Diss ETH No 13264

CELL-CELL AND CELL-SUBSTRATUM INTERACTIONS

IN THE LONG-TERM CULTURE OF ADULT CARDIOMYOCYTES

A dissertation submitted to the

SWISS FEDERAL INSTITUTE OF TECHNOLOGY ZURICH

for the degree of

Doctor of Natural Science

presented by

LIOUDMILA OLEGOVNA POLONTCHOUK

Diplom Biophysicist

Moscow State University named after M.V.Lomonosov, Moscow, Russia.

Born 11th November 1971

citizen of Russia

accepted on the recommendation of

Prof.Dr. H.M.Eppenberger, examiner

Prof.Dr. R.Weingart, co-examiner

Prof.Dr. E.Wintermantel, co-examiner

Zurich 1999

Content

II. TITANIUM DIOXIDE CERAMICS CONTROL THE DIFFERENTIATED PHENO-TYPE OF CARDIAC MUSCLE CELLS IN CULTURE

REGULATION OF THE INTERCELLULAR COMMUNICATION BETWEEN ADULT RAT VENTRICULAR CARDIOMYOCYTES IN LONG-TERM PRIMARY CULTURE

Summary

Regulation of the gap junction remodelling plays an important role in response to cardiac injury. Dissociated adult rat ventricular myocytes were used as an experimental system to study the re-establishment of cardiac gap junctions during the heart tissue regeneration in vitro. Gap junctions were assayed during the re-differentiation of the adult rat ventricular cardiomyocytes in long-term primary culture to gain insight into the process underlying their remodelling. The cells were examined for the presence of Cx40, Cx43 and Cx45 at the protein level using specific antibodies. Western blot analysis was done to study the expression patterns of connexins. Immunofluorescent labelling of the cells was performed to localise the channel proteins by means of confocal microscopy.

Imunofluorescent studies showed that cultured adult cardiomyocytes loose the normal pattern containing large gap junctions concentrated at the cell ends and exhibit many small junctions, which become uniformly distributed over the whole length of the cell contact membrane. These morphological transformations resembled the alterations in the organisation of gap junctions observed at the edges of an infarct during the active phase of healing. Double immunostaining studies indicated the localisation of connexins Cx40, Cx43 and Cx45 in the intercalated discs between cardiomyocytes. Their co-expression in the same cell and co-localisation in the same gap junction plaque raised the possibility for the heterotypic and/or heteromeric gap junction channels formation between the cardiac cells.

Western blot analysis showed time-dependent changes in the expression and phosphorylation of the connexins in the cultured cells. The total amount of all three cardiac connexins and the proportion of their phosphorylated forms to non-phosphorylated forms gradually increased during the re-establishment of the intercellular communication between the heart muscle cells in culture. The main connexin phosphorylation events were found to take place during and after the assembly of gap junctions within the cytoskeleton-associated regions of the cell-cell contacts in cultured cardiomyocytes. Connexin phosphorylation seems to be required to stabilise the intermolecular interactions within the new adhesion complexes formed between re-differentiated cardiomyocytes in vitro. The co-ordinated activation of the cytoplasmic and membrane-bound p70S6 kinase by TPA stimulates the expression of Cx43 and its phosphorylation in the plasma membrane. The elevated incorporation of the protein into sites of cell-to-cell contacts results in an increase of the metabolic coupling between the cardiomyocytes in culture.

Myocardial gap junctions display dynamic changes in co-ordination with cell behaviour. The results of the present study implicate multiple mechanisms for the regulation of intercellular communication by the gap junctions having different connexins. Some of them may be the results of the cell's switch to an early developmental program. Hence, the co-expression of cardiac connexins seems to play a major regulatory role in the heart morphogenesis and remodelling.

Zusammenfassung

Die Regulation der Wiederherstellung von Gap Junctions spielt eine wichtige Rolle, wie das Herz auf Schädigungen reagiert. Isolierte ventrikuläre Myozyten adulter Ratten dienten als in vitro System zur Untersuchung der Regeneration von Gap Junctions im Herz. Der Prozessablauf beim Wiederaufbau von Gap Junctions wurde während der Redifferenzierung ventrikulärer Myozyten aus dem Herz adulter Ratten in langzeitigen Primärkulturen verfolgt und mit Hilfe spezifischer Antikörper auf das Vorhandensein der Gap Junction Proteine Cx40, Cx43 und Cx45 untersucht. Das Expressionsmuster der Connexine wurde mit Hilfe von Western Blots studiert. Immunofluoreszenzmarkierung der Zellen wurde verwendet, um die Kanalproteine mittels konfokaler Mikroskopie zu lokalisieren.

Die Immunofluoreszenzstudien zeigten, dass adulte Kardiomyozyten in Kulturen das normale Verteilungsmuster der Gap Junctions, nämlich eine Konzentration an den Zellenden verlieren. Sie zeigten viele kleine Gap Junctions, die sich gleichmässig über die ganze Fläche der Zellkontaktmembran ausbreiten. Diese morphologische Veränderung ähnelt der Verteilung von Gap Junctions, wie sie an den Randen einer Infarktregion des Herzmuskels während der aktiven Heilungsphase beobachtet werden. Doppelte Immunofluoreszenzmarkierung lokalisierte die Connexine Cx40, Cx43 und Cx45 in den Glanzstreifen zwischen Kardiomyozyten. Ihre Expression in der gleichen Zelle und ihre gemeinsame Lokalisierung in der gleichen Gap Junction Plaque deuteten auf die Bildung heterotypischer und/oder heteromerer Gap Junction Kanäle zwischen den Herzzellen hin.

Western Blot Untersuchungen zeigten in Zellkulturen zeitliche Änderungen in der Expression und Phosphorylierung der Connexine. Die Gesamtmenge aller drei Connexine und das Verhältnis von phosphorylierten zu nichtphosphorylierten Formen stieg bei den Herzmuskelzellen in der Kultur während der Wiederherstellung der interzellulären Kommunikation allmählich an. Die Phosphorylierung der Connexine konnte hauptsächlich während und nach dem Zusammenbau der Gap Junctions innerhalb jenes Zellkontaktbereiche beobachtet worden, wo Interaktion mit dem Zytoskelett stattfand. Sie scheint in vitro zur Stabilisierung der intermolekularen Wechselwirkungen in den neu entstandenen Adhäsionskomplexen zwischen redifferenzierten Herzmyozyten wichtig zu sein. Nach der koordinierten Aktivierung der zytoplasmatischen und membrangebundenen p70S6 Kinase durch TPA wurden Expression und Phosphorylierung von Cx43 in der Zellmembran angeregt. Der erhöhte Einbau des Proteins gerade in Regionen, wo unter in vitro Bedingungen Zellkontakt stattfindet führte zu einer erhöhten metabolischen Kopplung zwischen den Herzmyozyten.

Gap Junctions im Herzen öffneten einen potentiellen Weg zu dynamischen, mit dem Verhalten der Zellen koordinierten Veränderungen. Die Ergebnisse der vorliegenden Arbeit, nämlich aus unterschiedlichen Connexinen zusammengesetzte Gap Junctions, implizieren mögliche unterschiedliche Mechanismen bei der Regulation der interzellulären Kommunikation. Einige davon könnten die Folge einer Umstellung der Zelle auf ein früheres Entwicklungsprogramm sein. Die gemeinsame Expression von unterschiedlichen Connexinen könnte eine regulatorische Funktion in der Morphogenese und im Remodeling des Herzens haben.

Introduction

1. Heart Structure and Function

The heart is a hollow organ, with muscular walls, which by its rhythmic contractions pumps blood through the vessels and cavities of the circulatory system. The heart is composed of two separate syncytiums (Fig. 1), the atrium syncytium that constitutes the walls of the two atria and the ventricular syncytium formed by the walls of the two ventricles. These syncytiums are separated from each other by fibrous tissue that surrounds the valvular openings between the atria and ventricles. The ventricles — the main working chambers of the heart — function under greatly different pressures and consequently vary in thickness and the total mass. However, the general architecture of all components (i.e., endothelium, muscle cells, capillaries, arteries, veins, nerves, etc.) is generally similar in both ventricles. Atrial architecture is, by and large, identical in both atria except that the sinoatrial (SA) and atrioventricular (AV) nodes are located in the right atrium close to the superior vena cava and near the atrial septum close to the AV junction, respectively.

The heart consists mainly of muscle, endothelial and fibroblastic cells. Soon after birth, cardiac myocytes lose their ability to proliferate, and the heart grows by increasing the size of its myocytes and increasing the number of non-myocytes. Cardiac muscle cells — ventricular and atrial cardiomyocytes — make up most of the adult myocardial mass; however, they comprise less than 30% of all the cells in the heart [Zak, 1973]. The other components of the cardiac tissue are:

Endocardium: The endocardium consists of endothelial cells that are indistinguishable from endothelial cells lining the capillaries.

Epicardium: The serosal surface of the heart consists of cells that have numerous villous processes similar to the mesothelial cells that cover all serous membranes.

Nervous system: Nerve cells, mostly autonomic unmyelinated fibres, are covered by a laminar coat. Often they are separated from the myocytes by fibroblasts and collagen. Sometimes only a very narrow space remains between them and the myocytes (~20 nm), so that both cell types share a laminar coat. As elsewhere, the nerve cells in cardiac muscle can be divided into parasympathetic (clear, cholinergic) and sympathetic (dense core, adrenergic) nerve endings.
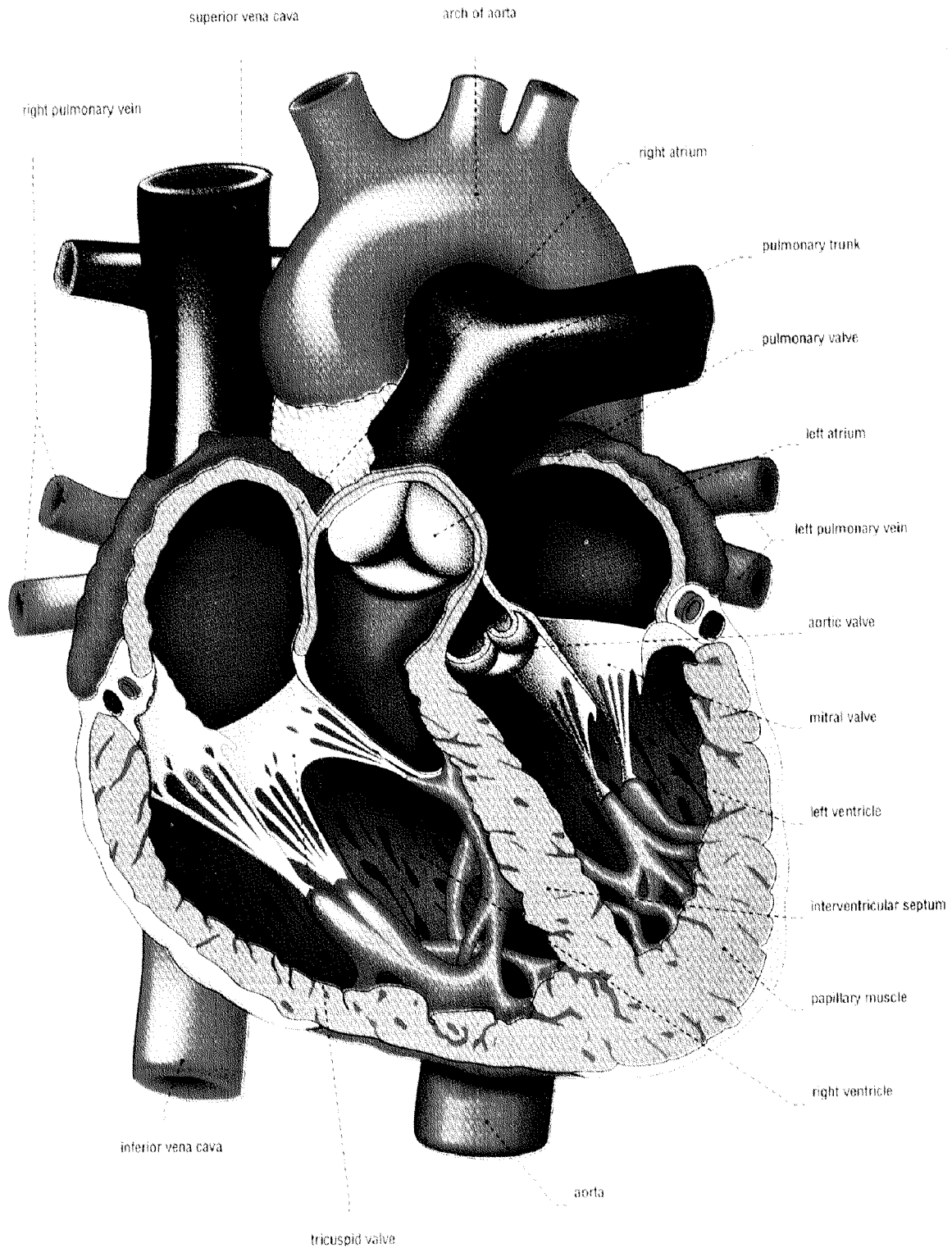
Fig. 1 Anatomy of the Heart

(from Diccionario Visual, Oxford University Press. ed. Quebec/Amerique International, 1995)

Vessels and capillaries: Arterioles and capillaries are lined by a continuous coat of endothelial cells that are not fenestrated except in the conduction cell bundles. Three or four capillaries are usually in contact with each myocyte. They are normally formed from a single or sometimes two endothelial cells joined by tight junctions [Weihe and Kalmbach, 1978].

Extracellular space: The ECS of the heart consists of a complex mixture of fibres, fibrils, and microthreads [Caulfield and Wolkowica, 1988]. It also contains a variety of proteins, negatively charged proteoglycans among them, as well as electrolytes, metabolites, and many formed elements. The formed elements comprise a complex weave of a fibrillar matrix, much of which is collagen, that holds myocytes, capillaries and nerves together by multiple connections. A mechanical analysis of the cardiac collagen microstructure showed that the elastic energy derived from a previous heart contraction is stored mostly in, and then released from, the collagen struts (i.e., the isotropic components of the system) [Ohayon and Chadwick, 1990]. 85% of the collagen's protein is type I, 11% type III, and the remainder is type V collagen [Weber et al., 1989]. Cardiomyocytes and capillaries are surrounded by the laminar coat formed by fibronectin, laminin and small collagen fibres. There are plenty of fibroblasts within the intercellular spaces. They do not have a laminar coat.

In the adult heart conventionally one distinguishes working myocardium (the primary function of which is contraction) from the conduction system (the primary function of which is the generation and conduction of electrical impulse). The myocytes of the conduction system are smaller than the working atrial or ventricular myocytes, moreover the actin and myosin filaments of the former are less organised, their sarcoplasmic reticulum less developed. However, the myocytes of the conduction system share with myocytes of the ordinary working myocardium four basic elements: 1) contraction, 2) autorhythmicity, 3) intercellular conduction, and 4) electromechanical coupling. The conduction system comprises of separate components with distinct functions. The sinoatrial node, which contains the leading pacemaker, generates the impulse, which is subsequently conducted via the atrial myocardium towards the atrioventricular node. After a delay the impulse is rapidly transmitted from the atrioventricular node via the bundle branches and peripheral Purkinje network. This pathway ensures a coordinated activation of the ventricular myocardium from apex to base (Fig.2).
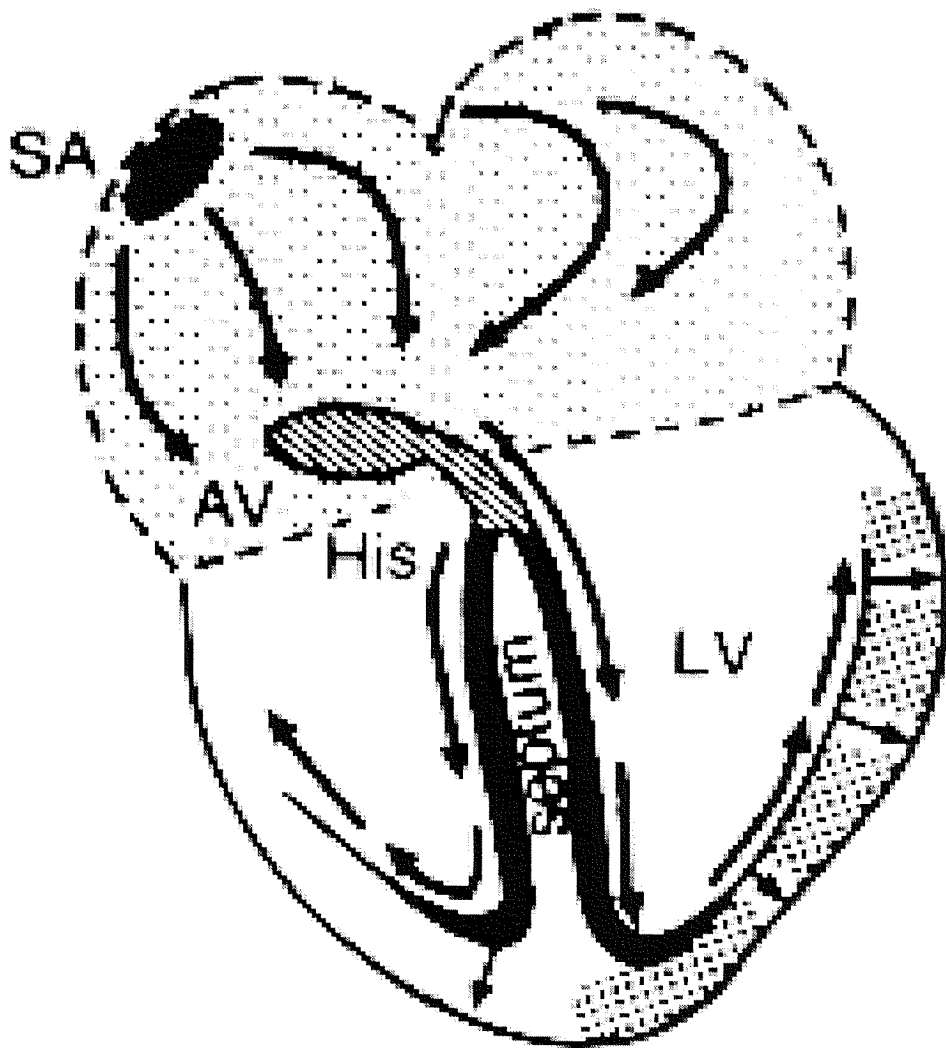
Fig. 2 Scheme of the Origin and Spread of the Cardiac Impulse

(from L.H.Opie (1991). The heart. Raven Press. N.Y.)

SA - sinoatrial node

AV - atrioventricular node

His - His bundle

LV - left ventricle

2. Cardiac Gap Junctions

2.1 Ultrastructure of Cardiac Muscle Tissue

Heart muscle is arranged in several muscle layers that are oriented at an angle to each other. This geometry simultaneously strengthens the wall and promotes a vector for the systolic heart twist which moves blood toward the cardiac outflow tract.
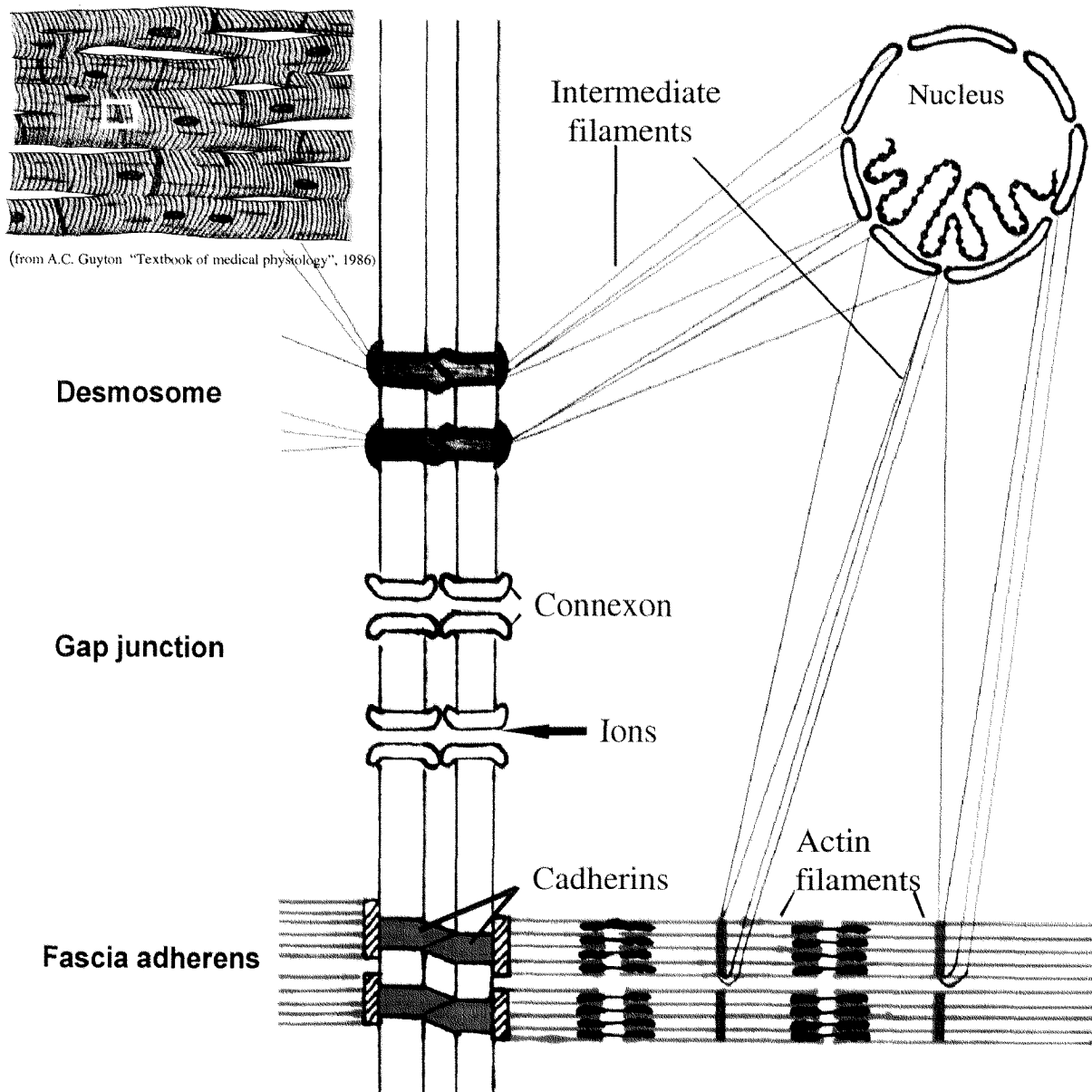
Fig. 3   Structure of the Intercalated Disk

The insert in Fig. 3 illustrates a typical histological picture of cardiac muscle, showing the cardiac muscle fibres arranged in a branching network. Cardiac muscle fibres are made up of many cardiac muscle cells connected in series with each other. This latticework formed by all myocytes defines the electrical current distribution within the tissue. Bundle geometry is maintained by junction complexes situated at cell ends. They are seen as angulated dark areas crossing the cardiac muscle bundles and are called intercalated discs. Cardiac myocytes are tightly apposed at the intercalated discs, which are mosaics of three kinds of junction complexes: a) desmosomes (macula adherens), b) adherent junctions (fascia adherens) and c) gap junctions (nexus) as depicted in Fig. 3.

The desmosomes and adherent junctions serve mainly an adhesive function. Gap junctions are the morphological structures providing one of fundamental physiological properties of cardiac muscle, which is the electrical coupling of all cardiac muscle cells. They provide the direct pathway for the cardiac electrical impulse propagation from the site of origin (in the sinus node) to the working myocardium of atria and ventricles, which finally leads to excitation contraction coupling in myocytes.

2.2 Structure of Gap Junctions

2.2.1 Microscopic Observations

The earliest description of what is now called a gap junction in cardiac muscle was reported by Sjoestrand et al. [1958] as seemingly fused membrane regions between cardiomyocytes, giving a pentalaminar profile in thin electron microscopy preparations. Later Barr, Dewey and Berger [1965], then Dreifuss, Girardier and Forssmann [1966], showed that the electrical coupling of cells in myocardium depends on the integrity of a particular membrane structure, the so-called nexus. These structures, now known as gap junctions, are formed between two cells by the close association of plasma membrane portions containing hexagonal arrays of particles [Revel and Karnovsky, 1967]: the connexons. Evidence that hexagonally packed structures were an integral part of the membrane was obtained from freeze-fracture studies of cardiac cells [Steer and Sommer, 1972]. In mammalian gap junctions the protoplasmic (P face) leaflet shows arrays of 4–5 nm particles at a centre-to-centre spacing of 9 –10 nm. The exoplasmic (E face) leaflet shows a similar array of pits. The particles in the P face represent complete channels partially exposed, the pits themselves are the impressions left as the hemichannels were extracted from the E leaflet. A central 2–2.5 nm lowering on the top of the

P face particles indicates a hydrophilic channel. Therefore, according to the first [McNutt, 1970] and subsequent models [Unwin, 1980], the gap junction consists of connexons (or hemichannels) that are composed of six protein subunits, which form a hydrophilic pore in their centre. A connexon, insulated from extracellular space, extends from one cell to the other across a narrow extracellular gap of about 2 nm. Connexons from apposing cells meet within the intercellular space to form the functional channels. The channel is 100–150 Å long and has the inner pore diameter of 12.5 Å [Beyer et al., 1995]. Gap junction channels are clustered in specialised membrane domains termed gap junction plaques.

Gap junctions comprise about 15% of the total intercalated disc profile length. Morphometric analysis of canine ventricular myocardium sectioned in three orthogonal planes [Hoyt et al., 1989] revealed that 80% of total gap junction membrane occurs in large, ribbon-like gap junctions oriented along the longitudinal cell axis in interplicate segments and usually having a profile length of one or two sarcomeres (Fig. 4). These gap junctions are the preferential sites of the electrical coupling of myocytes. The remaining 20% of gap junction membrane is represented by small gap junctions contained in the plicate segments that run transversely with respect to the long axis of the cell. An individual cardiac myocyte may have a number in the order of about 100 gap junctions connecting it to an average of about ten other myocytes.

Fig. 4 Architecture of the Intercalated Disk (rabbit myocardium, *91 750)

(from N.J.Severs "Gap junctional alteration in the failing heart". (1994) Eur.Heart.J. 15(D):53-57).

2.2.2 Connexins and the Molecular Architecture of Gap Junctions

The molecular structure of gap junctions was revealed by X-ray diffraction analysis of purified gap junction membranes [Caspar et al., 1977]. It was found that the gap junction hemichannels (connexons) are composed of six polypeptide subunits called connexins. Connexins form a group of related gap junction proteins encoded by a multigene family. They are now named according to the predicted MW from their cDNA sequence. Over the past decade these channel-forming proteins have been identified and characterised in nearly all organisms of the animal kingdom. The same connexin can be expressed in a variety of tissues and organs, and, on the other hand, more than one connexin type may be detected in the gap junction of the same cell type. Expression of Cx37, Cx40, Cx43, Cx45, Cx46 and Cx50 genes have been demonstrated in rat and mouse hearts either on the protein or on the mRNA level. The predominant connexins expressed in mammalian ventricular myocardium are Cx40, Cx43 and Cx45 [Davis et al., 1995]. The distribution of different connexins in specialised regions of the adult mammalian heart is shown in Fig. 5 [Davis et al., 1995; Kwong et al., 1998].

Sinoatrial node
Cx40>>Cx45>Cx43

Atria
Cx40, Cx43, Cx45

Atrioventricular node
Cx45>>Cx43>Cx40

Purkinje fibers
Cx40>>C43>Cx45

Ventricles
Cx43>Cx45
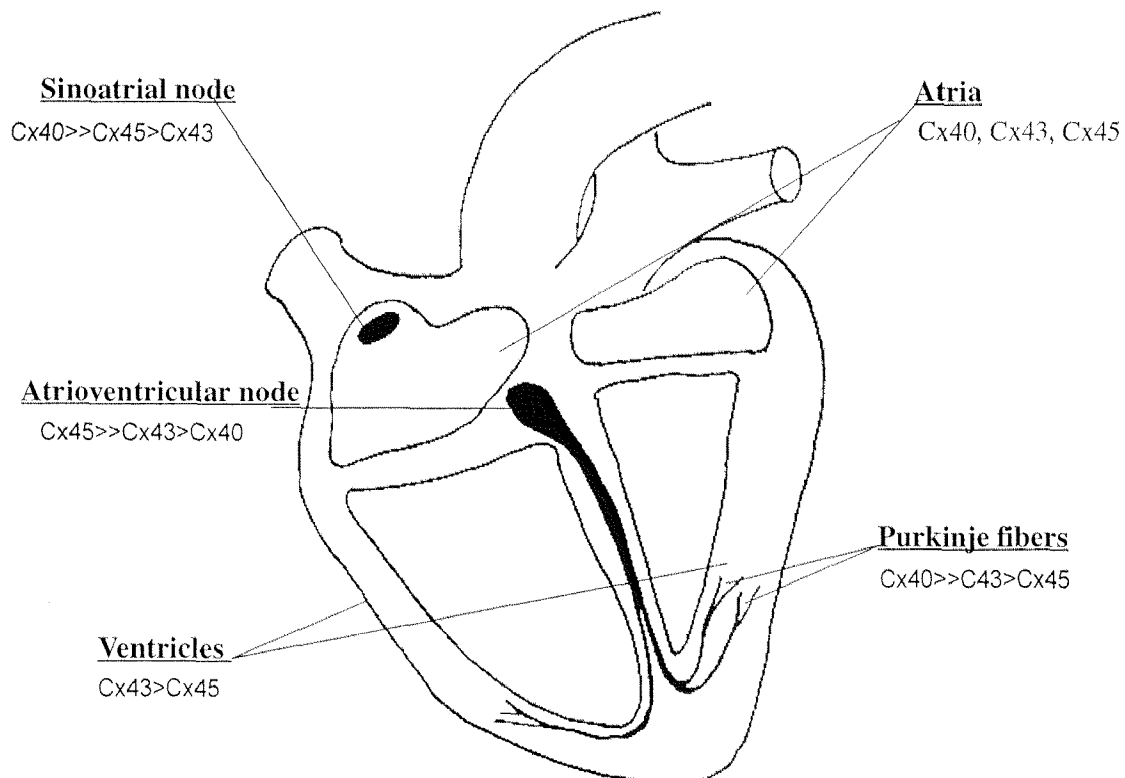
Fig. 5   The Specific Expression of Different Connexins in the Heart
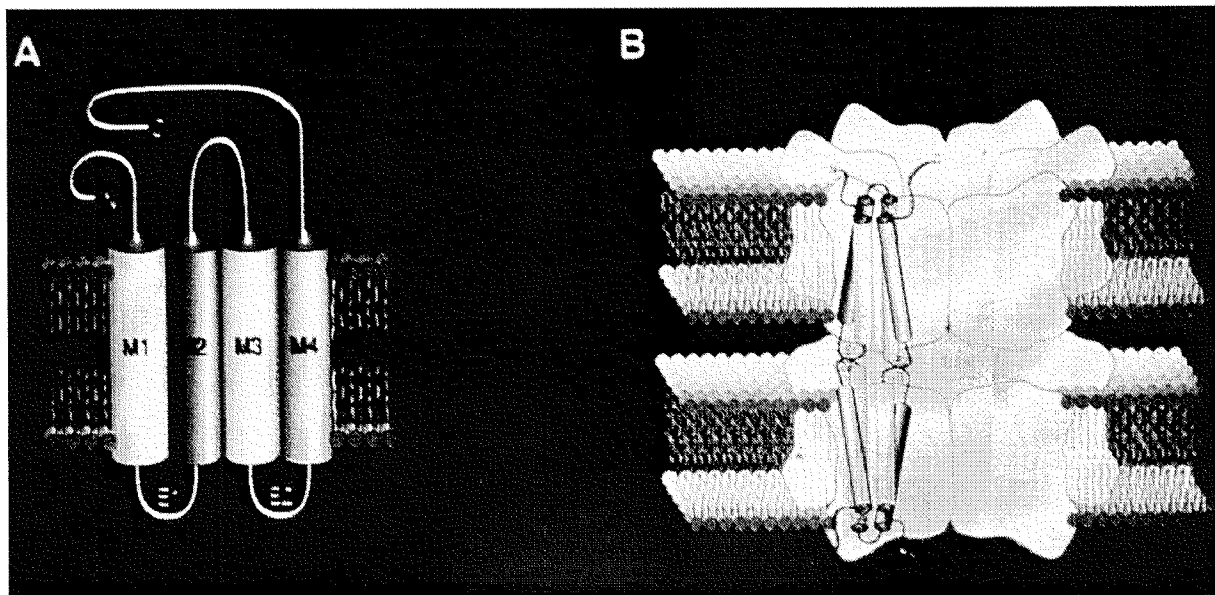
Fig. 6   Molecular Models for the Gap Junction Channel Structure

(from N.Kumar and N.B. Gilula. "The gap junction communication channels".(1996). Cell. 84:381-388)

A - model for the connexin membrane toplogy

B - model for the gap junction channel

All connexins have a similar membrane topology, as shown in Fig.6. The connexin molecule has nine specialised domains: the four transmembrane domains (M 1–M 4), the C-terminus, the N-terminus, two extracellular loops (E1 and E2) and the cytoplasmic loop (CL) between M 2 and M 3. The third membrane-spanning connexin domain (M 3) is located inside the gap junction channel lining the channel pore. Some of the polar residues repeatedly found within this domain are critical both for connexon transport into the plasma membrane and for gap junction channel permeability [Krutovskikh et al., 1998]. The extracellular loops contain highly conserved cysteine residues, which are necessary for the connexon docking in extracellular space. It was also found [Zhu et al., 1997] that the specificity of docking between hemichannels composed of different connexins is dictated by the tertiary structure of E1 and E2. The structure is influenced by the disposition of the transmembrane helices and plays a critical role in the formation of an intact gap junction between different cell types. In addition, the second extracellular loop, the amino acid sequence of which is less conserved among the investigated connexins, may be involved in the regulatory process of the gap junction channel gating [Krisciukaitis and Huelser, 1997]. The connexins are most divergent in their C-terminal domain with respect to length and amino acid sequence. The length of their intercellular

tail ranges from 18 amino acids in Cx26 to 191 in Cx46. The carboxy-terminal domain contains several phosphorylation sites and plays an important role in the chemical regulation of gap junctions. It can act as an independent domain which, under the appropriate conditions, binds to a separate region of the protein and closes the channel (as in the ball-and-chain mechanism of voltage-dependent gating of potassium channels) [Barrio et al., 1993; Morley et al., 1996]. The presence of a histidine residue at the N-terminal end of the cytoplasmic loop that acts as a receptor for the particle is conserved among connexins [Spray, 1990].

Connexons, composed of six connexins delineating a channel pore, are either homomeric, containing a single type of connexin, or heteromeric, containing multiple connexins. Additionally, adjacent cells can contribute identically or differently composed connexons, thus forming homotypic or heterotypic intercellular channels (Fig. 7).

| Connexon | Homomeric | Heteromeric | Homomeric | Heteromeric |
| Channel | Homotypic | Homotypic | Heterotypic | Hetereotypic |
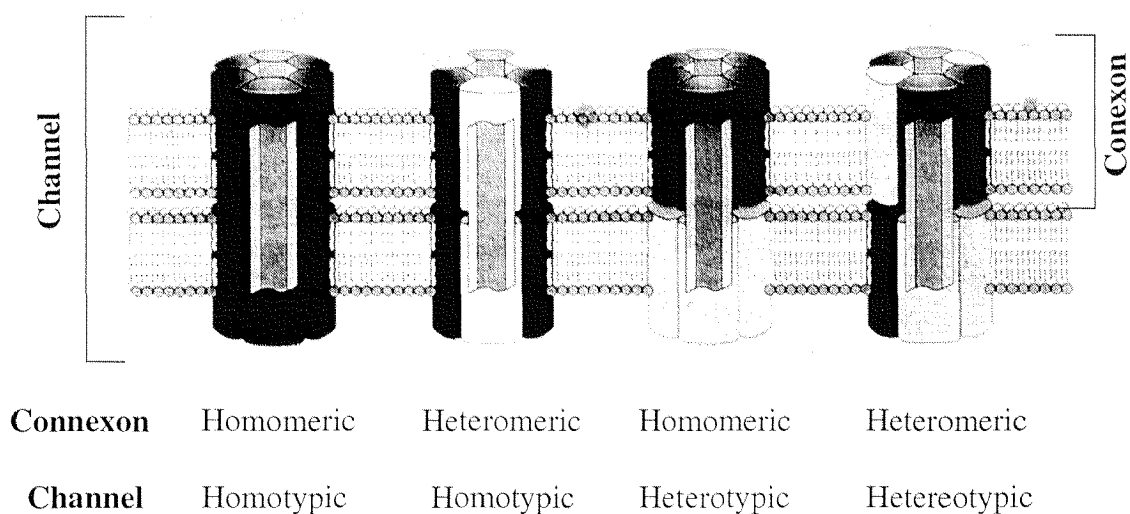
Fig. 7   Schematic Drawing of Possible Arrangements of Connexins to Form Gap Junction Channels

(from N.Kumar and N.B. Gilula. "The gap junction communication channels".(1996). Cell. 84:381-388)

2.2.3 A Three-dimensional Model of the Gap Junction Channel

Hydropathy analysis of the rat heart connexin 43 sequences predicts that hydrophobic transmembrane regions of the molecule could be folded as α-helices [Yeager et al., 1992]. Support for this model has been provided by CD spectroscopy [Cascio et al., 1990] and analysis of high angle X-ray diffraction patterns [Tibbits et al., 1990]. Electron cryo-microscopy and image analysis of frozen-hydrated, two-dimensional crystals of gap junction membrane channels formed by recombinant Cx43 (at resolutions of 7.5 Å in the membrane plane and 21 Å in the vertical direction) revealed that the transmembrane domains are packed as an α-helical bundle. These are a ring of transmembrane α-helices lining the aqueous pore and a second ring of α-helices in close contact with the membrane lipids. [Unger et al., 1999]. The dodecameric channel is formed by the end-to-end docking of two hexamers. The two connexons forming the channel are rotationally staggered with respect to each other. The model predicts that each subunit in such a connexon will interact with two connexin subunits in its apposing connexon via hydrogen bonds, hydrophobic interaction and ionic attraction (Fig. 8). Such an arrangement may confer stability in the docking of the connexons. In addition, the protein density forming the extracellular portal provides a tight seal to exclude the exchange of substances with the extracellular environment.

2.3 Biophysical Characteristics of Gap Junction Channels in the Heart

2.3.1 Conductive Properties

The current and molecular transfer through gap junctions depends on the size properties of the single channels, which include permeability, selectivity and unitary conductance. These considerations provide and distinguish the physical and electrostatic determinants for the transfer properties of a nexus.

First experiments with fluorescent tracer molecules revealed that substances with molecular weight (MW) of up to 1.2 kDa (or 12–14 nm in diameter) cross the channel independent of charge or nature [Schwarzmann et al., 1981]. Thus ions, second messengers such as cyclic nucleotides, inositol phosphates and diacylglycerol can be transported by the channels, but the passage of nucleic acids and proteins is not possible.
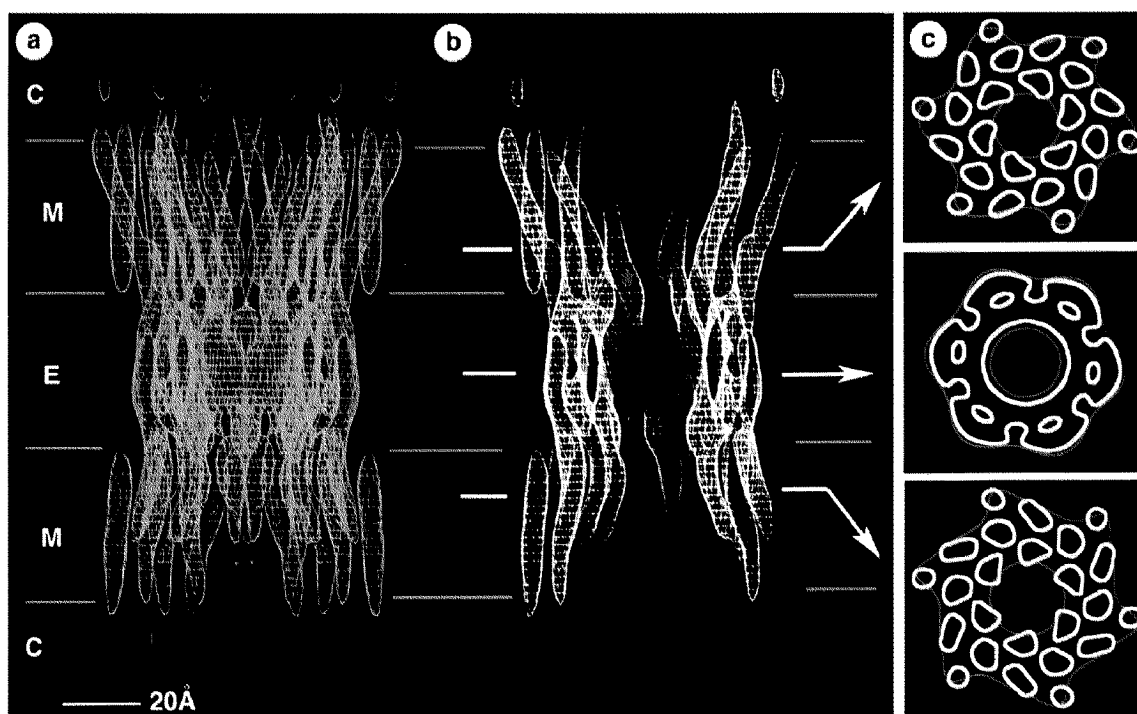
Fig. 8 Molecular Organization of a Gap Junction Channel

(a) A full side view is shown, and (b) the density has been cropped to show the channel interior. The approximate boundaries for the membrane bilayers (M), extracellular gap (E), and the cytoplasmic space (C) are indicated. The white arrows identify the locations of (c) the cross sections that are parallel to the membrane bilayers. The red contours in (c) are at 1 above the mean density and include data to a resolution of 15 Å. The yellow contours at 1.5 above the mean density include data to a resolution of 7.5 Å. The roughly circular shape of these contours within the hydrophobic region of the bilayers is consistent with 24 transmembrane helices per connexon. The maps in (a) and (b) were contoured at 3 above the mean, which tends to eliminate density that is less well defined, such as the cytoplasmic domains, which are contoured at 1.5 above the mean. The red asterisk in (b) marks the narrowest part of the channel where the aqueous pore is ~15 Å in diameter, not accounting for the contribution of amino acid side chains that are not resolved at the current limit of resolution. The noncrystallographic twofold symmetry that relates the two connexons of a gap junction channel has not been applied to the map. Hence, the similarity of the two connexons provides an independent measure of the quality of this reconstruction. (adopted from Unger VM, Kumar NM, Gilula NB, Yeager M. (1999) Three-dimensional structure of a recombinant gap junction membrane channel. Science. 283:1176-80)

However, the molecular permeability of gap junction channels is determined not only by the inner pore size. It has also been shown that the size (molecular weight or diameter) permeability limit to fluorescent tracers decreases reciprocally with an increasing negative charge of the permeant dye molecule [Brink et al., 1980], suggesting that gap junction pores contain fixed anionic charges and select for monovalent cations, predominantly K^+, under physiological conditions. Recent data [Veenstra et al., 1995] confirmed that there is an anionic site at or near the narrowest region of the connexin pore and that the ion permeation requires transient cation-anion interaction at this site.

Single channel recording technique applied to cardiac and other gap junctions has allowed another insight into the electrical properties of the gap junction channels. It was found that the diversity of connexins in various tissues is reflected in differences in unitary conductance of gap junction channels. Single channel studies of communication deficient HeLa cells stably transfected with the connexin cDNAs showed that each connexin forms gap junction channels with distinct transfer properties. It should be mentioned here that data obtained during the measurement of single channels events depend on the ions available as charge carriers in the pipette solutions used to fill microelectrodes. Therefore, care should be taken when comparing results obtained by different research groups.

Specific expression of connexins in distinct regions of the heart may regulate the velocity of the electrical impulse propagation between specialised compartments of cardiac tissue. For example, Cx40, which forms channels with the highest unitary conductance, has been found predominantly expressed in the conductive system and Purkinje fibres [Gourdie et al., 1993] where it supports the synchronous contraction of ventricles by quickly mediating excitation to them.

The conventional model for a gap junction channel, based on the structural and permeability data of early works, is an aqueous right cylindrical pore 8–14 Å in diameter and 16 nm in length. A major assumption of this model is that g_j is determined primarily by pore diameter. However, it was demonstrated in a recent study that the relative selectivity and permeability to ions and dyes in channels formed by different connexins was independent of channel conductance [Veenstra et al., 1995]. Cx45 channels, with the lowest g_j, were the most selective, as might be expected if the low g_j value were due to a narrow pore. Rat Cx43 has a smaller g_j of 61 pS compared to 190 pS for Cx40 in 110 mM Cs^+aspartate$^-$ [Valiunas et al, 1997; Valiunas, unpublished]. However, a different permeability to polysaccharides and organic cations suggest that the Cx40 pore is narrower than that of Cx43 [Veenstra et al., 1995]. These results

imply that weak electrostatic potentials associated with the pore of each connexin channel account for the gap junction channel conductance and permselectivity. No direct relation between connexin channel conductance and ionic selectivity or dye permeability was found by Veenstra et al. [1995]. Hence, these data are not consistent with the conventional simple aqueous pore model of a gap junction channel and suggest a new model based on electrostatic interactions. However, the molecular basis for the apparent selectivity in channel permeability is not known.

2.3.2 Gating

Gap junction channels, like other channels, are not static tubes and may be regulated by gating, enabling a cell to respond rapidly to various physiological events. Theoretically, a channel can close in an all-or-nothing or graded manner. The alteration in pore size has been envisioned either as a physical blockage (ball on a chain model) or as the rotation and tilting of the connexins (iris diaphragm model) [Unwin, 1987] (Fig. 9).

The experiments performed on induced pairs of neonatal rat ventricular myocytes [Valiunas et al., 1997] showed that Cx43 channels exhibit several prominent conductance states: a main open state, several substates, a residual (or partially closed) state and a closed state. Similar behaviour has been observed for the murine Cx40 channels [Bukauskas et al., 1995]. The residual state is attributable to incomplete channel closure. Functionally it exerts a higher restriction on ion permeation than does the fully open state. Therefore, the transition from the fully open state to the residual state serves to increase the ability of the channel to discriminate between ions. Subconductance states are interposed between the residual and the main open states. These could rarely be seen, preferentially in conjunction with short pulses of transjunctional voltage (V_j) of large amplitude or with long V_j pulses of intermediate amplitude.

The transitions of single channels between various conductive states may be differently controlled by chemical and electrical signals. Gating by transjunctional voltage is characterised by relatively fast (<2 ms) junction current (I_j) transitions between open and residual states. These may reflect rapid conformational changes of connexins, consistent with the iris diaphragm model of the channel closure. The existence of substates suggests that each connexin provides a subgate. Chemical gating tested with CO_2, alcohols and arachidonic acid exhibits slow (>15 ms) junctional current transitions between open (or residual) and closed states. Slow transitions may involve direct interactions between connexins and membrane lip-

ids (or membrane soluble pharmacological agents) inducing the slow modification of the channel structure. The experiments on preformed cell pairs [Bukauskas et al., 1997] also demonstrated a striking similarity between chemical gating and single channel behaviour at first channel opening during channel formation: both phenomena were characterised by slow I_j transition between open and closed states. Therefore, slow events implicate the channel insertion into or removal from the membrane. It seems that a slow gating mechanism involves a common gating element activated by different stimuli. Thus it has been shown that the structural bases for Cx43 channel closure are the same, regardless of the trigger: low pH_i, IGF or insulin exposure [Homma et al., 1998]. Moreover, each connexon acts independently, not relying on its partner to close the entire channel in response to acidification [Francis et al., 1999]. The results of recent findings demonstrate that the chemical gating of gap junction channels can be thought of as a reaction between a particle (the carboxy-terminal domain of connexins) and a receptor (the channel pore or some intermediary molecule) [Calero et al., 1998].

A

open   closed

B
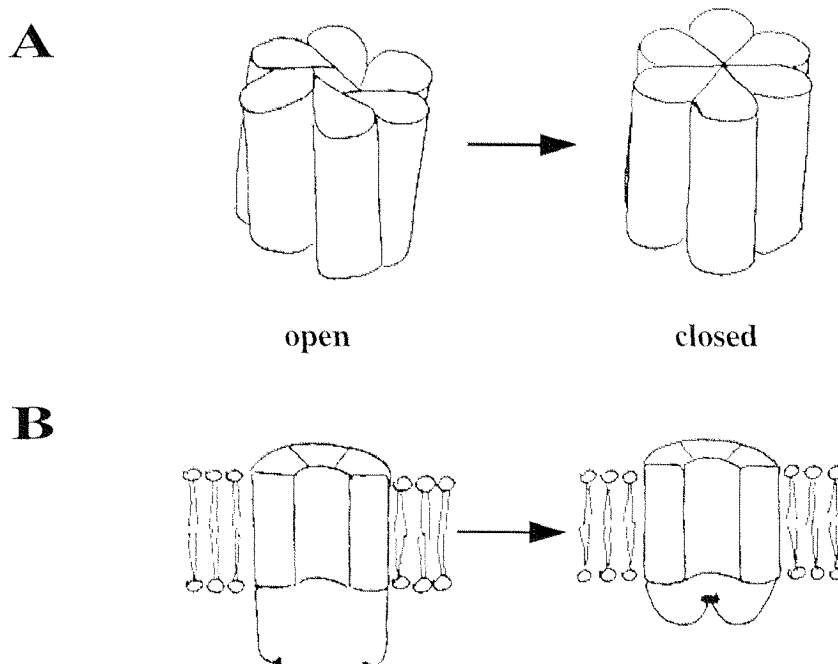
Fig. 9   Two Possible Mechanisms of the Gap Junction Channel Closure
A- iris diaphragm model; B- ball on a chain model. Only one hemichannel is shown.

In summary, all these data demonstrate that gap junction channels have several distinct conductive states. The transition between these states is differently regulated by various stimuli. Voltage gating induces fast conformational changes of the channel proteins in the mem-

brane similar to the rotation of an iris diaphragm, whereas a ball-on-chain model suggests a mechanism for the chemical gating of gap junction channels.

2.4 Regulation of Cardiac Gap Junctions

If the openings and closings of gap junction channels occur stochastically, macroscopic gap junctional conductance g_j is determined by the number of channels comprising the gap junction (n) multiplied by the conductance of each individual channel (g_j) and by the open-state probability (P_o) of the channels

$$g_j = n * g_j * P_o$$

Therefore, all the potential gap junction regulatory mechanisms described in the literature so far fall into one of two general categories depending on whether a mechanism induces rapid or long-term changes in the cell coupling. The first category describes mechanisms which quickly (within seconds or minutes) regulate the gating of pre-existing gap junctions affecting conductance or the open-state probability of the single channels; the second controls the balance of connexin synthesis, assembly and degradation over long periods of time.

2.4.1 Formation and Degradation of Gap Junctions in the Heart

Under standard conditions for myocyte dissociation, gap junctions are not normally split into their component membranes. Instead, they are retained as intact bimembranous structures with one or the other of the cells that originally shared them. The tearing often occurs at some distance from the junction plaque, creating a border of non-junctional membrane that can subsequently loop over and fuse with itself, thereby sealing off the potentially permeable junction from the exterior [Severs,1989]. The partitioning of junctions in this way might be expected to constitute a serious threat to the ionic integrity of dissociated myocytes. However, holes in the plasma membranes, created by the tearing out of gap junctions during myocyte dissociation, are repaired. The lesions are sealed over with a smooth, lipid-rich membrane, newly synthesised in subsarcolemmal vesicle clusters, continuous with the plasma membrane and form-

ing an intact closure [Severs, 1990]. The bimembranous gap junctions left in the membrane of dissociated cardiomyocytes are internalised by the cells. They form a vesicle with a circular profile (the so called annular gap junctions) and degrade by the usual pathway within proteosomes and lysosomes [Mazet et al., 1985].

The studies of isolated neonatal rat cardiomyocytes showed that if disaggregated cells are brought into close contact, cell coupling is re-established within minutes [Valiunas et al., 1997]. This observation suggests that the precursors of gap junction channels are present as hemichannels in cell membranes. This view is supported by evidence obtained in electrophysiological, and dye up-take experiments performed with single cells [Gupta et al., 1994; Li et al., 1996].

Axial aqueous channels are formed by docking hemichannels of adjacent cells. The theory of gap junction assembly which currently has the most support [Johnson et al., 1989; Musil et al., 1993], suggests that connexin proteins are assembled into hemichannels in an intracellular compartment before being inserted into the plasma membrane and distributed over the cell surface. Presumably the hemichannels in non-junctional membrane are routinely prevented from opening by regulatory molecules and the local calcium concentration. Thus a high-affinity binding site specific for purine cyclic monophosphate nucleotides is exposed during the synthesis, membrane integration or assembly of connexin channels and may play a role in keeping hemichannels closed while in cytoplasmic membranes [Bevans and Harris, 1999a].

It has been shown that Cx43 proteins are synthesised at the ribosomes on the endoplasmic reticulum (ER) and co-translationally integrated into ER-membrane with assistance of a chaperone-like assisting factor [Falk et al., 1995]. Synthesis is followed by early phosphorylation of Cx43 and transportation to the Golgi apparatus [Musil et al., 1991]. Connexins form oligomers in the trans-Golgi network [Musil et al., 1993] which are constitutively transported to the plasma membrane. These early phosphorylation events and the presence of adhesion molecules seem to be necessary for the assembly of connexons [Musil et al., 1990]. The extracellular loops of the connexins seem to be critical for the formation of the functional channel, since this process is inhibited by peptide analogues to the conserved regions of the extracellular domains in embryonic chick cardiomyocytes [Warner et al., 1995]. However, it has been recently shown that the primary sequence alone is not sufficient to determine the docking specificity. The tertiary structure of extracellular regions, influenced by the disposition of the transmembrane helices, also plays an important role [Zhu et al., 1997].

Cardiac connexins have a half-life of ~1.6 h as determined by pulse-chase experiments in cultured cells and isolated rat hearts [Laird et al, 1991; Beardslee et al., 1998]. Thus, the gap junction channels have a very rapid turnover rate, so that contacts between heart cells are highly dynamic [Hertig et al., 1996]. Regulation of connexin synthesis and degradation could play an important role in gap junction remodelling in response to cardiac injury.

2.4.2 Molecular Genetic Studies

To date, 14 different connexin genes localised in different chromosomes have been identified in the mouse genome and at least six other connexin genes have been isolated from other vertebrate species. For a review see Kumar and Gilula [1996]. Since orthologues of the latter six might exist in the mouse genome, the total number of vertebrate connexin genes is likely to exceed 20.

The majority of connexin genes have a simple structure in which the entire coding region is present within a single exon, although a new class has emerged that contains an intron within a coding region [O'Brien et al., 1996; Soehl et al., 1998].

The regulation of gene expression may be an important mechanism controlling temporal and tissue specific patterns of connexin distribution in the heart. Thus, mRNA transcripts of Cx37, Cx40, Cx43, Cx45, Cx46 and Cx50 genes have been demonstrated in rat and mouse hearts. For a review see Gros and Jongsma [1996]. However, the products of Cx40, Cx43 and Cx45 genes only are detected at the protein level in mammalian ventricular myocardium.

Cx43 is constitutively expressed in heart muscle. Analysis of Cx43 promoter by in vivo DNA footprinting identified several regions that showed differential protection in the heart as compared to other organs. One such region, located between nucleotides -34 and -71 (with respect to the transcription start site) in the mouse Cx43 promoter were shown to contain cis-activating sequence elements, which regulate the strength and specificity of the gene transcription [De Leon et al., 1994]. The sequence comprising nucleotides -36 to -52 contains a consensus AP-1 site [Chen et al., 1995]. The sequence between nucleotides -48 and -71 specifically binds a novel transcription factor, which has been recently identified by screening the rat cDNA library with a double-stranded DNA probe corresponding to nucleotides -34 to -71 [Oltra et al., 1997]. While the mechanisms that control expression of connexin 43 are not fully understood, most attention has focused on transcriptional regulation. The 3'-untranslated region (3'-UTR) of the Cx43 gene possesses regions rich in UA nucleotides (including four

AUUUA motifs), a feature that have been reported to confer mRNA instability and plays an important role in regulating the expression of Cx43 mRNA. It may be that at least part of the action of forskolin, retinoic acid and TPA may be mediated by it [Ou et al., 1997].

Unlike some other gap junction proteins, connexin 40 has a rather restricted pattern of expression in the heart. Developmental regulation of the connexin 40 gene expression in the mouse heart correlated with the differentiation of the conduction system [Delorme et al., 1995]. The mouse Cx40 gene contains a short first exon, an 11.4 kb intron, and a second exon containing the coding region and 3'-UTR. Exon 1 contains only 1 base, which differs between rat and mouse. It is closely preceded by a consensus TATA box and several consensus cis-acting regulatory elements in the upstream region. These flanking sequences contain a number of potential transcription factors binding sites (including AP-1, AP-2, and SP1). An area of ~300 bp in exon 1 can act as the basal promoter for Cx40 and contains an apparent repressor; both elements are important in the positive and negative regulation of Cx40 transcription [Seul et al., 1997].

The general genomic organisations of human and canine Cx45 genes are similar to the other mammalian connexins [Kanter et al., 1994]. The presence of transcription regulatory elements in the Cx45 gene has not yet been investigated.

2.4.3 Physiological Regulators of Cardiac Gap Junction Conductance

Four sets of factors which are of potential physiological relevance are known to affect g_j quickly. These are the concentration of small ions like H^+, Ca^{2+}, Mg^{2+} and Na^+, second messengers; transjunctional (V_j) or transmembrane (V_m) voltage and lipophilic agents.

It is known that in intact cells pH_i and pCa_i are interdependent. Elevation in the concentration of one cation leads to an increase in the concentration of the other [Vaughan-Jones et al., 1983]. A synergistic action of H^+ and Ca^{2+} in the regulation of gap junction conductance was demonstrated by Burt [1987] and by White et al. [1990] in neonatal and adult rat cardiomyocytes respectively. They demonstrated that a combined decrease in pH_i and elevation in Ca^{2+} blocked g_j, whereas either cation alone produced negligible effects. However, the molecular mechanisms by which H^+ and Ca^{2+} alter g_j are not resolved yet. It has been suggested that the histidine residue 95 may act as a pH sensor in Cx43 channels [Ek et al., 1994].

The results obtained in the same group also demonstrate that specific sequences within the carboxyl terminal (CT) region of Cx43 are required for pH-dependent gating of the Cx43 channel expressed in Xenopus oocytes pairs [Morley et al., 1996]. In addition, in vitro phosphorylation of Cx43 cytoplasmic tail was enhanced at lower pH [Rush et al., 1997]. Therefore, both mammalian and amphibian cells posses protein kinase(s) that can phosphorylate the CT domain of Cx43 in vitro in the regions between amino acid 261–280, 281–300, 364–373, and that this enzymatic activity increases at lower pH. These results indicate that phosphorylation processes could also contribute to pH gating.

An increase in the intercellular concentrations of Na^+ [De Mello, 1976] and Mg^{2+} [Noma et al., 1987] results in the reduction of the gap junctional conductance of cardiac myocytes by unknown mechanisms.

Gap junctional conductance can be modulated by cyclic nucleotides and ATP. Permeability of cyclic nucleotides can be connexin specific and some stoichometries and/or arrangements of connexin isoforms within a channel can distinguish between cAMP and cGMP [Bevans and Harris, 1999b]. Intracellular cAMP elevation, induced by β-adrenergic agonists or membrane permeable cAMP derivatives, increases g_j in cardiomyocytes within minutes, whereas intracellular cGMP derivatives decrease g_j in neonatal cardiomyocytes in the same time frame [Burt and Spray, 1988]. cAMP also increased the permeability of human Cx40 gap junction channels for Lucifer Yellow by 58% [van Rijen et al., 1997]. Intercellular communication may be modulated by direct interaction of the cyclic nucleotides with connexins, but the involvement of different protein kinases with the subsequent phosphorylation of gap junction proteins are more likely [Takens-Kwak, et al., 1992]. The up-regulation of macroscopic conductance of cardiac gap junctions by cAMP may play a role in the β-adrenergic regulation of the conduction velocity in the heart. ATP also has an important role as a physiological intracellular regulator of g_j. Reduction of $[ATP_i]$ to concentrations less than 0.1 mM leads to the total uncoupling of cardiac cells [Sugiura et al., 1990].

The sensitivity of the gap junction current to the resting membrane potential has not yet been obseved in cardiac cells. However, it has been recently described for rat Cx43 channels expressed in pairs of Xenopus oocytes that equal depolarisation of both cells decreases and equal hyperpolarisation increases g_j [Barrio et al., 1993]. In general, V_m-gating is represented by a relatively slow (~10 ms) transition of channels between open and closed states [Bukauskas et al.1997].

The dependence of gap junctional conductance on transjunctional voltage was investigated using the double whole-cell voltage clamp approach. If a transcellular voltage of 50–100 mV magnitude is established for a few seconds, g_j decreases with time from the initial instantaneous value ($g_{j,inst}$) to a steady-state rate ($g_{j,ss}$). A commonly used method to describe transjunctional sensitivity of gap junction channels is to fit the experimentally observed $g_j = f(V_j)$ relationship to the two-state Boltzmann equation (Spray et al., 1981):

$$g_{ss} = \left\{ \frac{\left(g_{max} - g_{min}\right)}{\left(1 + \exp\left[A\left(V_j - V_0\right)\right]\right)} \right\} + g_{min}$$

V_0 is a a voltage where g_{ss} lies half way between g_{max} and g_{min}, $A = zq/kT$ is a parameter quantifying voltage sensitivity (where z is the valence of charge q, k = Boltzmann's constant, and T = absolute temperature), g_{min} is a residual apparently voltage-insensitive, component always observed in gap junctions, and g_{max} is the maximum conductance.

Three assumption are made when this relation is applied: 1) gap junction channel gating is a two state first-order process, 2) all channels gate independently from each other, 3) all channels have identical opening and closing rate constants. Application of the Boltzmann relation to results obtained from cells expressing more than one type of connexin is not possible, because assumption three is then not satisfied. For instance, it will be inadequate in the case of cardiac gap junctions where co-expression and co-localisation of Cx43, Cx40 and Cx45 were demonstrated [De Maziere et al., 1993; Davis et al., 1995].

Recent studies demonstrated that cardiac gap junctions are moderately voltage sensitive [Rook et al., 1988; Wang et al., 1992; Valiunas et al., 1997], but this voltage sensitive behaviour of g_j can only be observed if g_j is low. There are two experimentally related reasons why voltage sensitive behaviour is not observed in large gap junctions. The first factor is the series resistance of the recording electrodes, which can cause a considerable drop in the applied transjunctional voltage with large transjunctional currents [Moreno et al., 1991]. The second factor is an additional drop in the applied transjunctional voltage due to the high current density in the cytoplasm near the gap junction channel mouths when large currents flow [Wilders and Jongsma, 1992]. The conductance of the single gap junction channel is not voltage dependent, but the ratio topen/tclosed depends on the applied transjunctional voltage [Rook et al., 1988]. The voltage dependence differs for the channels formed by different connexins: Cx45 chan-

nels are the most sensitive, followed by Cx40, while Cx43 channels are just slightly susceptible to transjunctional voltage [Dhein, 1998]. The physiological role of voltage sensitivity is still a matter of debate. It is possible that it is a mechanism protecting cardiac tissue from any depolarising or hyperpolarising influences.

Many lipophilic compounds have been examined for their uncoupling action on heart cells. g_j is reversibly reduced by linear alcohols such as heptanol and octanol [Ruedisueli and Weingart, 1989], volatile anaesthetics such as halothane [Burt and Spray, 1989] and by fatty acids [Burt, 1989]. These compounds do not affect unitary conductance, but reduce the probability that the channel is open (P_o). Lipophilic compounds may either directly interact with the channel proteins or non-specifically alter the fluidity of cholesterol-rich domains, important in gap junction coupling [Bastiaanse et al., 1992].

2.4.4   Modulation of Cardiac Gap Junctions by Phosphorylation

Phosphorylation, a common connexin modification, has been implicated in the gating of gap junction channels, connexin trafficking, assembly, insertion into the plasma membrane, degradation and retrieval from the plasma membrane.

The cardiac connexins Cx40, Cx43 and Cx45 appear to be phosphoproteins. The sequence of rat Cx43 intercellular carboxy-terminal domain allows phosphorylation by several protein kinases [Lau et al., 1996]: the serine residues 364, 368, 372 (Arg-X-Ser motif for PKA, PKG and PKC); 296, 365, 369, 373 (Arg-X-X-Ser motif for PKA, PKG, PKC and CaMK II); 244, 306 (Lys-X-X-Ser motif for PKG and PKC); 364, 368, 373 (Arg-X-Ser-X-Arg motif for PKC); 297, 364, 368, 372 (Ser-X-Arg motif for PKG and PKC); 262 (Ser-X-Lys motif for PKG and PKC); the threonine residue 290 (Lys-X-X-Thr motif for PKG and PKC); the tyrosine residue 265 (vSRC tyrosine kinase); and the serine residues 279, 282 and 255, which can be phosphorylated by MAP kinase. Phosphorylation of many of these sites has been confirmed by the two-dimensional tryptic phosphopeptide mapping and phosphoamino acid analysis of the protein isolated from cardiac cells radiolabelled with $^{32}P_i$ and by the in vitro phosphorylation of the specific peptides. However, the results obtained in situ should be very carefully taken over to the in vivo situation. For example, the distinct subset of the Cx43 phosphopeptides sensitive to the PKC activators in neonatal rat cardiomyocytes did not comigrate with those that were derived from the in vitro phosphorylation by PKC of a recombinant C-terminal Cx43 peptide (Cx43 [243–382]) [Saez et al., 1997].

Differences in the electrophoretic mobility observed for Cx43 have been shown to correlate with the presence of several distinct phosphorylated forms [Musil et al., 1990]. Treatment of the cells with drugs disrupting the intracellular vesicular traffic leads to the accumulation of intermediate phosphorylated forms of Cx43, suggesting that the initial phosphorylation of the gap junction protein occurs already before its incorporation into the cellular membrane [Puranam et al., 1993]. However, the subsequent phosphorylation steps occurring after the protein is translocated into the gap junction appears to be important for the regulation of the channel assembly [Musil and Goodenough, 1991]. The appearance of the phosphorylated forms is temporally associated with the localisation of immunoreactive Cx43 plaques into the cell membrane in myometrium during labour [MacPhee et al., 1997]. Phosphorylation may also target the protein for degradation. Thus, inhibition of lysosomal proteolysis in the isolated adult rat heart led to selective accumulation of phosphorylated Cx43 [Beardslee et al., 1998]. In addition, specific p34cdc2/cyclin B kinase phosphorylation of Cx43 causes its rapid internalisation and degradation in mitotic cells [Lampe et al., 1997]. Phosphorylation of Cx43 has also been proposed as the mechanism responsible for alterations in the unitary conductance and molecular permeability of gap junction channels in smooth muscle and cardiac cells [Moreno et al., 1994; Kwak et al., 1995].

The effect of connexin phosphorylation on the macroscopic current between cells depends on the kinases that control the phosphorylation process and on the type of the tissue. Some studies have reported that activation of PKA may enhance gap junction coupling in neonatal cardiomyocytes expressing Cx43 and Cx45 [Burt and Spray, 1988]. Furthermore, tumour promoting phorbol esters, which activate the classic isoforms of PKC, have been shown to increase g_j in the same cell culture [Spray and Burt, 1990]. PKG activation induced a reduction in the electrical coupling of neonatal rat cardiomyocytes, preferentially affecting the conductance of Cx43, but not of Cx45 gap junction channels [Kwak et al., 1995]. Tyrosine kinases can also phosphorylate Cx43 and thus inhibit gap junction communication in avian cardiomyocytes [Veenstra et al., 1992] and different cell lines [Crow et al., 1990; Swenson et al., 1990]. Activation of the Ras/Raf/MEK/MAPK cascade via epidermal growth factor receptors or by lisophosphatidic acid is responsible for the Cx43 phosphorylation and inhibition of gap junction communication in the rat liver epithelial cell line (T51B) [Kanemitsu and Lau, 1993]. MAP kinase also has been shown to phosphorylate Ser-255, 279 and 282 of an engineered construct corresponding to the C-terminus of Cx43 [Warn-Cramer et al., 1996]. The role of this kinase in the phosphorylation of gap junctions in cardiac tissue is uncertain.

All the data described above demonstrate that phosphorylation plays a role in regulating gap junction assembly and certain aspects of channel function. However, evidence for the involvement of other types of covalent modification(s) of connexins was obtained by free solution isoelectric focusing of Cx43 from the heart, brain and CI-9 cell samples [Hertzberg, 1997]. Cx43 from all three samples exibits pI variants of ca. 5.5, 6 and 7, rather than the pI 9 protein anticipated from cDNA sequence analysis. These pI variants comigrated on SDS-PAGE and were observed even after dephosphorylation of Cx43 by treatment with alkaline phosphatase, indicating that alteration of pI was relatively independent of phosphorylation. A shift in the pIs of these three isoforms towards anticipated values was observed in samples treated with alkali. The presence of the most acidic pI variant of Cx43 may be significant for gap junctions. It was lost after the treatment of CI-9 cells with monensin, inhibiting the connexin trafficking into the membrane in communication deficient insect cells. Biochemical analysis failed to detect connexin glycosylation, significant levels of acylation or tyrosine sulfation. The data suggest that some covalent polyanionic modification, not yet identified and not restricted to connexins or to mammalian cells, alters connexin pI without significantly affecting molecular weight.

2.5 Gap Junctions in Cardiac Development

The most comprehensive data on connexin expression in the developing heart are obtained from mice and rats. In the early myocardium, both the number and size of gap junctions are small but increase during cardiogenesis [Gros et al., 1978]. Gap junctions remain scarce only in the developing sinoatrial and atrioventricular nodes where low abundance of connexin expression corresponds with slow conduction velocities [Viragh et al., 1980]. The poor coupling of the nodal cells appears necessary to prevent the silencing of the pacing nodal myocytes by the much bigger atrial and ventricular myocardium [Joyner and van Capelle, 1986].

The products of connexin genes are developmentally regulated in rodent hearts. The transcripts of the connexin genes were detected only by RT-PCR in the mouse heart at 8.5 days post coitus (dpc), when the first rythmic contractions appear in the ventricular portion of the cardiac tube [Delorme et al., 1997]. At 9.5 dpc (and at further stages) all three connexins and their mRNAs, were detected by immunofluorescence (IF) or in situ hybrydisation (ISH) with a pattern of expression specific to each connexin. Cx43 was shown to be associated, although

in very small amounts, with the myocytes of the bulbus cordis (future right ventricle) and the common ventricular chamber (future left ventricle). In both rat and mouse embryonic hearts, Cx43 expression is higher in the trabecular ventricular component than in the compact ventricular component (septum and ventricular free wall) [Dahl et al., 1995]. This connexin was not however detected in the atrial tissue before 12.5 dpc. In contrast, Cx40 was observed as soon as 9.5 dpc, mainly associated with the myocytes of the common atrium. Cx40 was not detectable either in the common ventricular chamber or in the bulbus cordis before 10.5 dpc and 11.5 dpc, respectively. Between 10.5 and 11.5 dpc, Cx40 gene activation in myocytes was demonstrated to proceed according to a caudorostral gradient involving first the primitive atrium and the common ventricular chamber (10.5 dpc) and then the right ventricle (11.5 dpc). Thus, Cx40 is widely expressed in the 11.5 dpc embryonic heart, where it is detected in both the atria and ventricle primordia. Expression of Cx40 is maximal in the foetal period and declines towards birth. Cx40 expression in the left and right ventricles evolves independently, its mRNA disappearing 4 days earlier from the right than from the left ventricle, and earlier from the free wall than from the trabeculations [van Kempen et al., 1996]. From 14 dpc onwards, as the adult ventricular conduction system differentiates, Cx40 decreases in the trabecular network and is preferentially distributed in the ventricular conduction system of mice, rats, dogs, pigs, cows and humans [Delorme et al., 1995; van Kempen et al., 1995]. In addition, comparison of Cx40 and Cx43 distributions at the above developmental stages has shown that these connexins have overlapping (left ventricle) or complementary (atrial tissue and right ventricle) expression patterns [Delorme et al., 1997]. Moreover, Cx40 was found to disappear when the level of Cx43 became more abundant in the developing ventricular myocardium of different species [van Kempen et al., 1995]. These data suggest that abundant expression of Cx43 may lead to the suppression of that of Cx40.

Genetically engineered mice provide a novel tool for analysing the involvement of connexins during development. The dissection of cardiac defects in Cx43 knockout and transgenic mice showed that Cx43 gap junctions play an important role in conotruncal heart development, regulating the team migration of neural crest cells involved in cardiac morphogenesis [Lo and Wessels, 1998]. Although the consequences of transgenic gain versus knockout loss of Cx43 function were differnt, in both instances developmental abnormalities were localised to the right ventricle and outflow tract [Ewarts et al., 1997; Reaume et al., 1995], which are the target sites for a specific population of migrating neural crest cells [Fukiishi and Morris-Kay, 1992]. Therefore, observed phenotypes seem to arise from the perturbation of cardiac crest cells. Using an in vitro neural crest outgrowth assay, an enhanced rate of crest migration in

Cx43 transgenic embryos was observed, while crest migration in the Cx43 knockout mouse embryos was found to be inhibited [Huang et al., 1997]. Hence, changes in the abundance of crest cells could cause out-flow tract malformation and obstruction of myocardialisation of the endocardial ridges of the out-flow tract, a process which leads to the formation of the muscular outlet septum. This assumption is consistent with a recent finding that the out-flow tract myocardium in the Cx43 knockout mice retains an embryonic phenotype [Huang et al., 1998].

2.6 Cardiac Gap Junctions and Their Role in Heart Diseases

Studies of transgenic animals show that intercellular communication through gap junctions is critical for cardiogenesis [Reaume et al., 1995; Ewart et al., 1997] and normal cardiac electrophysiology [Willecke et al., 1998]. Moreover, the Cx43 perturbations are possibly involved in congenital heart defects. Recent medical genetic studies show that some mutations of the connexin 43 gene are linked to the hereditary severe cardiac malformation called visceroatrial heterotaxia (VAH) [Britz-Cunningham et al., 1995]. The VAH syndrome appears to arise by fundamental perturbation of left-right patterning in the heart. It clearly has a multigenic origin and exhibits a wide-ranging variability of phenotypes. Studies of the Cx43 gap junction channel defects in this dysfunction implicate gap junction communication in the establishment of left-right asymmetry in the heart. It is also interesting to note that five of six VAH patients harbouring Cx43 mutations showed defects associated with the pulmonary outflow tract, a region of the heart affected in the Cx43 knockout and transgenic mice. The phenotypes of these animals are clinically reminiscent of patients exhibiting malformations referred to collectively as subpulmonary stenosis or atresia with an intact ventricular septum [McQuinn, 1996]. In addition, looping defects in some Cx43 knockout mice were observed. They resulted in a heart configuration which is similar to a human cardiac malformation known as 'criss-cross' heart. The development of the D-configuration in the assembling loop of Cx43-deficient hearts was markedly retarded, so that the right ventricle retained a craniomedial position and was connected with the outflow tract by a more acute bend in ED10 and ED11 embryos. Due to the subsequent growth of the right ventricle, this condition usually evolves into a D-loop, but when it persists a criss-cross configuration develops, with the atrioventricular cushions rotated 90° counterclockwise, the position of the ventricular septum horizontal and a parallel course of the endocardial ridges of the outflow tract. Unfortunately,

it has not yet been investigated whether patients with either of these congenital heart anomalies have Cx43 mutations.

Abnormal myocardial impulse propagation is fundamental to the pathogenesis of important cardiac arrhythmia including ventricular tachycardia and atrial fibrillation. The conduction properties of normal atria and ventricles are determined by the number, size and 3-D distribution of their intercellular junctions. Gap junctions are usually located at the apical cell ends, i.e. with their transverse boundary in the longitudinal direction. However, the typical polarisation of Cx43 was lost in rat hearts after 24 hours of atrial fibrillation and connexin 43 was then distributed in a more disperse manner [Dhein et al., 1997]. Therefore, the alteration in the gap junction localisation may contribute to the formation of an arrhythmogenic substrate and the development of chronic atrial fibrillation.

Conduction velocity is dependent on active ionic currents and tissue structure as well as on the extent of intercellular coupling at gap junctions. An analysis of the electrophysiological features of heterozygous Cx43 +/- mice showed that these have a 44% slower epicardial ventricular conduction velocity of paced beats with no apparent differences in spontaneous heart rate or effective refractory period [Thomas et al., 1998]. Cx43 expression was reduced by approximately 50% in ventricular muscle of Cx43 +/- mice, but Cx45 expression was unchanged. The analysis of 3-lead surface electrocardiograms revealed a significant prolongation of the QRS complex in Cx43 +/- mice, consistent with the observed slow ventricular conduction. No differences in P wave duration were seen, suggesting that although atrial muscle expresses Cx43, no slowing of atrial conduction occurs in Cx43 +/- mice. Thus, Cx43 appears to be the principal conductor of intercellular current in ventricular muscle whereas Cx40 may serve this function in the atria. These proteins may therefore be chamber specific determinants of the conduction properties of atrial and ventricular muscles.

Cx40 knockout mice have also indicated an important role for this connexin in the rapid conduction of impulses in the ventricular conduction system. Cx40 is the predominant connexin known to be present in gap junctions between Purkinje fibres of the His bundle and the proximal portions of the left and right bundle branches [Bastide et al., 1993]. See also Fig. 5. These fibres mediate fast conduction of excitation from the atrioventricular node to the ventricles and are thus essential for co-ordinated myocardial contraction.

Two laboratories have independently knocked out Cx40 and found that the mice have a partial but not complete conduction block [Simon et al., 1998; Kirchhoff et al., 1998]. Cx40 null mice had normal sinus rhythm but frequently displayed notched or split QRS complexes

of increased duration, indicating abnormal ventricular excitation. Electrocardiograms also indicated a frontal plane axis deviation in many Cx40 knockout animals that is consistent with a partial block of conduction through the His/Purkinje system, leading to uncoordinated ventricular excitation. The lack of complete conduction block in Cx40 knockout mice may be explained by the fact that another connexin, Cx45, is also expressed in Purkinje fibres. Although Cx45 is enriched in the conduction system, unlike Cx40 it was also found in some adjacent fibres. The broader distribution of Cx45 may contribute to an abnormal spatial activation of the ventricles in the absence of Cx40, which normally provides a direct conduction pathway.

Important data about the role and regulation of gap junctions in the heart under pathological conditions were obtained during clinical investigations. For example, acute ischemia has been shown to lead to the uncoupling of cardiac muscle cells. This blockage was normally induced by a perturbation of the intercellular ionic balance and a loss of ATP [Wu et al., 1993; Dekker et al., 1996]; it seems to represent a protective mechanism in order to isolate the ischemic area and to prevent energy dissipation. The local disruption of cell coupling may contribute to the development of arrhythmia during the late phase of ischemia. Together with other factors it leads to a reduction in conduction velocity and to increased local inhomogeneity in action potentials [Gottwald et al., 1998].

Both the number and the arrangement of gap junctions are altered along the edges of infarct in dogs. The polarised distribution of gap junctions is lost during the active phase of the healing of damaged ventricular myocardium resulting in the remodelling of ventricular conduction pathways [Dillon et al., 1988]. In addition, the amount of Cx43 was found reduced three months after infarction [Saffitz et al., 1994]. In hypertrophied myocardium from chronically pressure loaded human left ventricles, Cx43 expression per myocyte was found to be not significantly different from normal, but was reduced by 40% per myocyte unit volume [Peters, 1996]. Subsequently, the changes in the extent of cellular coupling between cardiomyocytes leads to a slowing of conduction and probably contributes to the arrhythmogenic substrate in the chronic phase of ischemic heart disease.

Infection of cardiomyocytes with Trypanosoma cruzi induces Chagas disease, which is often associated with abnormal conduction in the heart. Pathogens suppress the Cx43 expression in the cells, which results in the reduction of cell coupling and cardiac dysfunction [Campos de Carvalho et al., 1994].

2.7 The Pharmacological Importance of Gap Junctions in the Heart

The blocking or activation of gap junctions may influence heart function under normal and pathological conditions. However, there are no drugs available that directly and specifically target gap junction proteins. Therefore, this chapter summarises different approaches which can be used to modulate gap junctions by natural or synthetic pharmacological agents.

There are several ways to affect gap junctions in the heart. They usually include the usage of 1) lipophilic drugs which directly interact with cell plasma membrane, 2) adrenergic stimulators coupled to down-stream protein kinases involved in signal transduction, 3) biologically active peptides, 4) genetic manipulation.

Since Johnson et al. [1980] first described the uncoupling action of higher linear alcohols on gap junctions between nerve cells, many lipophilic compounds have been shown to block gap junctions between the heart cells as well. Among them are heptanol, octanol, halothane, enflurane, long-chain fatty alcohols and acids. These substances can be used to reduce gap junction coupling so that the single channel events can be observed and characterised. However, it is important to note that the alcohols listed above can inhibit the Na^+ current and interfere with the Na^+/Ca^{2+} ionic exchange in cardiac tissue. Therefore, they should be carefully used in pharmacological experiments. The most specific drugs for gap junctions are palmitoleic and arachidonic acids. It has been found empirically that they reduce g_j at micromolar concentrations without affecting the unitary conductance. It is interesting that testosterone and 17β-estradiol derivatives in the concentration range 1 to 25 mM have been seen to reduce membrane fluidity and interrupt gap junction communication in rat ventricular myocytes in culture [Verrecchia, 1997]. Therefore, they may, like several other junctional uncouplers (e.g. heptanol), interfere with the plasma membrane structure, leading to perturbation of junction channel conformation with accompanying effects on channel functions.

Stimulation of β-adrenoreceptors by adrenalin or isoproterenol enhances gap junction coupling in cardiac cell pairs [De Mello, 1989]. Recently it has been also reported that stimulation of α-adrenergic and β-adrenergic receptors has an opposite influence on junction conductance in pairs of adult rat cardiomyocytes [De Mello, 1997]. For example, phenylephrine (10^{-6} M) reduced g_j by 45% within 2 min. via the PKC-dependant mechanism, whereas norepinephrine (10^{-6} M) or epinephrine (10^{-6} M) increased g_j by 56% and 3.6%, respectively. Their effects were larger if the α-1 adrenergic receptor was blocked with prazosin (10^{-6} M).

These results indicate that α-adrenergic receptor activation reduces g_j and interacts with β-adrenergic stimulation on junction conduction.

Acetilcholine is an important transmitter produced by parasympathetic synapses in the heart. The application of the parasympathomimetic drug carbacol led to the reduction of cellular coupling in cultured neonatal cardiomyocytes [Takens-Kwak and Jongsma, 1992]. The effect of carbacol was antagonised by the addition of alkaline phosphatase to the pipette filling solution used for the whole cell-patch clamp experiments. This fact suggests the involvement of a cytosolic phosphatase in the maintenance of the stable level of gap junction coupling between cardiac cells at least in vitro.

Angiotensin II is a mammalian hormone whose concentration in the blood inceases during heart hypertrophy. This biologically active octapeptide has been shown to reversibly reduce the cardiomyocyte cell coupling at concentrations higher than 10 nM. This effect could be suppressed by the inhibition of PKC and by the angiotensin receptor agonist DuP753. Some evidence points to the existence of an intracellular angiotensin system and receptors involved in the regulation of g_j in cardiomyocytes [De Mello, 1994]. Therefore, the specific inhibition of the angiotensin-converting enzyme could be an approach to prevent the uncoupling effect of angiotensin II in cardiac diseases.

Fibroblast growth factor-2 is an endogenous growth-promoting protein present in the heart in all developmental stages. It is believed to be involved in the processes of myocardial cell growth, differentiation, tissue angiogenesis and remodelling [Kardami et al., 1995]. It has been shown that the expression of FGFs is increased in hearts after myocardial infarction, especially at the borders between healthy myocytes and scar tissue where the postinfarction arrhythmia originates [Padua et al., 1993]. FGF-2 reduces coupling between neonatal cardiomyocytes in culture by inducing Cx43 phosphorylation within 30 minutes after administration [Doble et al., 1996]. Therefore, it may be that the blockage of intercellular communication plays a protective role during the initial phase of the heart injury, allowing the isolation of the damaged zone of tissue and preventing the enlargement of the ischemic area.

A newly emerged area in the field of cardiovascular drug development is the study of anti-arrhythmic synthetic peptides (AAPs) whose natural analogues were first isolated from bovine atria; they have been shown to enhance the synchronisation of the embryonic chick cardiomyocyte contraction in culture [Aonuma, 1980]. Recently a number of synthetic analogues were developed by Dhein et al. [1994]. Among them, AAP10 (NH2-Gly-Ala-Gly-4Hyp-Pro-Tyr-CONH2) exhibiting a semicyclic horseshoe-like molecular structure, seems to be the most

effective in the reduction of sustained ventricular fibrillation in the ischemic myocardium [Dhein , 1998]. AAP10 can enhance intercellular coupling in pairs of adult guinea-pig myocytes at nanomolar concentration [Mueller et al., 1997a]. The substance has been shown to bind to the specific membrane associated receptor and act via a PKC mediated mechanism [Dhein , 1998]. AAP10 also prevents a blockage of cell coupling in hypoxic heart tissue and may be an effective agent in treating arrhythmia [Mueller, 1997b].

In the future, the usage of genetic approaches such as overexpression of particular connexins may also be a way for the therapy of heart diseases that involve cellular uncoupling.

3. Long-term Primary Culture of Adult Rat Ventricular Cardiomyocytes

Dissociated adult ventricular cardiomyocytes serve frequently as an experimental system in several cardiological research disciplines. An advantage of the primary cell culture is that cells are fully differentiated and represent the cardiac phenotype, but lack interstitial tissue and other cell types, which can complicate measurements in whole tissue or animal models. Enzymatic digestion of ventricular tissue with type II collagenase yields single rod-shape cardiomyocytes (Fig.10 B). Establishment of the re-differentiated model for adult cardiomyocyte cultivation in the presence of 10-20% serum [Jacobson, 1977; Claycomb and Palazzo, 1980; Eppenberger et al., 1988] has allowed to maintain these terminally differentiated cells over several weeks in vitro.
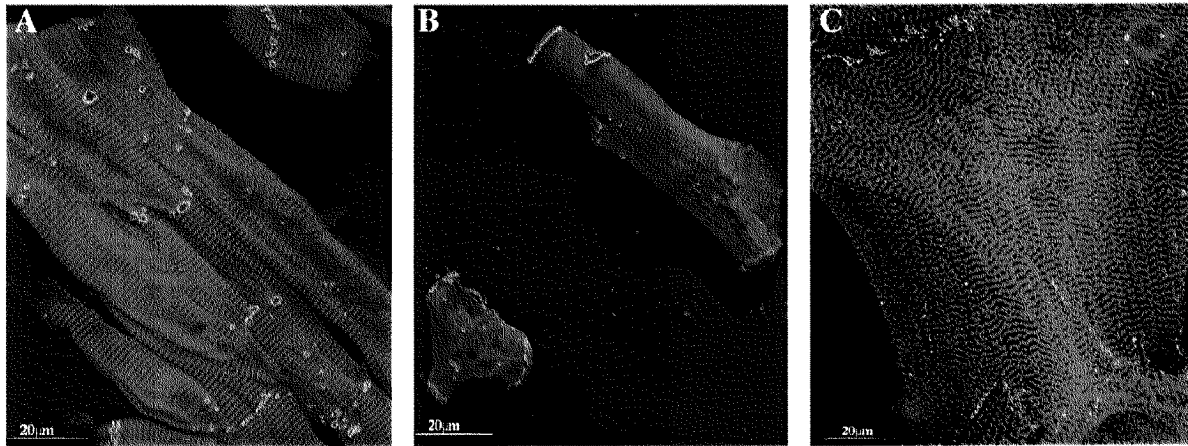
Fig. 10 Adult rat ventricular cardiomyocytes *in vivo* and *in vitro*

Cryosections of adult rat ventricle (a), freshly isolated cells (b), and cell cultures (c) were indirectly immunolabelled for Cx43 (green) and myomesin (red). Processing and 3-D reconstructions of confocal images were performed using the software Imaris.

During the first two days in serum-containing medium, the cardiomyocytes attach to the substratum and undergo complex modifications, which lead to spreading and re-differentiation. The cells grow in size, change from elongated cell shape to a polymorphic one, establish new cell-cell contacts, and form tissue-like sheets within several days with no signs of cell migration or cell division (Fig.10 C). Eventually they exhibit spontaneous rhythmic activity. These transformations resemble the processes associated with the adaptive enlargement of myocytes during cardiac hypertrophy that may occur as a result of cardiac dysfunction [Izumo et.al., 1987; Woodcock-Mitchell et al., 1989; Eppenberger-Eberhardt et al., 1990 and 1993; Chien et al., 1991; Boheler et al., 1992]. Hypertrophy is delineated from maturational growth by a number of characteristic changes in gene expression. These include the expression of immediate early genes [Dunnmon, 1990], some of which (c-fos, c-jun, Egr-1) encode transcription factors, re-expression of "foetal" ventricular myocyte genes (ANF, α-MHC, skeletal muscle α-actin) [Eppenberger-Eberhardt et al., 1990; Eppenberger-Eberhardt et al., 1993] and up-regulation of constitutive genes encoding myofibrillar proteins (MLC-2, cardiac muscle actin) [Tokola, 1994]. Therefore, detailed analysis of the heart cell re-differentiation in vitro provides information about the mechanisms involved in the remodelling of injured and hypertrophied myocardium. In addition, cardiomyocytes of adult rats in long-term culture represent a suitable model to study the regulatory mechanisms underlying the re-establishment of intercellular contacts and impulse propagation during heart failure treatments and tissue repair processes [Hertig et al., 1996].

4. The p70S6 Kinase and the Cell Growth

The phosphorylation of ribosomal protein S6 is a rapid and highly conserved cellular growth response that is observed during development and reaction to a variety of mitogenic and oncogenic stimuli [Decker, 1981]. This phosphorylation is correlated with regulation of translation of mRNA transcripts that contain a polypyrimidine tract at their transcriptional start site (5'TOP mRNAs) [Jefferies et al., 1997]. Although these transcripts represent only 100-200 genes, they can encode up to 20% of the cell's mRNA. This class of mRNAs code for many of the components of the protein synthetic apparatus [Meyuhas et al., 1996]. Failure to recruit these messages into polysomes suppresses the biogenesis of translational machinery required for cell cycle progression [Nasmyth, 1996].

Many protein kinases have been reported to phosphorylate S6 in vitro. However, based on the mode of activation and the ability to generate S6 phosphopeptide maps equivalent to those observed in vivo, only the mitogen-activated p70S6 kinase from mammalian cells [Jenoe et al., 1988] appear to be relevant.

4.1   Structure and Regulation of the Kinase

The p70S6 kinase is responsible for the phosphorylation of the 40S ribosomal protein S6 in mammalian cells representing the only identified well-recognised substrate [Proud, 1996]. The two isoforms of the enzyme, denoted p70S6 (αII) and p85S6 (αI) are generated from a single gene by alternative mRNA splicing and the use of an alternative translational start site [Grove et al., 1991]. The two isoforms are co-ordinately regulated and only differ by 23 amino acids at the amino terminus, where p85S6 contains a polybasic nuclear-localisation motif consisting of six consecutive arginine residues immediately after the initiator methionine residue. This segment is also responsible for the aberrantly slow mobility of the p85S6 isoform upon SDS-PAGE. The p85S6 is consequently located in the nucleus, whereas the p70S6 is predominantly cytoplasmic [Reinhard et al., 1994]. Little is understood concerning the role of the p85S6 in cell cycle progression. However, it is noteworthy that S6 is present in a free form in the nucleus and becomes phosphorylated at the same residues in response to mitogens as its cytoplasmic counterpart [Franco and Rosenfeld, 1990].
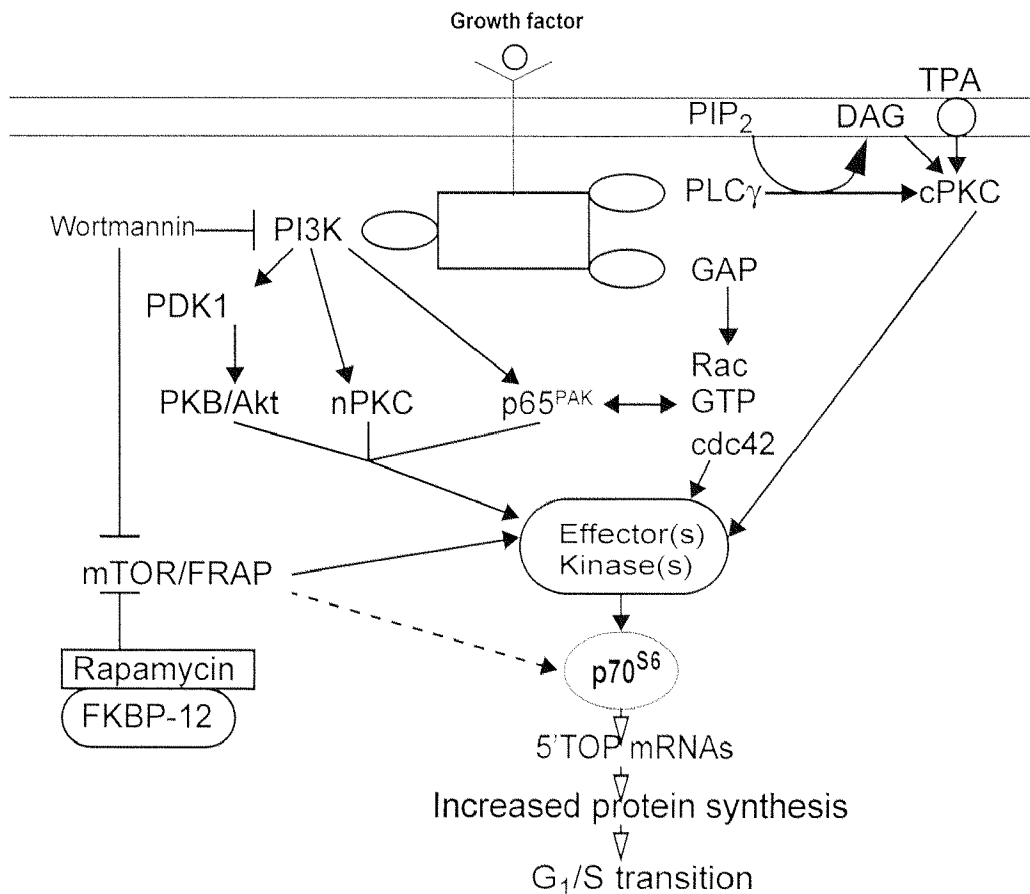
Fig. 11 The signalling pathways involved in the regulation of p70S6 activity

p70S6 is activated by phosphorylation at multiple sites. The phosphorylation of p70S6 is a complex process including multiple signal transduction cascades. The p85S6 is regulated in a co-ordinated fashion [Ming et al., 1994]. A huge number of experimental results obtained during the last decade demonstrated that p70S6 can be activated by virtually all mitogenic stimuli, including growth factors, cytokinases, phorbol esters, and oncogene products in different cell type [for a review see Chou and Blenis, 1995]. Combination of various experimental approaches provide clear evidence that activation of p70S6 is involved in the regulation of protein synthesis and is important for cell progression through G1. Accordingly, inhibition of p70S6 activation by microinjection of neutralising antibodies [Chung et.al., 1992] or by treatment of cells with the immunosupressant rapamycin, which selectively blocks p70S6 activation [Price, 1992], severely suppress cell cycle progression.

Rapamycin is a bacterial macrolide which depending on the cell type examined either abolished or severely inhibits the ability of cells to progress through the G1 phase of the cell

cycle [Lane et al., 1993]. At the molecular level, the inhibitory effects of rapamycin have been linked to its ability to selectively inhibit p70S6. The inhibitory effects of rapamycin are highly specific, as the kinase most closely related to p70S6, the 90kDa ribosomal S6 kinase (RSK), is resistant to the drug [Chung et al.,1992]. The inhibitory action of rapamycin is mediated by association with its cellular receptor, FKBP12 (FK506-binding protein), a peptidyl prolyl-isomerase (PPI) [Koltin et al., 1991]. This rapamycin-FKBP12 complex in turn targets a second protein, which is called TOR in yeast and mTOR, FRAP or RAFT1in mammalian system. Cloning of the yeast and mammalian homologues of TOR has revealed that these proteins are members of a novel family of PI kinase related kinases which contain a C-terminal lipid kinase domain, although no related lipid kinase activity has been demonstrated yet for any member [Hunter, 1995]. The scheme describing the signalling pathways that regulate the p70S6/p85S6 activation upon mitogenic stimulation is shown in Fig.11. It summarises derived from the most recent studies the major data consistent with this model.
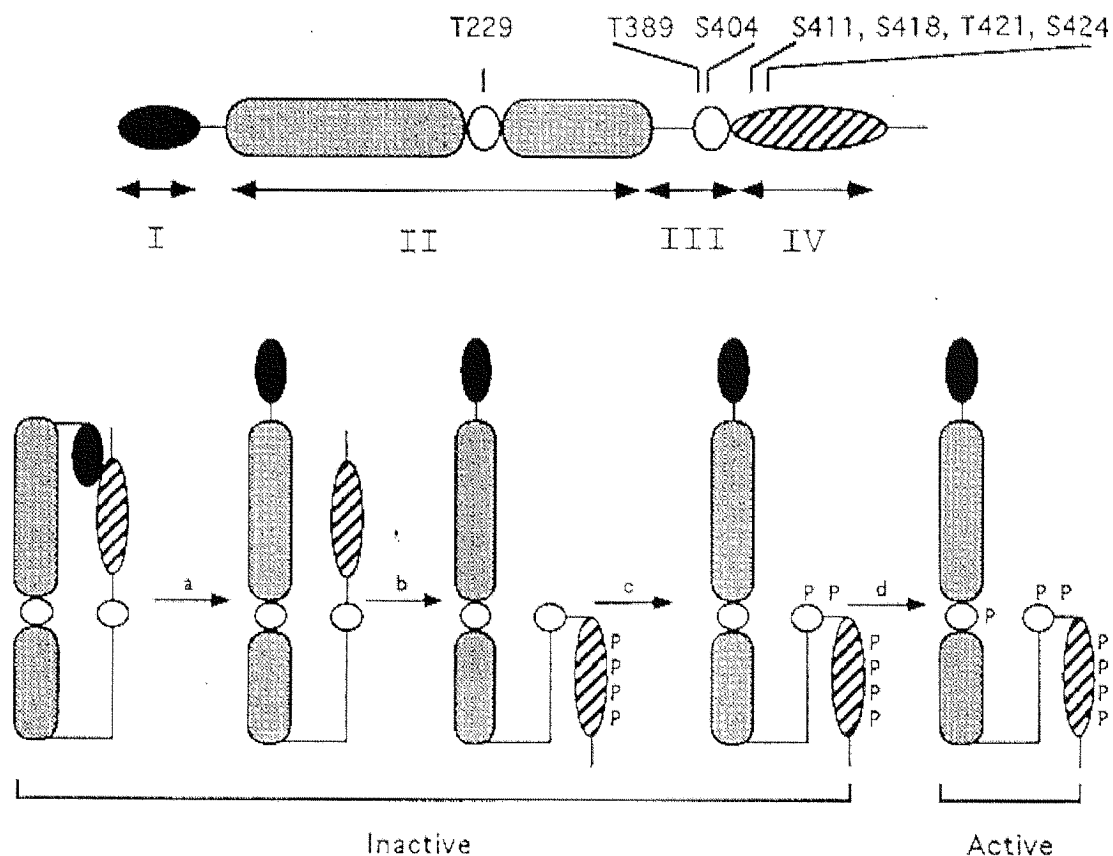
Fig. 12 Structural organisation of the p70S6 molecule

(from Pullen N. and Thomas G.(1997). "The modular phosphorylation and activation of p70S6". FEBS Letters. 410:78-82)

The p70S6 molecule can be roughly divided into four functionally significant domains or modules (Fig.12) [for a review see Pullen and Thomas, 1997]. Domain I extends from the N-terminus to the beginning of the catalytic domain and confers rapamycin sensitivity to p70S6 [Weng et al., 1995]. Domain II is catalytic. It contains the conserved acute site of mitogen-induced phosphorylation in the activation T-loop. Domain III links the catalytic domain with the carboxyl tail and contains two additional phosphorylation sites, which are essential for the kinase activation. All three sites are conserved in many members of the AGC family of Ser/Thr kinases and the calmodulin dependent protein kinase family [Pearson et al., 1995]. Domain IV is the autoinhibitory domain, which has significant homology with the substrate region of S6, and four closely clustered phosphorylation sites [Ferrari et al., 1992]. Activation of the kinase requires hierarchical phosphorylation of all these sites, culminating in the phosphorylation of the threonine in position 229 (Thr229) in the catalytic domain [Han et al., 1995]. The four-step model of the p70S6 activation process (Fig.12) predicts that at first a functional interaction between N-terminal and autoinhibitory domains is broken by mTOR/FRAP-mediated phosphorylation of the S/T-P sites in the autoinhibitory domain. This event allows a mitogen-activated kinase to phosphorylate Thr389, and in turn, propagate phosphorylation of Thr229 in the T-loop leading to the full activation of the enzyme. Recently a newly described kinase termed PDK I (a multifunctional effector downstream of the PI 3-kinase) has been demonstrated to selectively phosphorylate p70S6 at Thr229 thus mediating the last key step resulting in the 100% activation of the S6 kinase in vitro [Pullen et al., 1998]

4.2 The p70S6 Kinase in the Heart

Cells usually enter the cell cycle in response to a growth signal. Therefore, cell growth and proliferation are usually linked. However, cell growth is defined as the accumulation of mass (general protein synthesis), which does not necessarily lead to proliferation. Terminally differentiated mammalian cardiomyocytes lose the ability to proliferate soon after birth, so that the major contributor to postnatal enlargement of the mammalian heart is an increase in size (hypertrophy) of a fixed number of cardiomyocytes [Rakusan, 1984].

Studies with intact hearts both in vivo and in isolated perfused preparations as well as with neonatal and adult cardiomyocytes in cell culture have demonstrated that cardiac hypertrophic growth is the result of increased protein accumulation. This has been shown to be the result of an increased rate of protein synthesis, with relatively little change in the steady-state level of protein degradation [Morgan et al., 1992]. Available evidence indicates that at least 80-90%

of existing ribosomes in non-growing adult hearts are in the form of polysomes (i.e., they are already engaged in synthesising proteins) [Siehl et al., 1987]. Therefore, the availability of translation components and the rate of peptide chain initiation do not appear to be limiting to growth. Hypertrophy associated with the administration of thyroid, adrenergic hormones, phorbol esters (TPA as the most explored model) or hypertrophic response to pressure overload, is associated with increased cardiac ribosomal RNA content, RNA synthesis and accelerated ribosome formation [Zahringer and Klaubert, 1982; Morgan et al., 1987; Fuller et al., 1990; Bastie et al., 1990; Allo et al., 1991]. These data clearly demonstrate that an increase in ribosome content is an early, significant event that occurs during the hypertrophic growth of the heart. The p70S6 kinase represents one of several enzymes involved in the control of the ribosome formation and initiation of protein translation. Therefore, the examination of its regulation during the growth and re-differentiation of adult cardiomyocytes in vitro may help to elucidate mechanisms, which regulate cardiac hypertrophy.

Investigations performed so far aimed in this direction have been done using neonatal cardiomyocytes. It has been shown by Sadoshima and Izumo [1995] that the p70S6 kinase is activated by angiotensin II (AngII) and plays an essential role in the Ang II-induced increase in overall protein synthesis, but not in Ang II induced specific phenotypic changes in cardiac myocytes. It was later shown that Ang II activated p70S6 through AT1 receptors in cardiomyocytes [Takano et al., 1996]. Thus, Ang II contributes to the development of cardiac hypertrophy by activating p70S6. In addition, the activation of the p70S6 kinase has been demonstrated to be implicated in growth regulation of cardiac fibroblasts by PDFG-AA [Simm et al., 1997]. p70S6 also has the capacity to regulate gene expression. The results of Osawa et al. [1996] have demonstrated that a PI-3K/p70S6-dependent pathway is required for regulation of hexokinase II gene transcription by insulin in myotubes. The hexokinase facilitates the transport of glucose into cells and plays an important role in the energy supply in skeletal muscle, heart and adipose tissue. The work of Luo et al. [1996] has described the importance of the p70S6 activation for the transcription of the human mitochondrial NADP-dependent isocitrate dehydrogenase in lymphocytes after the mitogen stimulation. In the same study, heart and skeletal muscle have been shown to have the highest constitutive expression of the human mitochondrial NADP-dependent isocitrate dehydrogenase gene. The restricted expression of the gene in certain tissues suggests that this gene might have important functions in the heart, skeletal muscle, and activated lymphocytes. These last two observations indicate that p70S6 kinase may be involved in the regulation of other processes besides protein synthesis in the cells.

Objectives of the Study

The ability to isolate viable cells from heart tissue has enabled the cardiologists to study myocardial functions such as intracellular Ca^{2+} homeostasis, cell contractility, receptor properties, intracellular signalling mechanisms, excitation-contraction coupling, transport, and electrophysiology. In cardiac tissue, gap junctions are essential for the synchronization of the electrical activity of individual cells. The underlying mechanism involves propagation of the action potential from cell to cell by means of local circuit currents. Changes in the amount and spatial distribution of different connexins may lead to functional and developmental abnormalities of the heart [Reaume et al., 1995; Simon et al., 1998]. Alterations in the expression pattern and in the number of myocardial gap junctions also occur in ischemic and hypertrophic hearts where they contribute to the development of arrhythmia [Peters, 1996]. Therefore the investigation of intercellular communication between cardiomyocytes in culture represents a valuable way to obtain information on the electrophysiological behavior of intact cardiac tissue.

The aim of the studies presented in the first section of the thesis was to explore the functional consequences of the heart tissue regeneration investigating the expression and spatial distribution of the connexins during the re-establishment of the cell-cell contacts between adult rat ventricular cardiomyocytes in long-term primary culture. The first part of the work describes the dynamic of the cardiac connexin expression and phosphorylation during the growth and re-differentiation of adult rat ventricular cardiomyocytes in vitro. These results are compared with the data on the changes in the connexin phenotypes during the developmental hypertrophic growth of the heart in vivo.

Myocardial hypertrophic growth, characterised by an increase in the cell size , occurs during normal postnatal growth [Camacho et al., 1990], and as a concequence of pathologic conditions such as ischemia, hypertension and thyrotoxicosis in vivo [Chilian and Marcus, 1987] or as shown here during the cultivation of cardiomyocytes in the serum-containing media in vitro. The p70S6 kinase is the enzyme directly involved in the regulation of protein synthesis and transcription in the heart muscle cells under α_1-and-β_1-adrenergic stimulation [Simm et al., 1998]. Therefore, the experiments presented in the second part of the work were performed to investigate the role of the S6 kinase during the cardiac growth. In addition, the potential involvement of the p70S6 kinase in the signal transduction pathways leading to the connexin 43 phosphorylation in ARC was explored during the phorbol ester-stimulated activation of the enzyme.

Materials and Methods

1. Cell Culture

Methods Adapted and Further Developed in Our Laboratory [Eppenberger et al., 1988]

1.1 Isolation and Cultivation of Adult Rat Ventricular Cardiomyocyte (ARC)

Two main requirements for the isolation of viable adult cardiomyocytes are 1) prevention of tissue hypoxia during the isolation procedure; 2) avoidance of the "calcium paradox". The first problem was solved by maintaining the heart on an artificial circulation system, which provides an appropriate balance of salts, vitamins, amino acids, glucose, and dissolved oxygen at 37°C. Ventricular cardiomyocytes were isolated from the hearts of 2-month-old Sprague-Dawley-Javanovas rats by the retrograde perfusion method, where the perfusion medium enters the aorta and goes through the heart tissue via coronary arteries. Rats were anaesthetised with 0,35 ml 50 mg/ml Nembutal (Abbot Laboratories, IL, USA) / 200g body weight. While the rat slept, an incision was made below the diaphragm, the abdomen was opened and 0.2 ml 1000 i.e./ml heparin (Fresenius Medical Care AG, Switzerland) was injected into the vena cava to reduce the blood clots. The chest was opened by cutting up both sides of the rib cage and across diaphragm, pushing the "lid" of the chest up to fully expose the heart. The thymus, which appears like a pad over the heart, was removed with scissors to leave the aorta clearly in sight. The aortic arch was then cut with scissors; the heart was lift out and cut away from the body. The heart was immediately immersed in ice-cold M-199 medium (AMIMED AG, Switzerland) and quickly rinsed free of blood. The cannula, attached to the Langendorff perfusion apparatus was inserted into the aortic opening and the perfusion of the heart with the Ca^{2+}-free Joklik's medium (Cell Culture Technologies, Switzerland) was started. The aorta was tied to the cannula with cotton threads. Four hearts were used for every preparation (Fig.13). They all were simultaneously perfused with the Ca^{2+}-free Joklik's medium for at least 10 minutes at 37°C in order to dissociate the Ca^{2+} dependent contacts between cardiomyocytes. This first perfusion step was followed by 35-min perfusion with Joklik's medium containing 115 units/ml collagenase type II (Worthington Biochemical Corp., Freehold, NJ, USA). After removal of the atria, connective and valvular tissue, the left ventricle was opened

by an incision along the anterior free wall and the interventricular septum was dissected away. The ventricular wall tissue was then cut into few pieces, washed with Kraftbruehe (KB) solution (70 mM KCl, 30 mM K_2HPO_4, 22 mM glucose, 5 mM $MgSO_4*7H_2O$, 0.5 mM EGTA, 20 mM taurin, 5 mM creatin, 2 mM sodium pyruvate, 10 mM succinate, 5 mM Na-ATP, 2 mM 2-hydroxybutyric acid, pH 7.4) and finely chopped with scissors. The minced tissue was put into a siliconised Erlenmeyer flask with a screw cap and further digested in 5 ml per one heart KB solution containing 110 units/ml collagenase. The digestion has been performed for 10 minutes in a 37°C water bath under constant shaking by hand. The cell suspension was filtered through a 200 mm nylon filter and centrifuged at 70 g for 2 minutes. The resulting cell pellet was washed with Joklik's medium containing 0,5 mM $CaCl_2$. Thus, $CaCl_2$ was reintroduced gradually to intact cardiomyocytes. This step of calcium adaptation helps to avoid the "calcium paradox" — an irreversible cell damage during the transition from the Ca^{2+}-free solutions to the cell culture medium with physiological Ca^{2+} concentrations. Following an hour incubation in the M-199 medium supplemented with 0,1% FCS (Gibco Laboratories, Grand Island, NY, USA) and 5 mM creatine (Sigma Chemical Co., St.Louis, MO, USA) in the uncoated 100 mM Petri dishes (Nunc, Life Technologies AG, Switzerland), cardiomyocytes were suspended in culture medium M199 (AMIMED AG, Basel, Switzerland) supplemented with 20 mmol/L creatine (Sigma Chemical Co., St.Louis, MO, USA), 1% penicillin-streptomycin (Gibco Laboratories, Grand Island, NY, USA) and 20% FCS (Gibco Laboratories, Grand Island, NY, USA). Fibroblast growth was suppressed by addition of 10 µM cytosine arabinoside (Sigma, Chemical Co., St.Louis, MO, USA) to the growth medium. Plastic Petri dishes (Nunc, Life Technologies AG, Basel, Switzerland) were coated with 0.1% gelatine solution (Fluka, Switzerland) and air-dried during 4h at room temperature. The cell suspension was diluted to a density of $4*10^5$ viable cells/ml. Aliquots of the defined volume were plated into the cell culture dishes. Medium change was done after 2 and 7 days.

1.2 Drug Treatment

Starting on day 7 of culture, cardiomyocytes were incubated in the medium containing 200 nM phorpbol 12-myristate 13-acetate (TPA) for a week. 2 mM stock solution of TPA (Sigma, Buch, Switzerland) in dimethyl sulfoxide (DMSO) (Fluka, Switzerland) was added to the cell culture medium every 2 days and the final concentration of DMSO in each dish was 0.001%.

Rapamicyn (Calbiochem-Novabiochem Co., USA) was used to block the effect of TPA in cultured cardiomyocytes. Rapamycin was added every day from day 9 on to the culture medium of TPA treated and untreated cells at a final concentration of 0.1 nM. Stock solution of rapamicyn in DMSO (Fluka, Switzerland) was used and the concentration of DMSO in the cell culture medium was 0.001%.
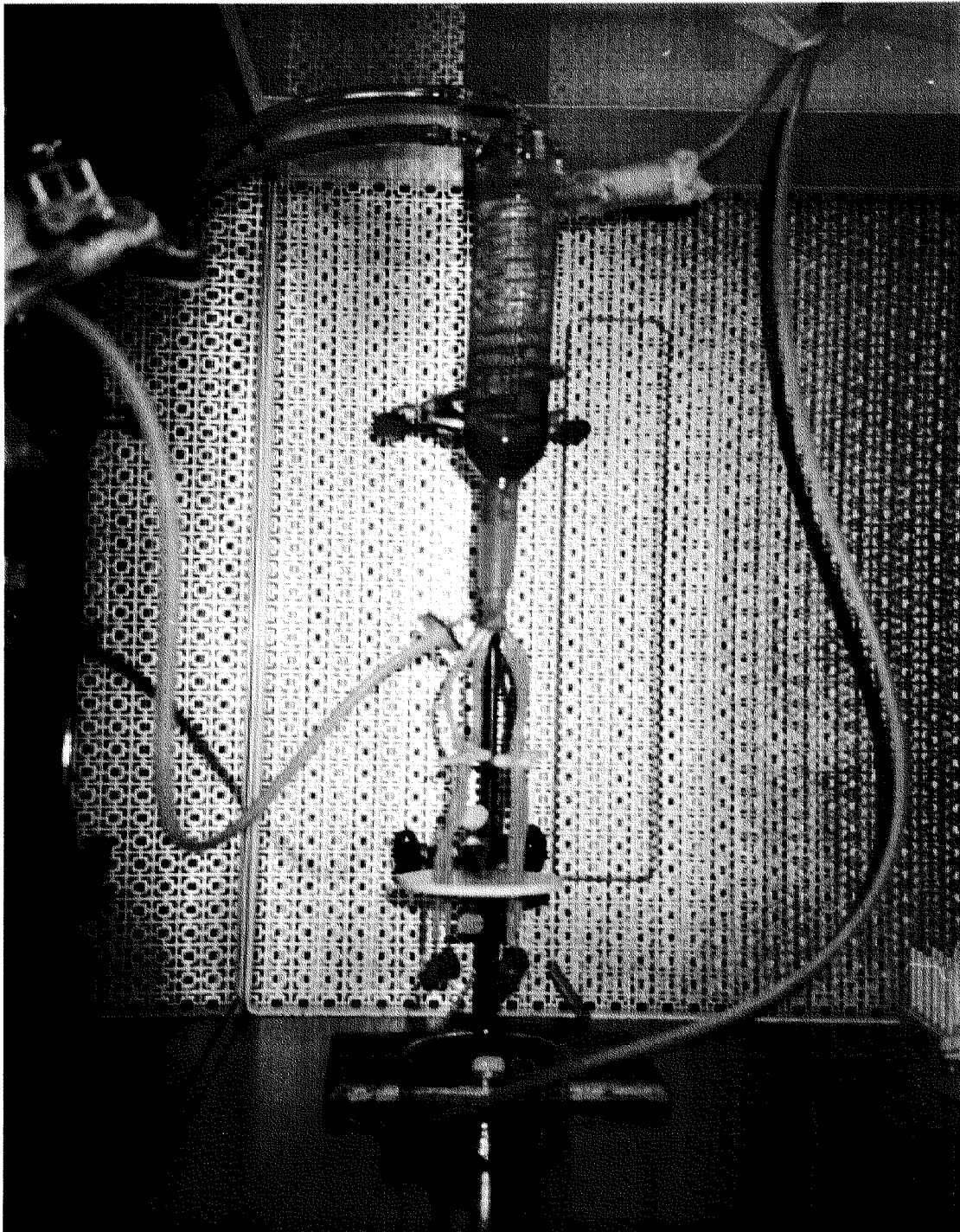
Fig.13 System for Perfusing the Rat Hearts

1.3 Ca²⁺-Depletion Experiments

7-day-old ARCs were incubated in Joklik's medium (Cell Culture Technologies, Switzerland) containing 5 mM EGTA for 3 hours at 37°C. Subsequently cells were washed and kept for 1 hour in Joklik's medium at room temperature to inhibit the protein sorting and allow the protein turnover at former sites of cell contacts. The disruption of the intercellular contacts was monitored visually and ARC were collected for the protein analysis or fixed for immunofluorescence at the indicated time points. To recover the Ca^{2+}-dependent intercellular contacts between cardiomyocytes, ARC were incubated in the standard cell culture medium at +37°C overnight [Hertig et al., 1996].

1.4 Isolation and Cultivation of Neonatal Rat Cardiomyocytes (NRC)

Hearts of new-born rats at postnatal day one were dissected and the ventricles were used to isolate cells by enzymatic digestion with 110 units/ml collagenase type II (Worthington Biochemical Corp., Freehold, NJ, USA) and 0.6 mg/ml pancreatin (Gibco BRL, Grand Island, NY, USA) in ADS buffer (120 mM NaCl, 20 mM HEPES, 1 mM NaH_2PO_4, 5 mM glucose, 5 mM KCl, 0.8 mM $MgCl_2$, pH 7.4). After isolation, cardiomyocytes were purified from other cell types by centrifugation in Percoli gradient and plated in Petri dishes (Nunc, Life Technologies AG, Switzerland) coated with 0.1% gelatine (Fluka, Switzerland). The plating medium consisted of 68% Dulbecco's MEM (AMIMED AG, Switzerland), 17% medium M199 (AMIMED AG), 10% horse serum (Gibco BRL, Grand Island, NY, USA), 5% FCS (Gibco BRL), 200 mM glutamine (AMIMED AG) and 1% penicillin/streptomycin (Gibco BRL). After one day, the medium was replaced by maintenance medium containing 78% Dulbecco's MEM (AMIMED AG, Basel, Switzerland), 20% medium M199 (AMIMED AG), 1% horse serum (Gibco BRL), 200 mM glutamine (AMIMED AG), 1% penicillin/streptomycin (Gibco BRL) and 10^{-4} mM phenylephryne (Sigma Chemical Co., St.Louis, MO, USA).

1.5   Isolation and Cultivation of Embryonic Rat Cardiomyocytes (ERC)

14-day pregnant Sprague-Dawlea-Javanovas rat was anaesthetised with 0,35 ml 50 mg/ml Nembutal (Abbot Laboratories, IL, USA) / 200g body weight. The uterus with embryos was cut out and kept in medium M199 on ice. The embryos were taken out, their hearts were dissected and collected in ADS buffer (120 mM NaCl, 20 mM HEPES, 1 mM NaH$_2$PO4, 5 mM glucose, 5 mM KCl, 1 mM MgSO$_4$, pH 7.4). Ventricle tissue was minced and digested with 110 units/ml collagenase type II (Worthington Biochemical Corp., Freehold, NJ, USA) and 0.6 mg/ml pancreatin (Gibco) in ADS buffer. The cell suspension was filtered through the Nylon filter and centrifuged at 80g for 6 minutes. The cells were cultivated under the same conditions as those described for the neonatal rat cardiomyocytes. Glutamine was left out of the cell culture medium in order to prevent fibroblast overgrowth.

2.   Cell Fractionation

2.1   Isolation Cytoplasmic and Membrane Fractions

ARC cultured for 2 weeks were washed three times with ice-cold PBS and collected in 50 mM β-glycerophosphate buffer (pH 7.4), containing 250 mM sucrose, 1 mM EGTA, 0,34 mM CaCl$_2$ (calculated to give a free Ca^{2+} concentration approximately 100 nM), 1 mM PMSF and 10 mg/ml leupeptin. Cells were homogenised by 15 strokes of a Polytron homogeniser (Kinematika AG, Switzerland), lysed by a cycle of freeze-thawing and sonificated on ice for 5 minutes in the ultrasound bath (Transsonic Digitals) at 140% power. The homogenate was centrifuged at 100 000 g for 15 min, and the supernatant was saved as the cytosolic fraction. The pellet was resuspended in 50 mM β-glycerophosphate buffer (pH 7.4), containing 1 mM EGTA, 1% Triton X-100, 1 mM PMSF and 10 mg/ml leupeptin, and incubated on ice for 1 hour. After centrifugation at 100 000 g for 15 min, the supernatant was collected and saved as the membrane fraction. The purity of the cytoplasmic and membrane fractions has been evaluated by assaying for the activity of marker enzymes. Before loading on SDS-PAGE, samples of the cytosolic and membrane fractions were mixed with Laemmli electrophoresis buffer (50 mM Tris-HCl pH 6.8, 10% glycerol, 2% SDS, 5% b-mercaptoethanol, 0,005% Bromophenol blue).

2.2 Isolation of Nuclei

Cultures were placed on ice, washed twice with cold PBS saline, and rinsed once in a Buffer I containing 10 mM Tris-HCl, pH8.0, 10 mM NaCl, 2.5 mM $MgCl_2$, and 5 mM DTT. The dishes were scraped with the same buffer (0.5 ml per 100 mm dish) and incubated on ice for 15 minutes. Cells were gently homogenised by passaging through the 22G needle. An equal volume of the Buffer I supplemented with 0.6M sucrose and 0.6% Triton X-100 was added to the cell suspension, which was layered over an equal volume of Buffer I containing 0.6M sucrose and centrifuged at 1500g for 10 min at +4°C. The nuclear pellet was resuspended in 50 mM Tris-HCl, pH 8.0, 5 mM $MgCl_2$, 0.1 mM EDTA, and 20% glycerol and pelleted by centrifugation at 1500g for 10 min. The nuclear pellet was resuspended in Laemmli buffer prior to loading on SDS-PAGE

3. Marker Enzyme Assays

3.1 Alkaline Phosphodiesterase I: Plasma Membrane Marker

The reaction mixture consisting of one part of 10 mM sodium thymidine 5'-monophosphate, p-nitrophenyl ester (Sigma, Switzerland) substrate solution, one part of 0.1M Tris-HCl buffer (pH 9), and two parts of water was warmed up to 37°C. Samples of the membrane or cytoplasmic fractions containing 10 mg of the total protein were added to the reaction mixture and incubated at 37°C. Three samples of each fraction were prepared and analysed in parallel. After 2 hours, the reaction was stopped by addition of 1 ml of 0.5M glycine/0.5M sodium carbonate buffer to the tubes containing membrane proteins. The absorbance was read at 410 nm. The samples of the cytosolic fraction were incubated overnight to allow readings well enough above background. Enzyme activity was expressed as absorbance units/ minute.

3.2 Lactate Dehydrogenase: Cytosol Marker

1 ml of the reaction mixture was prepared combining 0.02 ml NADH solution (10mg/ml in water), 0.5 ml of Trap 450A (10 mM triethanolamin, 20 mM EDTA, pH7.6), 0.45 ml H2O and 0.01 ml of the cytosolic or membrane sample containing 10 mg of the total protein. The reaction was started by addition of 0,02 ml of 120 mM sodium pyruvate and the decrease in absorbance was monitored at 340 nm at room temperature. Enzyme activity was expressed as

decrease in absorbance units/minute. Triple sets of identical samples were analysed for each reaction.

4. Protein Analysis

4.1 Preparation of Whole Cell Lysates

Cells were washed with TBS and scraped from the dish or put directly after isolation in an extraction buffer containing 62,5 mM TRIS-HCL (pH6.8), 20% SDS, 10 mM EDTA, 5% glycerol, 700 mM b-mercaptoethanol and 1 mM PMSF. The lysates were boiled for 5 min and centrifuged at 13000g for another 5 min at RT. The supernatant was taken and used for SDS-PAGE protein analysis. Laemmli sample buffer (50 mM Tris-HCl pH 6.8, 10% glycerol, 2% SDS, 5% b-mercaptoethanol, 0,005% Bromophenol blue) was added to the lysates prior electrophoresis.

4.2 Protein Determination

The protein content of the cardiomyocyte lysates was estimated with the Lowry method. 1 µl of the cell lysate was added to 500 µl of 10% TCA solution and left on ice for an hour. Precipitated proteins were collected by centrifugation at 13000g for 15 min at +4°C and the supernatant was discharged. The rest of TCA was carefully removed using small pieces of a filter paper. The pellet was solubilised by vortexing in 1 ml of 0.1 N NaOH containing 2% Na_2CO_3, 0.01% $CuSO_4$ and 0,02% K-Na-tartrat and incubated for 10 min at room temperature. 100 µl of a folin reagent (Merck, Germany) was added to the solution, which was then incubated at +60°C in water bath for 10 min. The absorbance at 750 nm was measured at room temperature and the amount of proteins was estimated using the standard curve, which was plotted using aliquots of 1mg/ml BSA solution in water.

4.3 Immunoblot Analysis

15-50 micrograms of total protein was loaded on and resolved by a 12,5% SDS-polyacrylamide gel using the Mini-PROTEAN II Electrophoresis Cell (BioRad,CA, USA). Proteins were electrically transferred to nitrocellulose membranes (Schleicher&Schuell, Germany) using Semi-dry blotting and visualised with Ponceau red. After blocking with a milk blocker

(40 mM TRIS, pH 7.5, 0.1% Tween-20, 4% (w/v) milk powder), they were incubated with primary antibodies. Secondary antibodies coupled to peroxidase (Cappel Research Reagents, PA, USA) were detected with the iodophenol/luminol reaction system.

4.4 Densitometric Analysis

Immunoblots were incubated for 90 seconds in the iodophenol/luminol reaction mixture and exposed to X-ray films for 1 minute to detect the chemiluminescent signals. Connexin bands were imaged on a ScanJetIIcx (Hewllett Packard) scanner. Pictures were digitised and analysed with the NIH Image1.61/fat software (Macintosh). After subtraction of the background grey scale values, the gray scale values of the connexin signals at defined time points were normalised to those in freshly isolated cells, which were assigned a 100% value. Statistical analysis of data was performed in Microsoft Excel. The results are presented as mean ± S.D.

4.5 Alkaline Phosphatase Treatment

15 µg of total protein from the cell lysates were resuspended in 0.5 ml of a phosphatase reaction buffer (50 mM Tris-HCl (pH 8), 10 Mm $MgCl_2$, 150 Mm NaCl and 1 mM PMSF) and treated with 5 units of alkaline phosphatase from calf intestine (1000 units/mg; Boehringer Mannheim, Germany). The reaction was carried out in the Slide-A-Lyzer cassettes (Pierce, USA) at 37°C for 3h while being dialysed against the buffer mentioned above containing 0.05% SDS, 1 mM $ZnCl_2$ and 0.35 g/L solid PMSF. For control samples 10 mM Na_3 -phosphate was added to the phosphatase reaction buffer. The reaction was terminated by addition of a 10% TCA solution and incubation on ice for an hour. After precipitation, proteins were washed twice with cold (-20°C) acetone and dissolved in 20 ml of Laemmli sample buffer. Samples were electrophoresed on 12,5% SDS gels and analysed by immunoblotting as described above.

4.6 Immunoprecipitation of Connexin 43

Immunoprecipitations were carried out at +4°C. Aliquots of the whole cell lysate obtained as described above (see Preparation of Whole Cell Lysates) containing 20 mg of total protein were diluted in 0.5 ml of an IP buffer (100 mM NaCl, 20 mM $Na_3B_4O_7$, 15 mM EGTA, 15

mM EDTA, 10 mM N-ethanolamid, 1.5% Triton X-100, 0.02% Na N$_3$, 1 mM PMSF, pH 8.5) and incubated with 5 µg of polyclonal anti-Cx43 antibodies for 2 h at +4°C on the rocking platform. To collect the antibody-antigen complexes, 50 ml of Protein A Plus/ProteinG Agarose beads (Calbiochem-Novabiochem Co., USA) were added and incubated with the lysates for another hour with gentle shaking. Immunoprecipitated proteins obtained after centrifugation at 2500 g for 4 minutes were washed five times with the IP buffer and subjected to SDS-PAGE and immunoblot analysis as described before.

5. p70S6 Kinase Assay

5.1 Preparation of Cell Lysates

After 7 days in culture ARCs were treated with TPA or rapamycin as described above (see "Drug Treatment") for one week in order to stimulate or inhibit the p70S6 kinase activity respectively. The cells were cultured in 100 mM Petri dishes (Nunc, Life Technologies AG, Switzerland). At least four of such dishes were used to purify sufficient amounts of the kinase. The dishes were placed on ice and washed three times with cold TBS. The cells on each plate were scraped into 0.5 ml of Lysis buffer A (50 mM TRIS-HCl pH 7.3, 120 mM NaCl, 15 mM pyrophosphate, 1 mM EDTA, 5 mM EGTA, 20 mM NaF, 1 mM benzamidine, 1% NP-40 and 1 mM PMSF) and homogenised with 15 strokes of a Polytron homogeniser (Kinematika AG, Switzerland). The homogenate was centrifuged at 13 000 g for 10 min at +4°C in a bench-top microfuge (Heraeus Instruments, Germany) followed by a high-speed centrifugation at 100000 g in a Beckman Airfuge (Beckman, USA) for 1.5 h at +4°C. The supernatants were frozen in liquid nitrogen and kept at − 80°C until required.

5.2 Purification of the p70S6 Kinase from Cultured Adult Rat Cardiomyocytes

Aliquots of the cell lysates containing 100 µg of total protein were diluted in 1 ml of Lysis buffer A and incubated with 5 µg of anti-p70S6 antibodies or control rabbit IgG for 2 h at +4°C. The immunocomplexes were incubated with 50 ml of Protein A Plus/Protein G Agarose beads for 1 h at +4°C with gentle shaking and then pelleted by centrifugation at 2500 g for

4 minutes. The immunoprecipitates were washed twice with Lysis buffer A containing 1% BSA, twice with the same buffer containing 1M NaCl, once with a dilution buffer (50 mM MOPS pH7.1, 10 mM $MgCl_2$, 2%(w/v) Triton X-100) and resuspended in 20 ml of the dilution buffer containing 1 mM DDT. The suspended immunocomplexes were assayed for the p70S6 kinase activity. To confirm that equal amounts of S6 kinase protein were immunoprecipitated in each reaction, aliquots of the samples were boiled with Laemmli electrophoresis buffer and subjected to SDS-PAGE analysis. The proteins were visualised by staining the gels with a GELCODE Blue Stain Reagent (Pierce, Socochim SA, Switzerland).

5.3 In Vitro Phosphorylation and S6 Peptide Assay

100 µl of the reaction mixture contained 25 mM TRIS-HCl (pH7.3), 50 mM EGTA, 5 mM Mg-acetate, 0.1% b-mercaptoethanol, 1 µg PKI, 100 µM ATP, 10 mCi [γ-^{32} ATP] and 10 µg of S6 peptide (RRLSSLRA; Calbiochem-Novabiochem Co., USA) or 10 µg of Cx43 peptide (GPLSPSKDCGSPKYAYFNGC; Zymed Laboratories Ltd, USA) were warmed up to +30°C and dispensed in the immunoprecipitates. After 30-min incubation at +30°C, the reaction was stopped by sedimentation of the kinase immunocomplex absorbed onto agarose beads. The equal aliquots of supernatant were spotted on 15*15 mm squares of p81 filter paper (Whatman, UK), washed 5 times for 10 minutes each in 75 mM (0.4%) phosphoric acid. After the final wash with acetone, the filter pieces were dried and counted by the Cerenkov technique.

6. RNA Analysis

6.1 RNA Isolation and Northen Blot Analysis

Total RNA was isolated from cardiac myocytes using the single step guanidinium thiocyanate-phenol-chloroform extraction method [Hood and Simoneau, 1989]. The RNA concentration was estimated by measuring absorbance at 260 nm. RNA samples (15 µg) were subjected to electrophoresis on a 1% agarose/formaldehyde gel containing 0.1 mg/ml of ethidium bromide, capillary blotted onto a nylon membrane (Boehringer Mannheim, Germany) and cross-linked to the membrane by UV light.

Blots were hybridised to the cDNA probe generously provided by Dr. Haeflinger (Department of Internal Medicine B, University Hospital; Lausanne) containing the entire coding region of Cx43 cDNA (Beyer et.al.,1987). The generation and detection of the alkaline phosphatase labelled cDNA probe was performed using an AlkPhos Direct kit from Amersham Life Science (Amersham Switzerland, Switzerlan). All standard protocols were followed exactly.

7. Immunocytochemical Analysis

7.1 Immunostaining Procedures

Ventricular cardiomyocytes were either directly fixed and permeabilised in methanol (5 min at $-20°C$) or fixed in 3% PFA (15 min at RT) and then permeabilised in 0,2% Triton X-100 (10 min at RT). The cells were incubated with primary antibodies (overnight at $+4°C$ or 1 h at RT), washed with PBS and exposed to the treatment with secondary antibodies for 1h at room temperature in the dark. The preparations were rinsed in PBS and mounted in galat-glycerol mounting medium.

7.2 Antibodies

A monoclonal antibody raised against residues 252-271 of rat Cx43 was from Zymed Laboratories Ltd (USA). A polyclonal antibody directed to a synthetic peptide corresponding to the amino acid sequence 314-322 of rat Cx43 was a generous gift of Dr. D. Gros (IBDM, Laboratoire de Génetique et Physiologie du Dévelopment, UMR C9943, Faculté des Science de Luminy, Marseille, France) [El Aoumari et al., 1990]. Polyclonal antibodies raised against mouse Cx45 and Cx40 were kindly provided by Drs. O. Traub (Institute for Genetics, University of Bonn Römerstrasse 164, D-53117 Bonn, Germany) [Bastide et al., 1993] and J.A. Haefliger (Department of Internal Medicine B, University of Lausanne Rue du Bugnon, CH-1011 Lausanne, Switzerland) respectively. The monoclonal antibody against myomesin was raised in the laboratory of Prof. H.M.Eppenberger (Institute for Cell Biology, ETH-Zurich, Switzerland). Anti-phosphoserine, anti-phosphothreonine and anti-phosphotyrosine monoclonal antibodies, as well as a monoclonal anti-α-actinin antibody (clone EA-53) were purchased from Sigma (USA). A polyclonal antibody, which recognises residues 482-501 at the C-terminus

of the p70S6 kinase, was obtained from Santa Cruiz (USA). A monoclonal antibody against ABL-70 glycoprotein of medial Golgi cisternal membrane were produced in the group of Dr. August (Dept. of Pharmacology and Molecular Science, Johns Hopkins University School of Medicine) and generously provided by Dr.Taylor (Institute for Cell Biology, ETH-Zurich, Switzerland). A monoclonal antibody recognising H-69 glycoprotein of rough endoplasmic reticulum [Hughe and August, 1981] were kindly given by Dr.Taylor (Institute for Cell Biology, ETH-Zurich). F-actin specific reagents phalloidin-RITC and phalloidin-Cy5 binding to all isoforms of actin were purchased from Molecular Probes (Germany).

The secondary antibodies FITC-coupled goat anti-mouse IgG and FITC-coupled goat anti-rabbit IgG were purchased from Cappel Research Reagents (USA). The secondary antibody TxRed-coupled goat anti-rabbit IgG was purchased from Jackson Immuno Research Laboratories (USA).

8. Confocal Microscopy and Image Processing

A laser-scanning confocal microscope equipped with an argon/krypton mixed gas laser (Leica TCS NT), fitted onto a microscope (Leica DMIRB-E, FL APO objective lens 63, N.A. 1.4), was used to obtain optical sections of the cells grown in culture dishes. Image processing was performed with a Silicon Graphics Workstation using the software Imaris (Bitplane AG, Switzerland) [Messerli et al., 1993].

9. Dye-transfer Assay

Intercellular coupling was assessed by the extent of Lucifer yellow (Sigma Chemie, Switzerland) transfer between cultured ARCs. Glass Femtotips with the inner diameter of 0.5 mm (Eppendorf, Germany) were backfilled with a 5% (w/v) solution of Lucifer yellow (Li^+salt) in the intracellular saline containing 120 mM KCl, 10 mM NaCl, 3 mM MgATP, 1 mM $MgCl_2$, 1 mM $CaCl_2$, 10 mM EGTA (pCa ~8) and 5 mM HEPES (pH 7.2). Cardiomyocytes were microinjected with the LY solution by 1s pressure pulses (P1= 1400 hPa, P2 = 350 hPa) with the help of Eppendorf's Microinjector and Micromanipulator (Germany). Dye injection of the 14-day-old cells were performed at room temperature, viewed with an epifluorescence and phase contrast microscopy with an Axiovert inverted microscope (Zeiss, Germany) and recorded using a CCD camera (Kappa, Videotek AG, Switzerland). 3 minutes after the Lucifer

yellow injection, the number of fluorescent cells were counted and used as an index of junctional transfer. 30 measurements were performed in control, TPA and/or rapamycin treated cultures in parallel. The results were reproduced in two different cell preparations. After microinjection, the cell density was controlled in every cell culture dish. Cardiomyocytes were incubated with a 0.25% trypsin solution in PBS (Sigma, Switzerland) at +37°C for 15 minutes. The number of cells was calculated using the "Assistant"-Hemocytometer chamber (Scherf Praezision, Germany).

10. Statistics

Statistical analysis of all data was performed in Microsoft Exel. The results were represented as mean ± SD from n different cell preparations. Student's t-test was used to evaluate the significance of the observed effects. Values P<0.01 were accepted to be significant.

Results

1. Expression and regulation of Connexins

1.1 Expression of Cx43

1.1.1 Northern Blot Analysis

Total RNAs from adult rat cardiomyocytes at different stages of their development in vitro were examined for Cx43 using a specific cDNA probe. Under stringent conditions, a single 3.0-kb band was clearly detected in all samples with the Cx43 probe (Fig.14). The results of Northern blot analysis demonstrated that the level of the Cx43 mRNA expression remained constant during the whole period of the adult ventricular cardiomyocytes growth in culture.
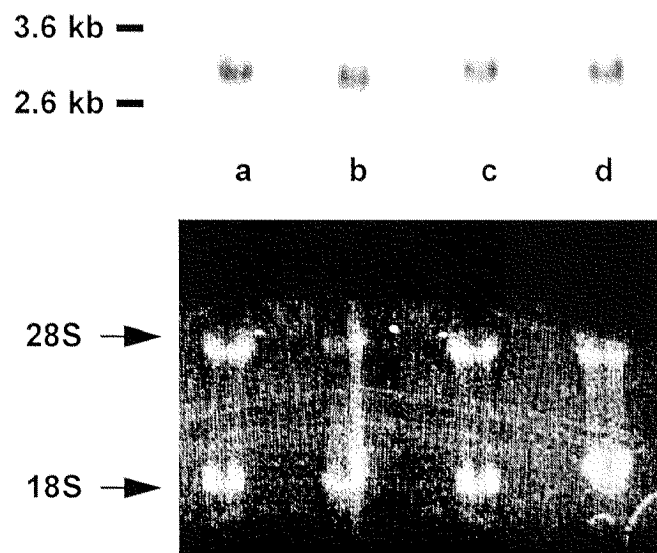

Fig.14 Northern Blot Analysis of Cx43

Total RNAs were isolated from freshly isolated adult rat ventricular myocytes (lane a) and from ARC at days 2(lane b), 7 (lane c) and 14 (lane d) of culture. The lower half of the figure shows ethidium bromide staining of 18S and 28S ribosomal RNAs in the samples before transfer to membrane.

1.1.2 Western Blot Analysis

Fig. 15 shows the results of the immunoblot analysis of ventricular cell lysates prepared at different times after isolation. At first, an epitope-specific polyclonal antibody directed against residues 314-322 of the cytoplasmic C-terminal domain of rat Cx43 was used for the immunoblot analysis (Fig. 15A). In the case of freshly isolated myocytes (a), the antibody recognised three bands migrating at 42, 45 and 47 kDa, respectively. After two days in culture, only the 42 kDa band was present (b). Subsequently, the 45-and 47-kDa bands reappeared gradually with time. First signs of a recovery were detectable after 4 days in culture (c). At around that time, the cells started to form synchronously beating clusters. After 8 days in culture, the 45 and 47 kDa bands were clearly visible (d). After 14 days in culture (e) these two bands were more prominent than those in freshly isolated cells. In contrast, time course studies of the 42 kDa band remained virtually unchanged.

Western blot analysis of the same cell lysates with a monoclonal antibody raised against residues 252-271 of the Cx43 carboxyl terminus detected only a single band migrating at 42 kDa (Fig. 15B). Immunoblots showed the decrease of the antibody binding during the reformation of the intercellular contacts between the cardiomyocytes in culture. The carboxy-terminal region of the Cx43 molecule between residues 252-271 is known to contain several phosphorylation sites. However, the antibody seems to recognise only a non-modified epitope. The results of these experiments implied that the specific phosphorylation of the Cx43 cytoplasmic tail may induce the epitope masking and reduce the binding affinity of the Cx43 monoclonal antibody to the antigen.

1.1.3 Analysis of the Cx43 Phosphorylation

Fig. 16 illustrates the results of a study examining the phosphorylation state of Cx43. Cell lysates of freshly isolated myocytes (a and b) and myocytes kept for 8 days in culture (c and d) were examined. Prior to SDS-PAGE and Western blotting, the cell lysates were incubated with calf intestine alkaline phosphatase to dephosphorylate proteins. In the presence of 10 mmol/L phosphate, a phosphatase inhibitor, immunoblot analysis with the polyclonal anti-Cx43 antibody showed the expression of three bands corresponding to 42, 45 and 47 kDa (a and c) . Alkaline phosphatase treatment alone led to the disappearance of the 45 and 47 kDa bands and a concomitant increase of the 42 kDa band (b and d). Hence, the band with the lower molecular weight, i.e. 42 kDa, represents the non-phosphorylated form of the protein
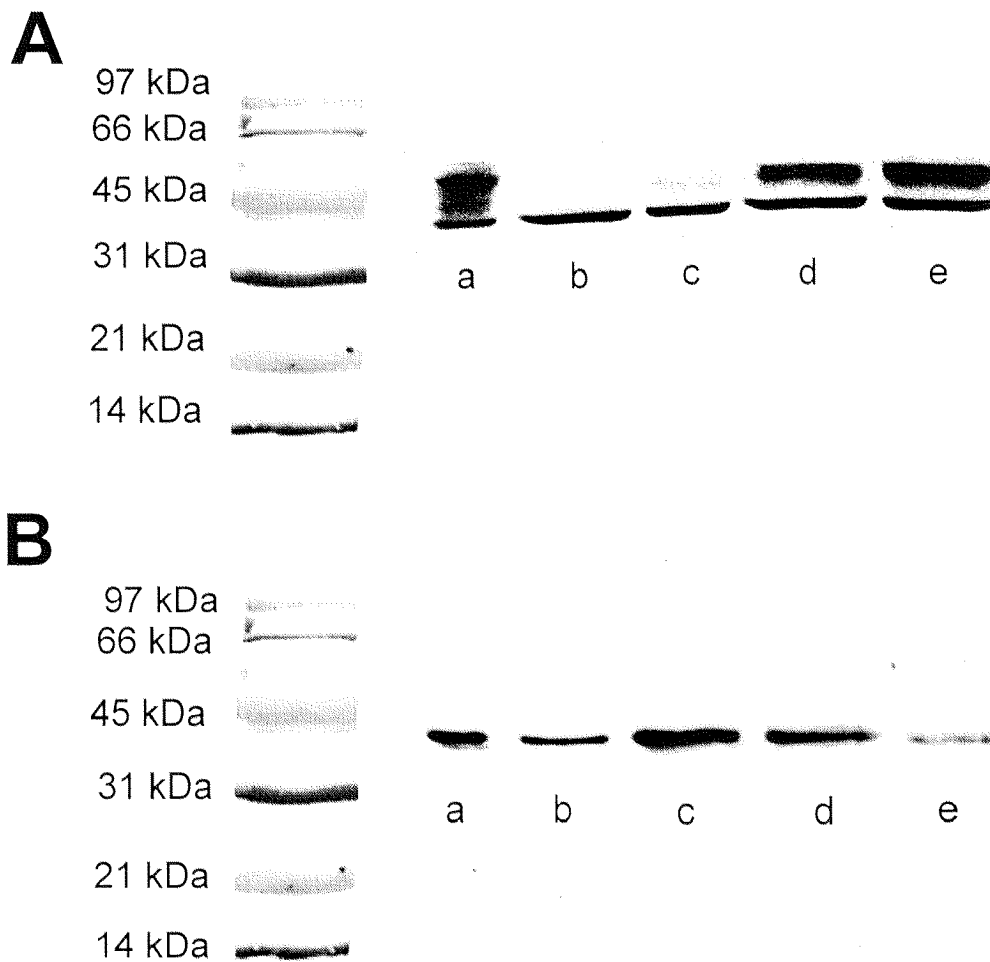
Fig.15 Cx43 Expression during the Re-differentiation of Adult Rat Ventricular Myocytes In Vitro

A - Western blot analysis of the cardiomyocyte lysates with the anti-Cx43 antibody raised against amino acid residues 314-322 of rat Cx43 shows three bands migrating at 42, 45 and 47 kDa respectively. The bands with a slower electrophoretic mobility may represent the phosphorylated isoforms of the Cx43 protein. Lanes contain protein extracts from freshly isolated (a) and kept in culture for 2 (b), 4 (c), 8 (d) and 14 (e) days ventricular myocytes.

B - The anti-Cx43 antibody produced against amino acid residues 252-271 of rat Cx43 recognises a single 42-kDa band in the lysates of freshly isolated (a) and cultured for 2 (b), 4 (c), 8 (d) and 14 (e) days adult rat ventricular myocytes.

(will be referred as Cx43-NP) and the two bands with the higher molecular weight, i.e. 45 and 47 kDa, correspond to the phosphorylated isoforms (will be referred as Cx43-P1 and Cx43-P2, respectively). Therefore, the reestablishment of cell-cell contacts and synchronous contractions of cardiomyocytes in vitro appears to correlate with the increase of the Cx43 phosphorylation in the carboxy-terminal region of the molecule between residues 252-271.

66 kDa ━

45 kDa ━

a   b   c   d
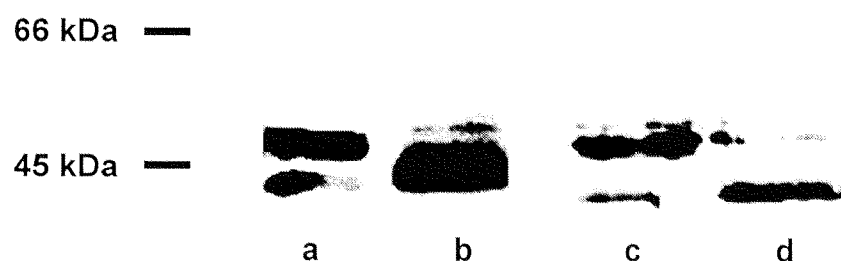
Fig.16 Dephosphorylation of Cx43 with Alkaline Phosphotase

Cell lysates of freshly isolated (lanes a and b) and 8 days cultured (lanes c and d) cardiomyocytes were incubated with calf intestine alkaline phosphatase prior SDS-PAGE and Western blotting. In lines a and c the reaction was performed in the presence of phosphatase inhibitor (10 mM phosphate). Alkaline phosphatease treatment (lines b and d) caused dissapearence of the upper bands and a concominant increase in the 42-kDa band corresponding to the non-phosphorylated isoform of Cx43.

Proteins can be phosphorylated at tyrosine, serine or threonine amino acid residues. To obtain an information at which residues Cx43 was phosphorylated in cultured ARCs, cardiomyocyte extracts were immunoprecipitated with the polyclonal anti-Cx43 antibodies as described in "Materials and Methods". Immunoprecipitated Cx43 protein was then analysed for the presence of the specific phosphorylation by Western blotting with monoclonal anti-phosphotyrosine, anti-phosphoserine and anti-phosphothreonine antibodies. As shown in Fig.17, Cx43 appeared to be phosphorylated only on serine residues (lane b). There was no sign of tyrosine or threonine phosphorylation of Cx43 (lanes c and d).

66 kDa   ━

45 kDa   ━

              a   b   c   d
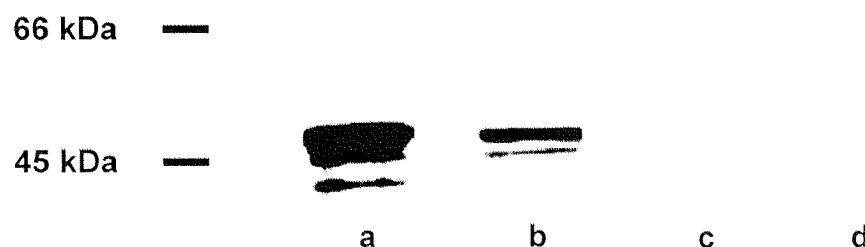
Fig.17 Cx43 is Phosphorylated on Serine Residues

Cx43 was immunoprecipitated from the lysate of 8 day-old ARCs using the poly-
clonal anti-Cx43 antibody, which recognises all three isoforms of the protein. Immu-
noprecipitated material was analysed by Western blotting with the polyclonal anti-
Cx43 antibody (lane a), and anti-phosphoserine (lane b), phosphothreonine (lane c),
phosphotyrosine (lane d) antibodies.

1.1.4 Localisation of the Various Forms of Cx43 in the Cells

To assess whether the non-phosphorylated isoform and the phosphorylated isoforms of
Cx43 have a different intracellular distribution, an immunoblot analysis of the cardiomyocyte
membrane and cytosolic fractions was performed using the polyclonal anti-Cx43 antibody,
which recognised all three isoforms of the protein. The purity of the cytoplasmic and mem-
brane fractions has been always checked by assaying for the activity of marker enzymes - lac-
tate dehydrogenase and alkaline phosphodiesterase I for cytosol and plasma membrane respec-
tively. Only the preparations where 95% of the lactate dehydrogenase activity was detected in
the cytosolic fraction and not less then 80% of the alkaline phosphodiesterase I activity was
associated with the membrane fraction were used for the experiments. The results of Western
blot showed that all three isoforms of Cx43 reside in the plasma membrane (Fig.18A lane a).
In addition, a small amount of Cx43-NP was detected in the cytosolic fraction of the cells
(Fig.18A lane b). The contamination of the cytosolic fraction with membrane proteins during
the cell fractionation seemed to be unlikely. Hence, the morphological localisation of Cx43 in
cultured ventricular cardiomyocytes was examined by indirect immunofluorescent labelling of
the cells with the anti-Cx43 antibodies. Primarily, formaldehyde fixed and detergent perme-
abilised ARCs were incubated with the rabbit polyclonal anti-Cx43 (res.314-322) antibody
and then exposed to the treatment with the mouse monoclonal anti-Cx43 (res.252-271) anti-
body; the signals from both primary antibodies were detected using the fluorescently labelled

anti-rabbit IgG and anti-mouse IgG secondary antibodies respectively. Actin cytoskeleton was visualised by labelling the cells with a rhodamin-coupled phalloidin. The signals from the anti-Cx43 antibodies and filamentous actin were simultanously recorded by means of confocal microscopy, so that it was possible to monitor the localisation of the proteins in the same cells. A typical picture is shown in Fig.18B. Re-differentiated adult ventricular cardiomyocytes demonstrated a pattern of the punctate Cx43 staining localised mainly in the sites of intercellular contacts. However, a weak intracellular signal was detected as well. It corresponded exclusively to Cx43-NP, which is the only Cx43 isoform recognised by both anti-Cx43 antibodies. Therefore a non-phosphorylated isoform of Cx43 was found to be present in the plasma membrane and in the cytoplasm of the re-differentiated cardiomyocytes, whereas Cx43-P1 and Cx43-P2 resided only in the junctional membrane. Surprisingly, Cx43-NP was also seen in the non-junctional regions of the cell surfaces (see an arrow in Fig18B a and c).

Fig.18   Cellular Localisation of Different Cx43 Isoforms in the Cultured Adult Cardiomyocytes

A - the lysates of the membrane (lane a) and cytosolic (lane b) fractions of ARC cultured for 14 days were analysed by Western blotting with the polyclonal anti-Cx43 antibodies, which recognises all isoform of the protein.

B - confocal images of a 14 day cardiomyocyte culture in standart medium. (a) - double immnustainign of the cells for Cx43 using monoclonal Cx43 antibody (FITC, green) specific for the non-phosphorylated isoform of Cx43 and polyclonal Cx43 antibody (TxRed, red), which recognises all three isoforms of the protein; yellow colour indicates the colocalisation of the signals from both antibodies and indicates the presence of the non-phosphorylated isoform of Cx43 at the sites of cell-to-cell contacts. (b) - the same cells were stained for total F-actin using the Cy5-labelled phalloidin shown in blue. (c) - overlay of the images shown in a and b.

A

45 kDa —

a   b
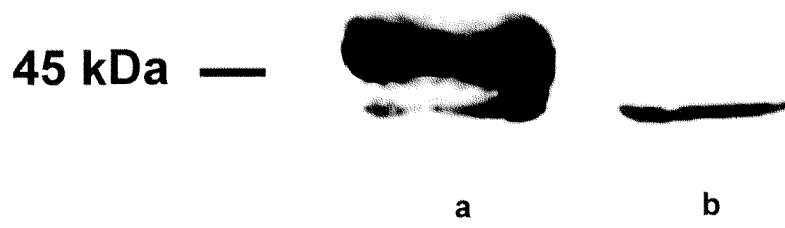
B
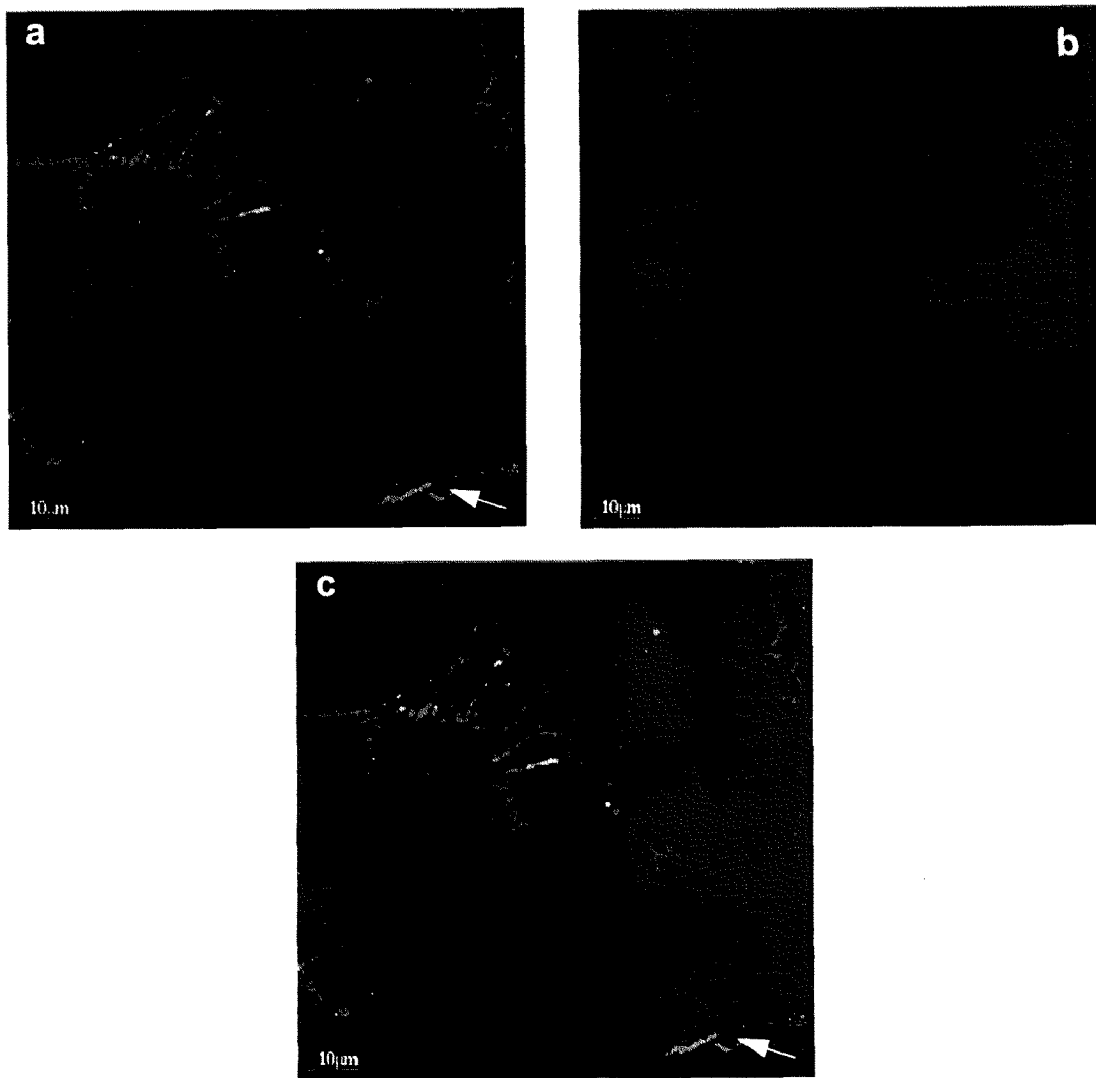
1.1.5 Phosphorylation of Cx43 during the Formation of Intercellular Contacts

Cell-to-cell contacts between the re-differentiated cardiomyocytes were subjected to quick artificial disintegration to determine whether the phosphorylated state of Cx43 can be affected by the disruption of the functional intercellular junctions. ARC cultures were incubated in the Ca^{2+} free medium with EGTA for two hours at 37°C to break down the Ca^{2+} dependent adhesive complexes and for one more hour at RT to prevent the transport of newly synthesised proteins to the plasma membrane. This treatment resulted in the splitting of the cardiac gap junctions and the subsequent increase of the non-junctional membrane area. Immunoblot analysis of the cell lysates with the polyclonal anti-Cx43 antibodies demonstrated that the disruption of the intercellular contacts between cardiomyocytes in culture led to the selective accumulation of the non-phosphorylated isoform and a concominant decrease in the phosphorylated isoforms (Fig.19 lines a and b). Immunocytochemical localisation of Cx43 in the cardiomyocytes after Ca^{2+} depletion experiments confirmed this finding. The cell preparations were double immunolabelled with the monoclonal and polyclonal anti-Cx43 antibodies. The superimposed signals from both antibodies indicated the cell borders along the splitting junctions (Fig.20B). At the same time, the double immunostaining of the cardiomyocytes with an anti-N-cadherin antibody and the monoclonal anti-Cx43 antibody showed that the non-phosphorylated isoform of Cx43 could still reside in the sites of the former intercellular contacts even if cadherins have been already degraded intracellularly (Fig.20C). The phosphorylated forms of Cx43 were not detected after the disruption of the cell-cell adhesion between cardiomyocytes.

45 kDa ▬

a   b   c

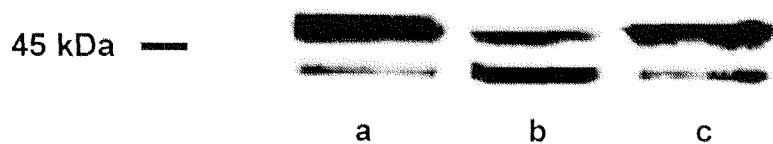## Fig.19 Cx43 Phosphorylation after Ca^{2+} De- and Replenishment

14 day ARC were incubated in the Ca^{2+} medim with EGTA to dissociate the intercellular junctions, lysed and subjected to the immunoblotting with the polyclonal anti-Cx43 antibody. Lane a - the lysate of the control culture incubated in the standart medium; th e extract prepared from ARC after removal (lane b) and re-addition of Ca^{2+}.

The process of the disruption of the Ca^{2+}-dependent intercellular contacts between cardiomyocytes was reversed by an overnight incubation of the cells in the standart cell culture medium at 37°C. The recovery of the intercellular communication resulted in the increase in the phosphorylated forms of Cx43 as was detected by Western blot (Fig.19 lane c) and the immunofluorescent analysis of the cells (Fig.20D). Taken all together, these results indicate a correlation between processing of Cx43 to the phosphorylated forms and the acquisition of ability to incorporate into the sites of the cell-to-cell contacts.
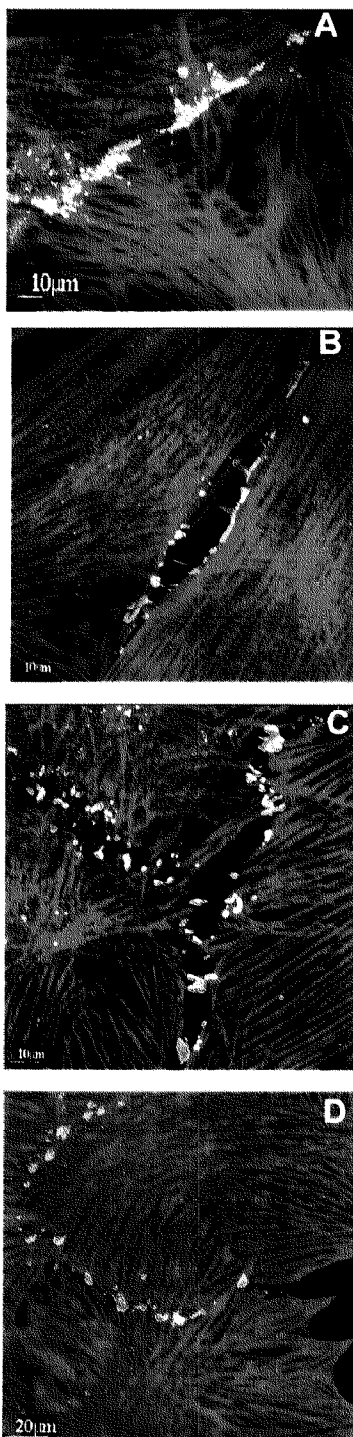
Fig.20 Dynamics of the Cell-to-Cell Contact Dissociation and Re-assembly in the Cardiomyocyte Primary Cultures

A - Adult rat ventricular cardiomyocytes cultured for 14 days were immunostainined for Cx43 with the monoclonal (FITC, green) anti-Cx43 antibody and for N-cadherin with the polyclonal anti-Pan cadherin antibody (Cy5, blue). F-actin was visualised by rhodamin-phalloidin (red). Under standard conditions, the signals from all proteins were localised in the regions of the intercellular contacts (shown in white).

B - Incubation of the same cells in the Ca^{2+}-free medium with EGTA initiated the separation of the intercalated disk-like structures between ARC. The cardiomyocytes were indirectly immunolabelled for Cx43 with the monoclonal (FITC, green) and the polyclonal (Cy5, blue) anti-Cx43 antibodies. Rhodamin-phalloidcomplexes decorated filamentous actin are shown in red. White and light green colours indicate the localisation of non-phosphorylated isoform of Cx43 along the boders of the splitting cell-to-cell contacts.

C - Cardiomyocyte junctions disrupted by Ca^{2+} depletion were indirectly immunolabelled for Cx43-NP with the monoclonal anti-Cx43 antibody (FITC, green), for cadherin with the polyclonal anti-N-cadherin antibody (Cy5, blue) and for F-actin with rhodamin-coupled phalloidin (red). The non-phosphorylated isoform of Cx43 was detected in the sites of the former cell-to-cell contacts (green), while cadherin has disappeared from the cell periphery and is localised intracellularily (violet).

D - Cardiomyocyte cultures incubated in the standard cell culture medium containing Ca^{2+} overnight restored their cell adhesion complexes, which are visualised by double immunolabelling of the cells with the monoclonal anti-Cx43 antibody (FITC, green) and the polyclonal anti-Pan cadherin antibody (Cy5, blue). F-actin cytoskelton is detected by rhodamin-phalloidin staining. White colour indicates the colocalisation of all three proteins in the regions of the intercellular contacts.

1.2 Expression of Cx40

1.2.1 Immunoblot Analysis

Fig.21A shows the results of a Western blot analysis using a polyclonal antibody directed against mouse Cx40, C-terminal amino acid residues 231-331. In freshly isolated cardiomyocytes, this antibody specifically recognised a single band migrating at 38 kDa (a). However, two bands of 38 and 41 kDa were detected in myocytes kept in culture for 2(b), 4(c), 8(d) and 14(e) days. HeLa cells transfected with mouse Cx40, revealed the same two bands (f; positive control) and parental HeLa cells yielded no signal (g; negative control).
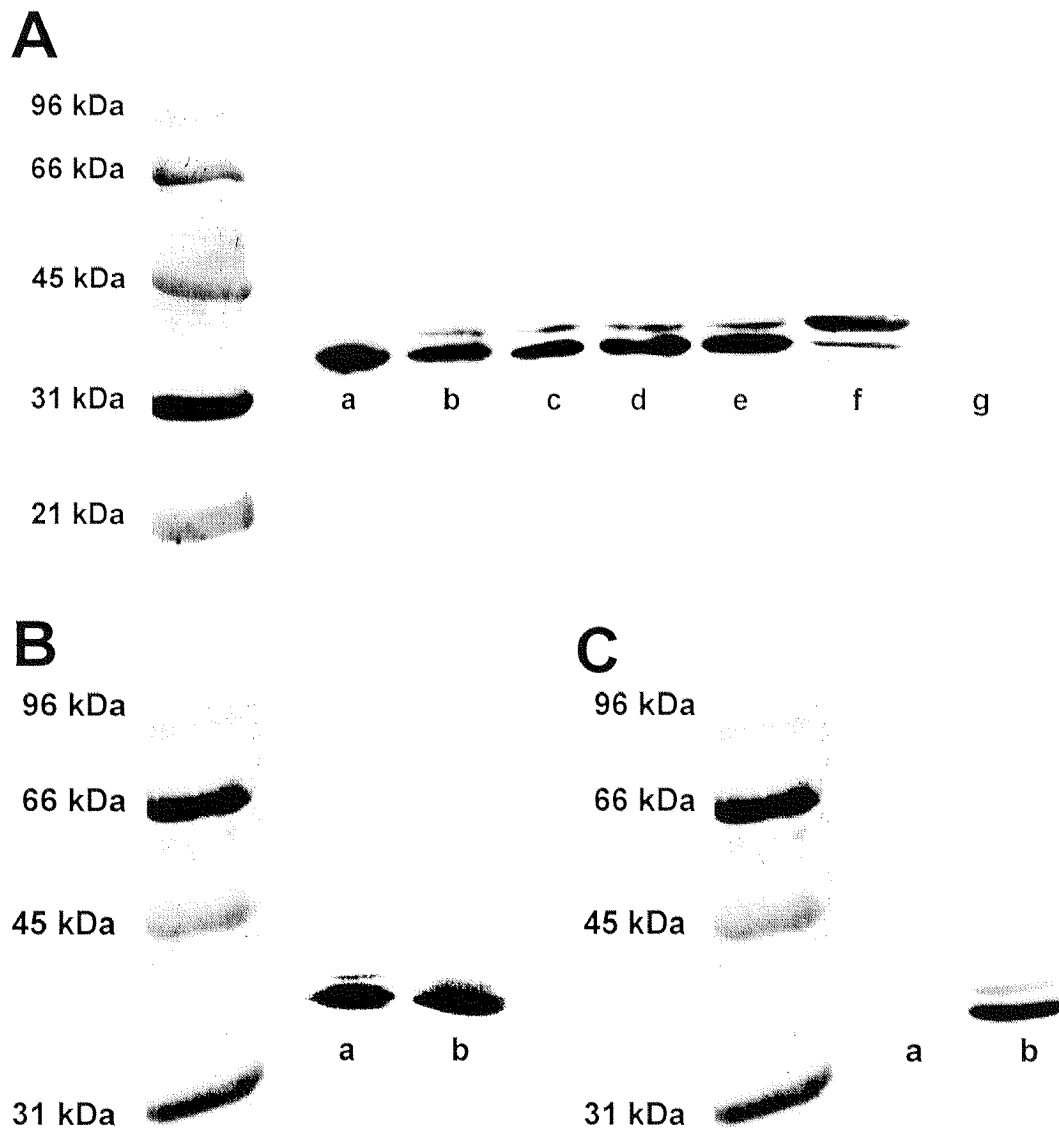
Fig.21 Expression of Cx40 in Re-differentiating Myocytes and HeLa Cells.

A - Western blots of cell lysates with a polyclonal antibody directed against the residues 231-331 of mouse Cx40. The antibody recognised two bands migrating at 38 and 41 kDa. Myocytes: freshly isolated (a) and kept in culture for 2 (b), 4 (c) and 10 (d) and 14 days (e). HeLa cells: wild type (e), transfected with mouse Cx40 (f).

B - Phosphorylation state of Cx40. Lysates of myocytes kept in culture for 8 days. Alkaline phosphatase caused removal of the upper band (b), concomitant addition of phosphatase inhibitor prevented it (a).

C- Western blot analysis of the cytoplasmic (lane a) and membrane (lane b) fractions with the anti-Cx40 antibody shows that both, the non-phosphorylated and phosphorylated isoforms of the protein reside in the plasma membrane.

1.2.2 Examination of the Protein Phosphorylation

Using the same antibody, the phosphorylation state of Cx40 was also examined. Fig. 21B documents the results. The lysates of cells kept in culture for 8 days were treated with alkaline phosphatase as described above (see Expression of Cx43). Incubation of the sample with alkaline phosphatase led to an almost complete loss of the 41 kDa band (b). In the control, where the phosphatase inhibitor was added, both bands of Cx40 can be seen (a). Clearly, the 38 kDa band reflects the dephosphorylated form of the protein and the 41 kDa band its phosphorylated isoform. The results indicate that the phosphorylated form of Cx40 increases with time of the cell re-differentiation while the non-phosphorylated form remains virtually constant. The immunoblot analysis of the membrane and cytosolic fractions of the cells with the anti-Cx40 antibody showed that both isoforms of Cx40 reside in the plasma membrane of cultured cardiomyocytes (Fig.21C lane b).

1.2.3 Immunocytochemical Localisation of Cx40 in the Cardiomyocytes

The localisation of Cx40 and Cx43 in pairs of myocytes was studied using the indirect double immunolabelling of cells with a monoclonal anti-Cx43 antibody and a polyclonal anti-Cx40 antibody. Fig.22 shows the confocal images of freshly isolated cardiomyocytes (A) and cells in culture for 2(B), 4(C) and 8(D) days. The panels document the complex structural changes of the cellular architecture during re-differentiation; after rounding up first, the cells spread out and formed processes. The cardiomyocytes turned from rod-shaped to polymorphous and increased their size and volume. Each panel shows fluorescence signals of three different colors. Green and red localise Cx40 and Cx43, respectively, and yellow shows colocalisation of Cx40 and Cx43. The fluorescent signals of both connexins were primarily seen in the intercalated discs. The co-localisation of fluorescent signals suggests that Cx40 and Cx43 are co-expressed in the same cell and localised within the same gap junction plaque

Fig.22 Localisation of Cx40 and Cx43 in Gap Junctions of Cardiomyocytes

Double immunostaining with primary antibodies raised against Cx40 and Cx43 and a secondary antibody linked to a fluorescent marker. Light microscopy pictures obtained from freshly isolated cells (A) and cells kept in culture for 2 (B), 4 (C), and 8 days (D).

The fluorescent labels were localised in the intercalated disks. Green and red localise with Cx40 and Cx43, respectively, and yellow indicates the co-localisation of Cx40 and Cx43.

1.3 Expression of Cx45

1.3.1 Western Blot Analysis

Fig.23 shows the Western blot of ventricular cell lysates performed with a polyclonal antibody raised against an epitope consisting of 138 carboxy-terminal amino acids of mouse Cx45 [Butterweck et al., 1994]. This antibody recognised two bands with a molecular weight of 45 and 49 kDa in freshly isolated myocytes (a) and in myocytes kept in culture for 2 (b), 4 (c), 8 (d) and 14 (e) days. As previously reported, this antibody detected the same bands in lysates from mouse kidney cells and HeLa cells transfected with mouse Cx45 [Butterweck et al., 1994]. The lower band reflects the dephosphorylated form, the upper band the phosphorylated form. Hence, like in the case of Cx43, the signal from the dephosphorylated isoform of Cx45 was more intense than the signal from the phosphorylated protein at time t = 2 days and 4 days (compare Fig.15A and Fig.23). Furthermore, the amount of both isoforms decreased during the first two days and increased from day 2 to day 14 of cardiomyocyte development in culture.

96 kDa

66 kDa

45 kDa

          a   b   c   d   e

31 kDa

21 kDa

14 kDa
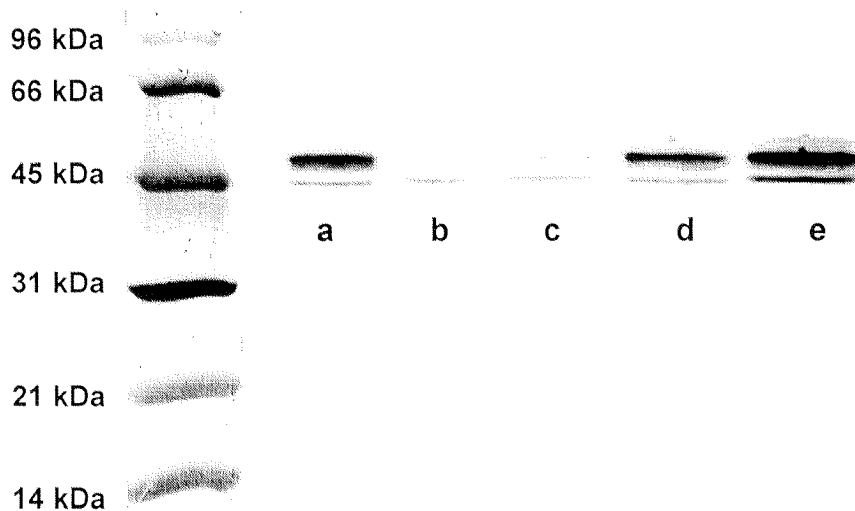
Fig.23 Expression of Cx45 during Re-differentiation of Cardiomyocytes.

Western blots of cell lysates with a polyclonal antibody directed against 138 C-terminal amino acids of mouse Cx45. The antibody recognised two bands with a molecular weight of 46 and 49 kDa. Freshly isolated cells (a) and cells kept in culture for 2 (b), 4 (c) and 10 (d) and 14 days (e). The upper band corresponds to the phosphorylated form of Cx45, the lower band to the de-phosphorylated isoform.

1.3.2 Immunocytochemical Analysis

Double immunostaining was used to examine the distribution of Cx43 and Cx45 connexins in cultured ventricular cardiomyocytes. Fig.24 depicts confocal images of freshly isolated cells (A) and cells after 2(B), 4(C) and 8(D) days in culture. The pictures shows fluorescently labelled connexin proteins concentrated at the intercalated discs. The green and red colors indicate Cx43 and Cx45, respectively; accordingly a yellow signal points to co-localization of Cx43 and Cx45. The level of the Cx45 expression in cardiomyocytes was strongly down regulated during the first days in culture, only detectable on the blots, but not with immunofluorescent labelling of cells (compare Fig.23b and Fig.24B). However, cells cultured for an extended time (Fig.24 C and D) indicated a co-localisation of Cx43 and Cx45, demonstrating that Cx43 and Cx45 are co-expressed in the same cell and are present at identical gap junctions.
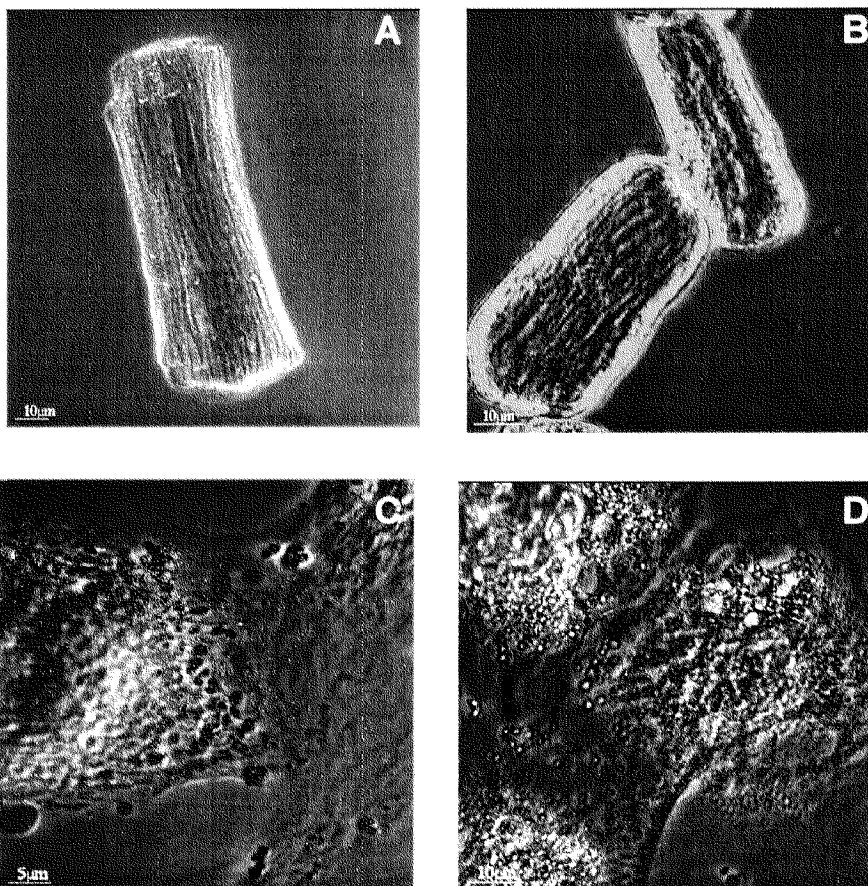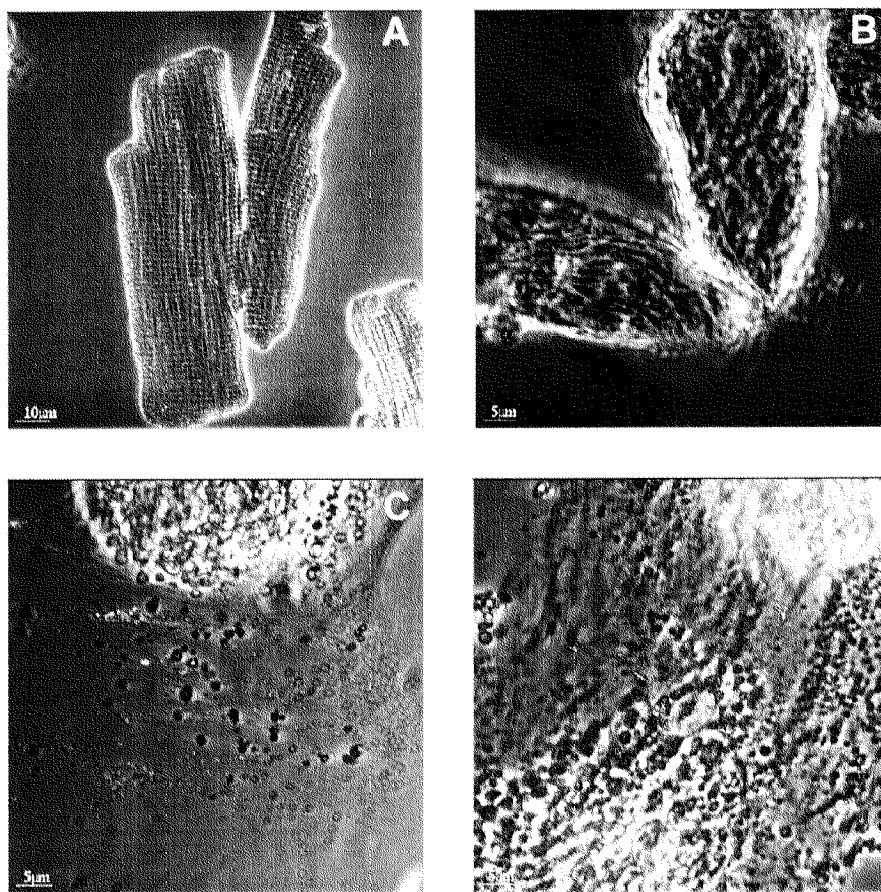

Fig.24 Localisation of Cx43 and Cx45 in Gap Junctions of Cardiomyocytes

Double immunostaining with primary antibodies raised against Cx43 and Cx45 and fluorescently labelled secondary antibodies. Light microscopy pictures obtained from freshly isolated cells (A) and cells kept in culture for 2 (B), 4 (C), and 8 days (D).

The fluorescent labels were localised in the intercalated disks. Green and red localise with Cx43 and Cx45, respectively, and yellow shows the co-localisation of Cx43 and Cx45.

1.4 Quantification of Connexin Expression

Table 1 summarises the results of a quantitative analysis of immunoblots. Extracts obtained from 10^5 cells were collected at different times after cell isolation, electrophoresed on the same SDS-PAGE and electrotransferred to nitrocellulose membranes. Three membranes containing proteins of the same cell lysate were prepared in parallel and incubated with antibodies against Cx40, Cx43 and Cx45, respectively. The chemiluminescent signals from immunolabelled proteins were detected by exposure to X-ray film. The expression levels for each connexin were determined from densitometric scans of the films. The level of the connexin expression in freshly isolated cells was set to 100%. Four complete experiments of this kind were performed.

According to Table 1, Cx40 underwent a moderate up-regulation. Between times t = 0 days to 14 days, the expression level increased monotonically by about 25%. In contrast, Cx43 exhibited a biphasic behavior, i.e. an initial down-regulation was followed by a pronounced up-regulation. Within 2 days after isolation, the expression level was about half as large. Thereafter, it increased continuously. At time t = 14 days, it was nearly doubled when compared with control. Cx45 showed a similar biphasic time profile. When compared with control, at time t = 2 days the level was half as large, at time t = 14 days it was twice as large. Hence, the initial down-regulation and subsequent up-regulation were virtually superimposable with those of Cx43. These results are consistent with the data presented by the individual immunoblots (see Figs. 15A, 21A and 23) and immunostaining experiments (see Figs. 22 and 24).

Table 1

	$t = 0$ days	$t = 2$ days	$t = 4$ days	$t = 8$ days	$t = 14$ days
Cx40	100%	$101 \pm 1\%$	$106 \pm 1\%$	$112 \pm 2\%$	$126 \pm 3\%$
Cx43	100%	$56 \pm 13\%$	$75 \pm 15\%$	$127 \pm 12\%$	$191 \pm 41\%$
Cx45	100%	$53 \pm 15\%$	$74 \pm 9\%$	$88 \pm 15\%$	$180 \pm 67\%$

The data represent means $\pm$ S.D. from 4 complete experiments. Representative immunoblots performed with anti-Cx43, anti-Cx40 and anti-Cx45 antibodies are shown in Figs 2A, 8A and 10, respectively.

The dynamics of the connexin expression described above may reflect changes of protein expression in single cells or alterations in number of cells expressing the specific connexins. To distinguish between these possibilities, we have visually examined the cardiomyocytes cultured for different periods of time, immunofluorescently labelled with antibodies against Cx43, Cx45 and Cx40. Cells were double immunolabelled with anitibodies against Cx43 and Cx40 and against Cx43 and Cx45 in parallel. Hence, two sets of 100 cells randomly selected were analysed in each sample. Three complete experiments of this sort were carried out.

Cx43 was present between all cardiomyocytes irrespective of the time after isolation. This implies the increase of Cx43 in the immunoblots reflects increased expression of Cx43 in each cell. Cx40 was expressed in ~20% of the cells in each sample. Likewise, this suggests that the increase of the Cx40 content observed in the Western blots is due to the enhanced expression of Cx40 expression in single cells. Cx45 was detected in ~10% of freshly isolated ventricular cardiomyocytes and in 83% of the cells cultured for 8 days. This indicates the the increase of Cx45 in the immunoblots is broght about by increased number of cells expressing Cx45.

Unfortunately, data from immunoblots and immunofluorescence cannot be used to determine and compare the expression levels of different connexins in single cardiomyocytes. This is because each primary antibody exhibits a different affinity for its respective epitope as well as for the secondary antibody.

1.5 Expression of Cx40 and Cx45 during Rat Heart Development

1.5.1 Western Blot Analysis of the Proteins

The cell lysates prepared from freshly isolated embryonic (14 dpc), neonatal (P1), and adult rat ventricular cardiomyocytes and from 14 days old re-differentiated ARCs were subjected to the immunoblot analysis with the anti-Cx40 and anti-Cx45 antibodies. All samples contained equal amounts of total protein. Typical outcomes are shown in Fig.25. Cx40 was found to be expressed as phosphorylated and non-phosphorylated isoforms during late foetal and early neonatal development of the rat heart (Fig.25A lines a and b). The proportion of the Cx40 phosphorylated isoform to the non-phosphorylated one decreased during the cardiomyocyte differentiation in vivo, while the expression level of the protein increased in neonatal cardiomyocytes in comparison to the embryonic cells. The phosphorylated isoform of Cx40 was not detected in freshly isolated adult ventricular cardiomyocytes, however it reappeared again in the re-differentiated cells (compare Fig.25A lines c and d). Anti-Cx45 antibodies rec-

ognised two bands in the lysates of cardiomyocytes at all developmental stages in vivo and in vitro. The highest level of the Cx45 expression and phosphorylation was observed in freshly isolated NRCs (Fig.25B lane b). The expression of the protein was dramatically reduced in the postnatal ventricular myocardium (Fig.25B lane c) and then slightly elevated again in the car-diomyocytes cultured for a week in vitro (Fig.25B lane d). Hence, these data demonstrated that the level of the cardiac Cx40 and Cx45 expression and phosphorylation decreases during the transition from the neonatal stage to the adult stage in vivo and increases during the growth and re-differentiation of adult ventricular cardiomyocytes in vitro.
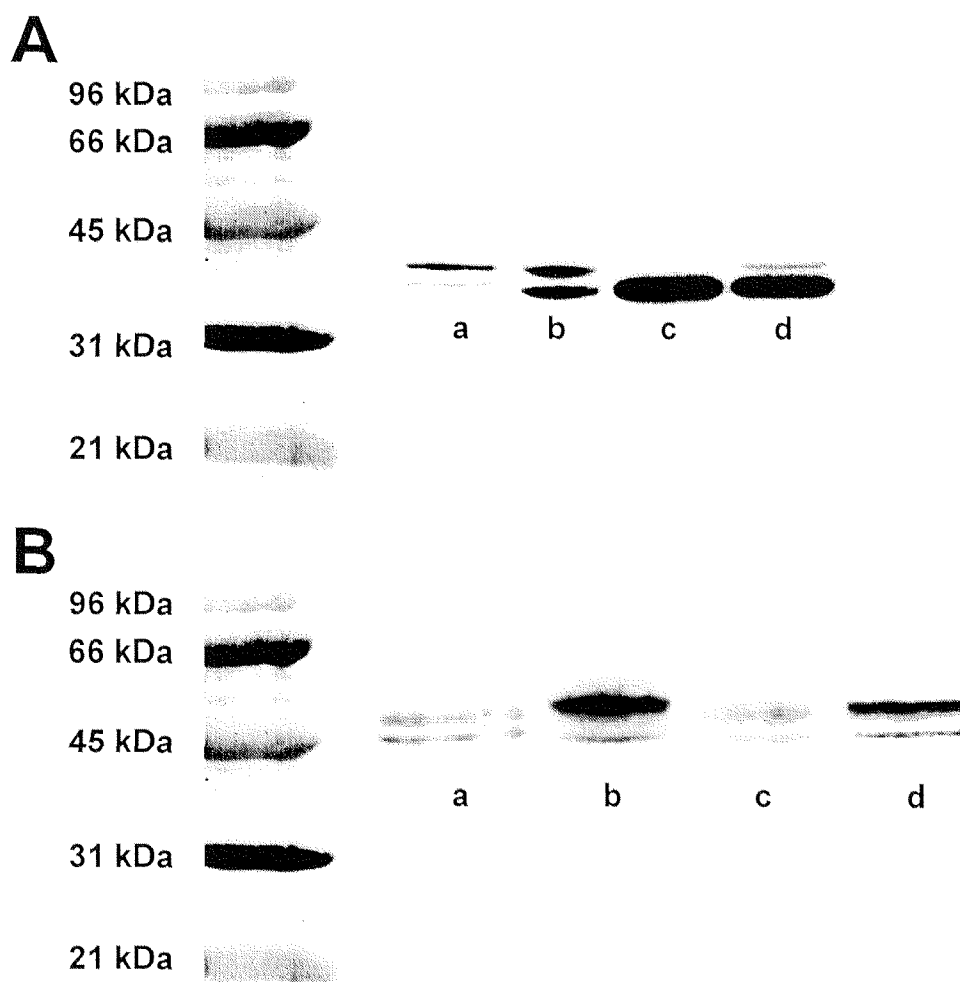
Fig.25 Expression of Cx40 and Cx45 during the Cardiomyocyte Growth *In Vivo* and *In Vitro*

A - Immunoblot analysis of the cell lysates of the embryonic (a), neonatal (b), adult (c) rat ventricular myocytes and 14 day-old ARC (d) with the anti-Cx40 antibody.

B - Western blot of the cell extracts prepared from the embryonic (a), neonatal (b) and adult (c) rat ventricular myocytes, and 14 day-old ARC (d) with the anti-Cx45 anti-body.

2. p70S6 in Ventricular Cardiomyocytes

2.1 The Ribosomal S6 Kinase during Cardiac Growth and Development

2.1.1 Immunofluorescent Labelling of the Cells

To characterise the distribution of the p70S6 kinase in the adult rat ventricular cardiomyocyte, double immunostaining of the cells was performed using an antibody raised against residues 482-502 of the p70S6 C-terminal domain and an anti-a-actinin antibody. In freshly isolated cells the signal from the p70S6 antibody was seen mainly in the plasma membrane of the former intercelular contacts at the cell ends (Fig.26A). In ARC cultured for two days in vitro, p70S6 was found to localise in the submembrane regions at the leading edges of spreading cells (Fig.26B). These are known sites of active cytoskeleton remodelling, where the local activation of protein synthesis may be essential for the quick targeting of new molecules to the places where needed most. The immunostaining of the cells maintained for more then four days in culture revealed an increase in the expression of p70S6 in cytoplasm (Fig.26C-D). The specific membrane and nuclear p70S6 signals were also seen in the cells cultured for two weeks in vitro(Fig.26E).

2.1.2 Western Blotting

The anti-p70S6 antibody generated against amino acid residues 482-501 at the C-terminus of the p70S6 kinase recognised a single band migrated at 60 kDa in the lysates of freshly isolated cells (Fig.27A lane a). It corresponded to the p70S6 kinase as was reported earlier by others [Kozma et al., 1990]. At the same time, the antibody revieled two bands at 60 kDa and 62 kDa in the cells cultured for two days (Fig.27A lane b). The appearance of a third 85 kDa-band could also be seen at Western blots of the cardiomyocyte lysates after four days in culture (Fig.27A lane c). The analysis of the cell samples run on the same gel and transffered to the same membrane in parallel demonstrated that the intensivity of the signal from the anti-p70S6 antibody increased eventially during the cardiomyocyte growth in vitro (Fig.27A lines d and e). The presence of two forms of the kinase with a higher molecular weight may be explained by the phosphorylation state of the protein. To test this possibility, aliquots of the immuno-

precipitated S6 kinase were incubated in the presence of 10 units of calf intestinal alkaline phosphatase.

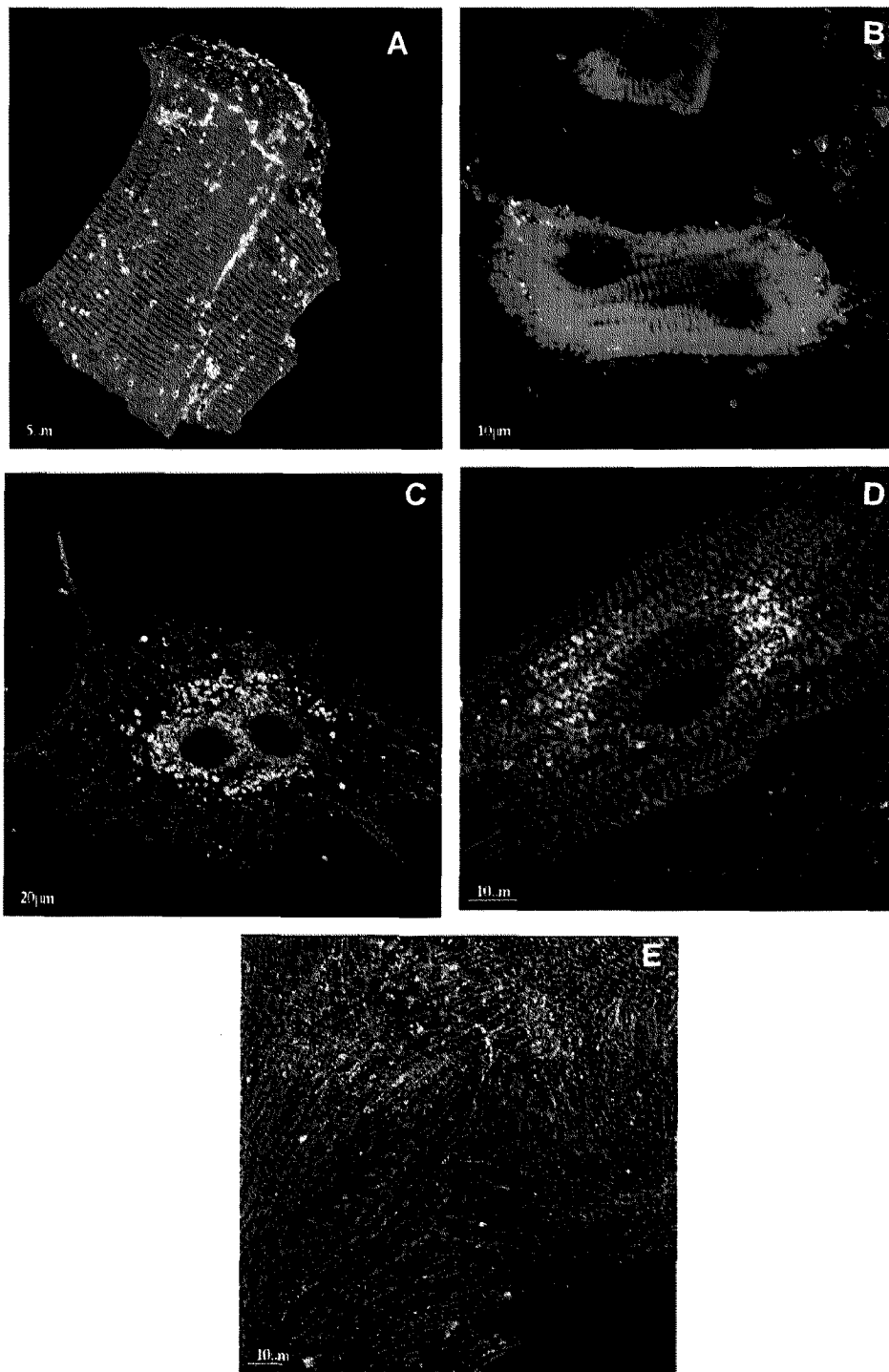**Fig.26 Localisation of the p70S6 Kinase in Adult Ventricular Cardiomyocytes**

Freshly isolated (A) and cells cultured for 2 (B), 4 (C), 8 (D) and 14 (E) days cells were double immunolabelled with the antibodies against α-actinin (TxRed, red) and p70S6 (FITC, green).

The activity of the phosphatase was inhibited by addition of 10 mM Na_3-phosphate in the control sample. After this treatment, the mobility of both kinase preparations was evaluated by Western blot analysis. The results showed that the 63-kDa band was absent. At the same time the amount of the enzyme migrated at 60 kDa increased after the phosphatase treatment (Fig.27B lane a). The pattern of the p70S6 mobility on SDS-PAGE did not change in the control sample: all three isoforms could be detected (Fig.27B lane b). Thus, the difference in molecular weights between the 60-kDa and 63-kDa isoforms of the p70S6 kinase may be explained by phosphorylation of the protein.

However, the 85-kDa form of the protein was unaffected by dephosphorylation. The appearence of the alkaline phosphatase resistent 85-kDa isoform of the S6 kinase on Western blot correlated with the increase of the nuclear signal of the anti-p70S6 antibody in the cells. The antibody is able to recognise a nuclear isoform of the enzyme, which has been shown to run as a 85-kDa protein on the 12.5% SDS-PAGE [Grove et al., 1991]. Therefore it is very likely that the 85-kDa protein detected on Western blot represents the nuclear isoform of the p70S6kinase. Western blot analysis of the cytoplasmic and membrane fractions of 14 day-old ARCs demonstrated that 85- kDa isoform of the kinase localises in the cytoplasm (Fig.27B lane c), whereas the 60-kDa isoform resides in the plasma membrane of cultured cells (Fig.27B lane d). The 63-kDa phosphorylated isoform of the kinase was found in both, membrane and cytoplasmic fractions of the cardiomyocytes.

The data described before provided evidence that the expression of the S6 kinase is up regulated during the re-differention of adult ventricular cardiomyocytes in long-term primary culture. To compare the regulation of p70S6 during the growth of ventricular myocytes in vitro and in vivo, cell lysates of the embryonic, neonatal and adult cardiomyocytes were subjected to immunoblotting analysis with the p70S6 antibody. The results are shown at Fig.28. They demonstrate that the expression of the enzyme and particularly its 85-kDa isoform is up regulated in the cardiomyocytes isolated from the ventricles of newborns (lane b) in comparison to those from embryos (lane a) and adults (lane c). However, the level of the p70S6 expression became higher again in the adult ventricular cardiomyocytes, which were kept in culture for two weeks (lane d). Therefore the expression of the p70S6 kinase was found to be up regulated during the growth and development of ventricular cardiomyocytes in vivo and in long-term primary culture.
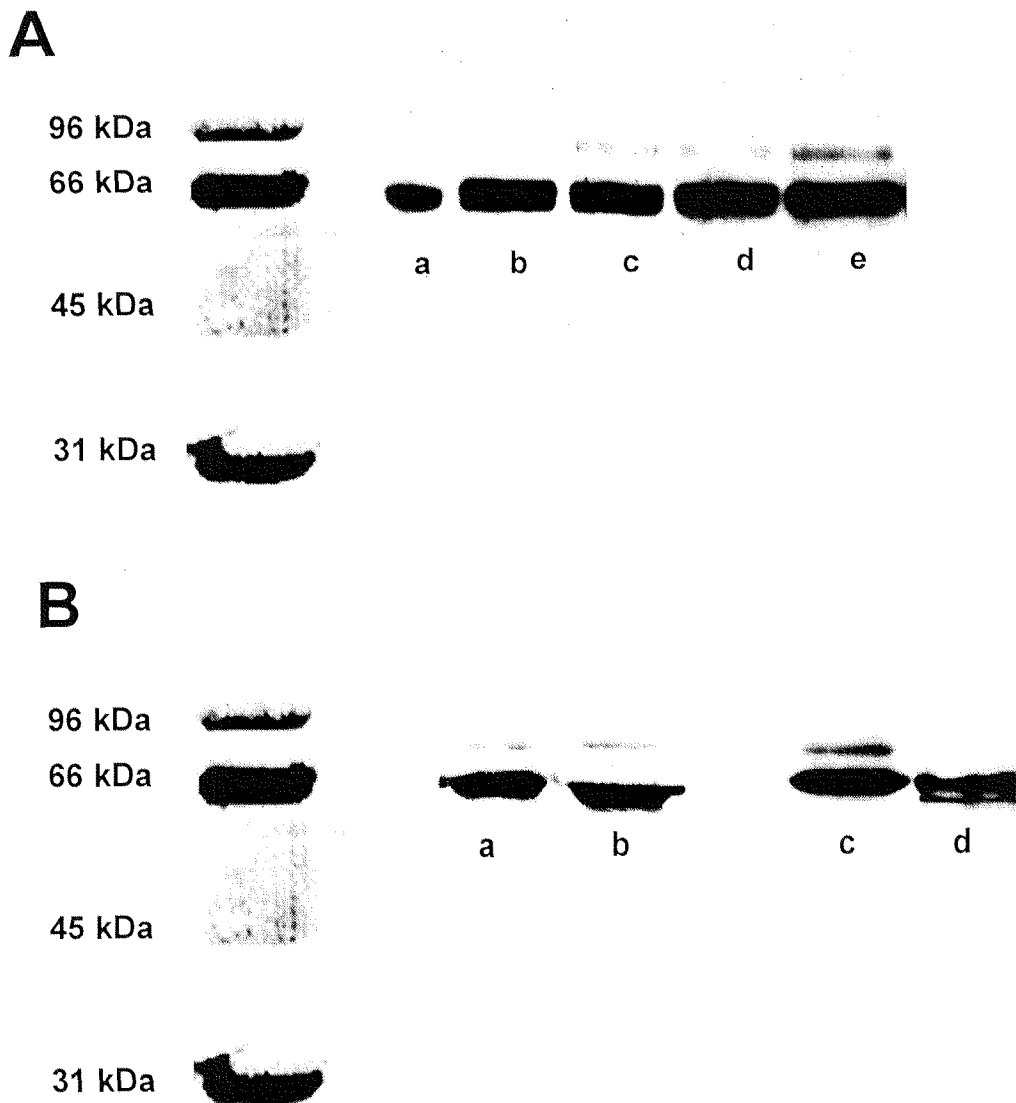
Fig.27 Expression and Subcellular Distribution of p70S6 in ARC

A - Cell lysates of freshly isolated (a) and cultured for 2 (b), 4 (c), 8 (d), 14 (e) days cardiomyocytes were subjected to immunoblot analysis with the anti-p70S6 antibody.

B- The cell lysates of the 14 day ARC were incubated with alkaline phosphatase in the presence (a) or absence (b) of the phosphatase inhibitor and analysed by Western blotting with the anti-p70S6 antibody. Lines c and d represent the results of the immunoblots of the cytoplasmic and membrane fractions of the 14 day cells with the anti-p70S6 antibody.
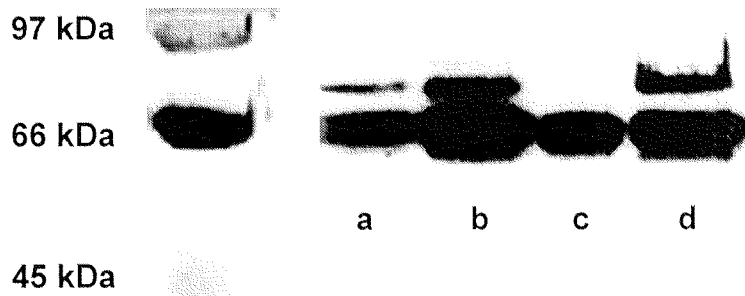
Fig.28 Regulation of the p70S6 Expression during the Cardiac Growth *In Vivo* and *In Vitro*

Cell lysates from freshly isolated embryonic (a), newborn (b) and adult (c) ventricular myocytes and 14 day ARC (d) were assayed for the p70S6 kinase by immunoblotting.

2.1.3 Activation of p70S6 during the Growth and Re-differentiation of ARC *In Vitro*

The activity of the p70S6 kinase is known to be regulated by phosphorylation. Therefore, the appearence of the phosphorylated isoform of the kinase detected by Wetern blot analysis may indicate the activation of the enzyme. Activation of p70S6 during the adult cardiomyocytes growth in vitro was estimated by measuring its ability to phosphorylate the S6 synthetic peptide RRLSSLRA, which is a substrate for the p70S6 kinase. This technique has been shown to be the definitive method for quantifying the p70S6 activity [Pelech et al., 1986].

The anti-p70S6 immunoprecipitates were obtained from the lysates of freshly isolated and cultured cells. Equal amounts of the enzyme from each preparation were used for the in vitro phosphorylation assay. The RRLSSLRA phosphorylating activity of the p70S6 kinase was examined using γ^{32}P-ATP added to the reaction mixture. Samples with addition of the heat inactivated kinase were used as controls. After the protein kinase assay, the peptide was absorbed to the P81 phosphocellulose paper and the excess of γ^{32}P-ATP was washed away at low pH. To measure the γ^{32}P-ATP incorporation, each sample was counted by detection of Cherenkov irradiation. The cytosolic extracts from the cardiomyocytes cultured for two weeks in vitro were discovered to contained the 6.5-fold enhanced kinase activity in comparison to those from freshly isolated cells, where the kinase activity appeared to be only 1.2-fold higher than that in the controls (Fig.29). Hence, the p70S6 kinase is activated during the cardiomyocyte growth and re-differentiation in vitro.
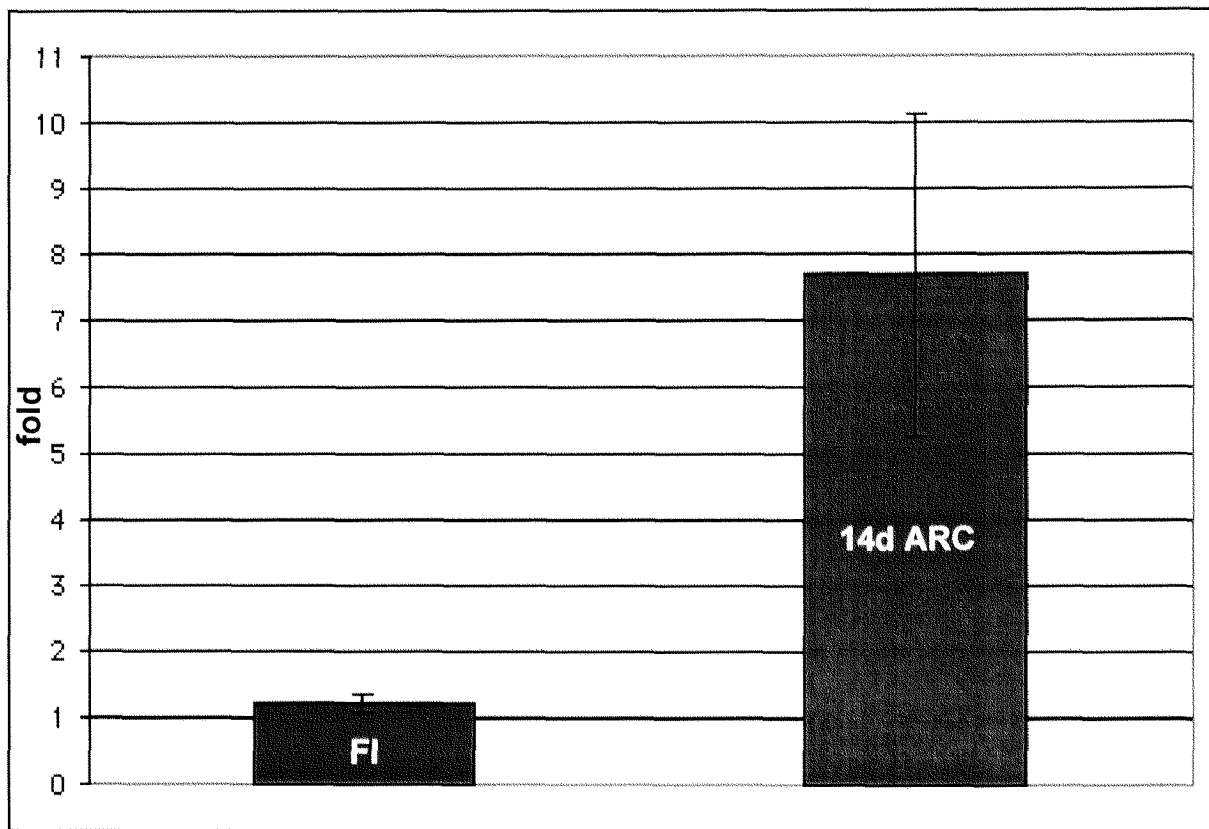
Fig.29 The Ribosomal p70S6 Kinase is Activated during the Re-differentiation of Adult Ventricular Cardiomyocytes *In Vitro*

Cell extracts of freshly isolated and 14 day ARC were immunoprecipitated with the anti p70S6 antibody and subjected to the p70S6 kinase assay using the synthetic S6 peptide as a substrate. Fold induction values represent the averages of four experimens. The control activity of the enzyme from the boiled samples of freshly isolated and cultured ventricular myocytes designated as 1 for freshly isolated and cultured cells respectively. The results are presented as mean ± SD, P<0.05.

2.2   The   Intercellular   Communication   between   Adult   Rat Cardiomyocytes *In Vitro*: Involvement of the p70S6 Kinase

2.2.1   Intercellular Communication between the Cells Treated with TPA

Started at day 7 in culture, a week incubation of ARC in the medium with 200 nM TPA resulted in the increase of the intercellular communication in the 14 day-old cardiomyocyte cultures as was estimated by the extent of Lucifer Yellow CH (LY) intercellular transfer determined 3 min after microinjection of the dye (Fig.30). In the control cultures, microinjected LY passed to 17 ± 5 neighbouring cells. Cell coupling was significantly increased between the TPA-treated cells: the dye passed to 37 ± 8 adjacent cells. The cell density did not differ significantly and was $4\cdot10^5$ cells/cm2 and $3.8\cdot10^5$ cells/cm^2 in the control and TPA-treated cultures respectively.

2.2.2   Expression of Cx43 and Cx40 in the TPA Treated Cardiomyocytes

Lucifer Yellow does not pass through channels formed by Cx45 and, therefore,one could selectively assess changes in the Cx43 and/or Cx40 expression in the cultured ventricular cardiomyocytes.

Western blot analysis with the polyclonal anti-Cx43 antibodies demonstrated an increased amount of the Cx43 protein in the cells after a week of incubation with TPA (Fig.31A lane b). At the same time, the level of the Cx43 mRNA expression did not changed in the cultures treated with TPA (Fig.31B lane b). The expression of Cx40 was unaltered after the long-term exposure of cardiomyocytes to TPA as was shown by immunoblotting the cell lysates with the anti-Cx40 antibody (Fig.31A lane e). Therefore, the Cx43 expression at the protein level was mainly affected by long-term treatment of the cardiomyocytes with TPA.

Double immunostaining of the cardiomyocytes with the antibodies against two different epitopes of the Cx43 molecule indicated a co-localisation of the signals from both antibodies under control conditions (Fig.32A). In contrast, cardiomyocytes exposed to TPA for a week showed positive staining only with the polyclonal antibody raised against residues 314-322 at the Cx43 C-terminus (Fig.32B). Phosphorylation or another posttranslational modification of Cx43 in the region between residues 252-271 could be responsible for the epitope masking and the loss of the antibody sensitivity after TPA treatment.
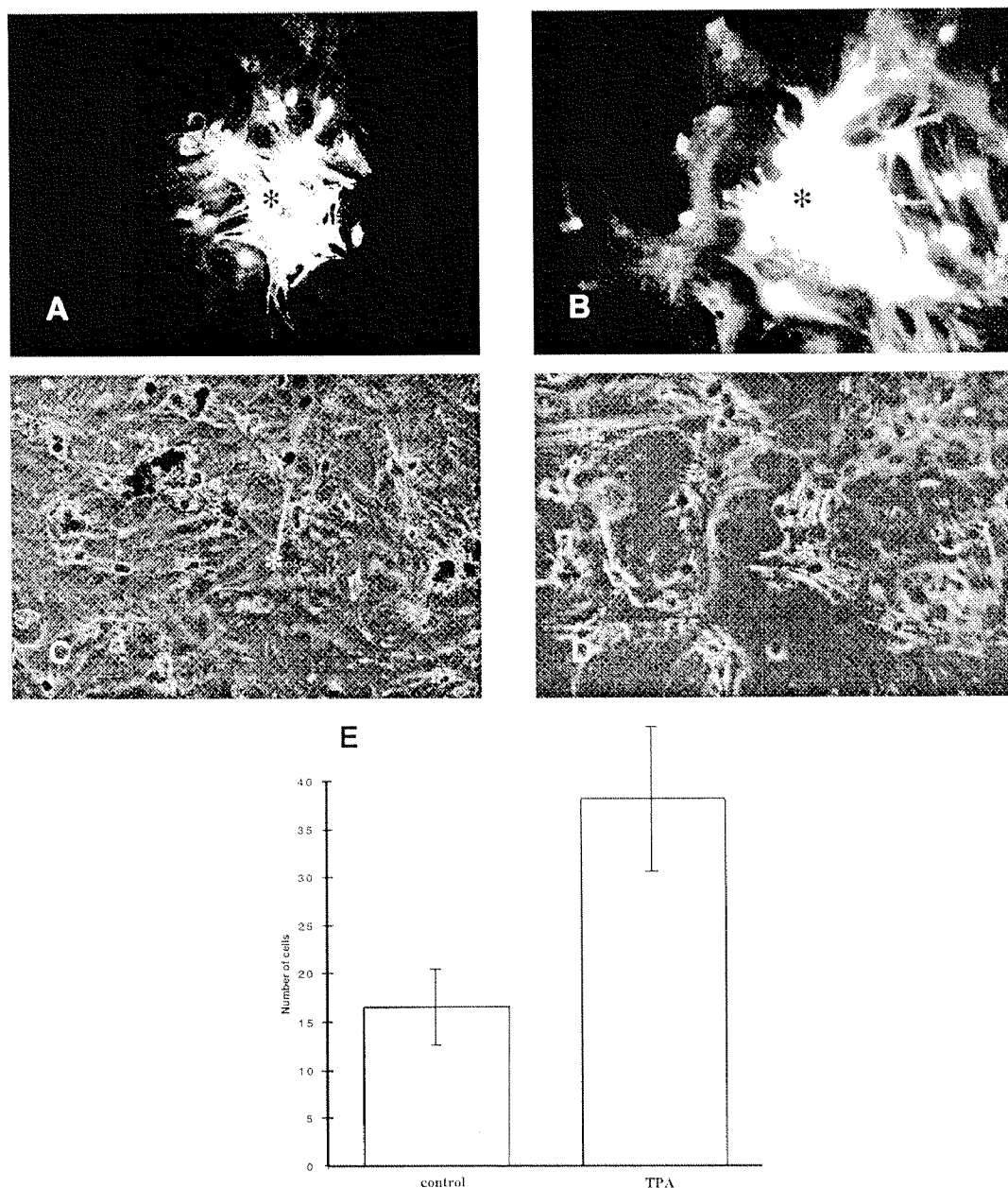
Fig. 30 Effect of TPA on Dye Transfer between Adult Rrat Cardiomyocytes

Cells are 14 days in culture. A - Transfer of Lucifer Yellow from a prelabelled micro-
injected cell (asterisk) to neighbouring cells under control conditions. Fluorescence
was monitored 3 min.after the microinjection of LY. B- Photomicrograph of a prepa-
ration showing increase of dye transfer between ARCs treated with 200 nM TPA for
7 days. C and D - Phase contrast micrographs of the cultures shown in A and B respec-
tively. E - Statistical diagram shows that under control conditions cardiomyocytes are
extensively coupled to each other as measured with LY. 200 nM TPA considerably
increased the extent of dye diffusion after the one week incubation with the cells. Val-
ues are mean numbers of fluorescent cells± SD of 30 dye injections.

A

97 kDa

66 kDa

45 kDa

31 kDa

B

2.6 kb

3.6 kb

a   b
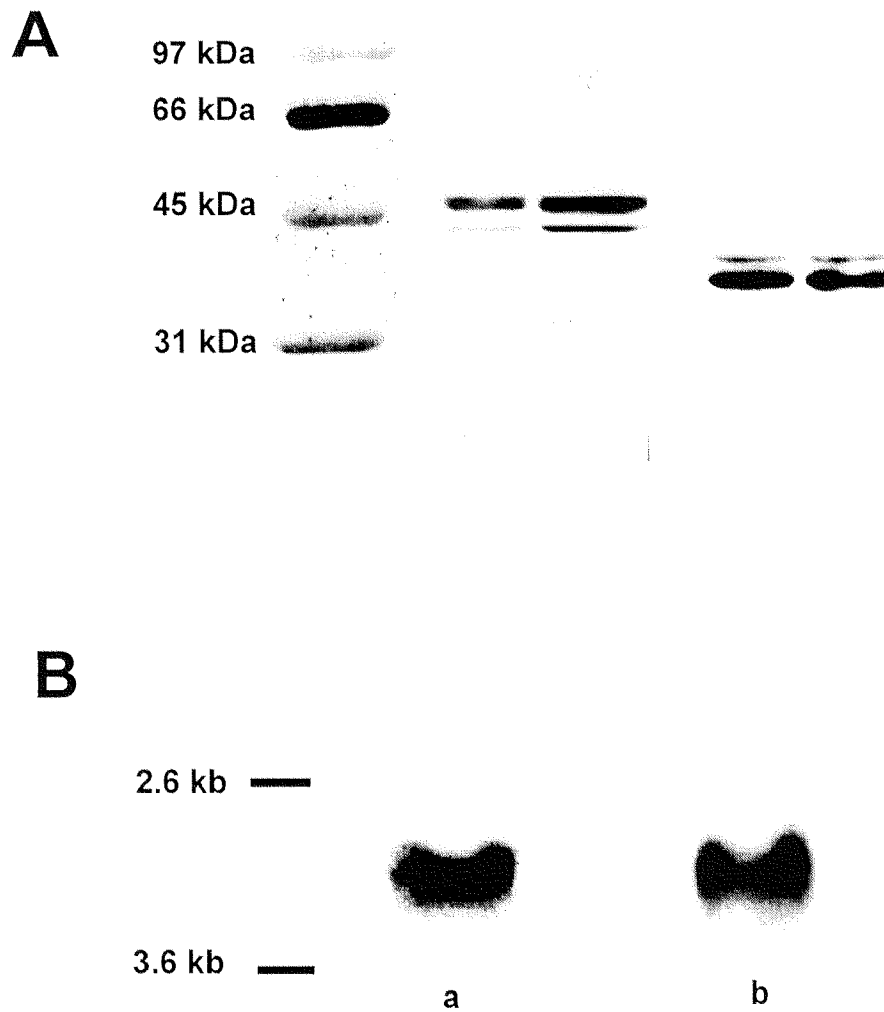
Fig.31 Effect of TPA on the Cx43 and Cx40 Expression

A- Immunoblot analysis of control (lanes a and c) and TPA treated (lanes b and d) cultures of adult rat cardiomyocytes with the anti-Cx43 (lines a and b) and the anti-Cx40 (lanes c and d) antibodies.

B - Northen Blot Analysis of Cx43. Total RNA were isolated from the adult rat ventricular myocytes cultured under standard conditions (lane a) or in the presence of 200 nM TPA (lane b), fractionated in a 1% agarose-formaldehyde gel, blotted onto nylon membranes, and hybridised with the alkaline phosphatase-labelled Cx43 probe. A single 3.0-kb band corresponding to the Cx43 mRNA was clearly detected in both samples. Cx43 mRNA expression did not change in the TPA treated cells.
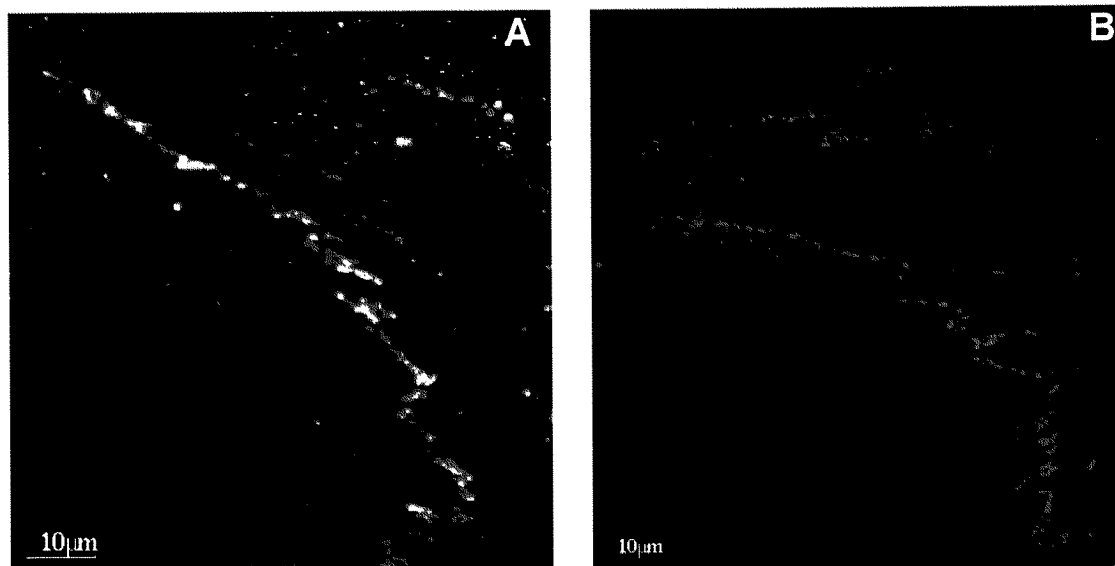
Fig.32 Immunolabelling of Cx43 in TPA treated Cells

ARC were double immunostained for Cx43 using the monoclonal anti-Cx43 antibody
raised against amino acid residues 252-271 (FITC, green) and the polyclonal antibody
against residues 314-322 (TxRed, red) at the Cx43 C-terminus. Panels show a specific
punctate labelling at the intercalated disks between cardiomyocytes (yellow: superim-
position of green and red). A - Control. B - TPA treated cells.

2.2.3 Long-term Treatment with TPA leads to p70S6 Activation in the Cardiomyocytes

TPA has been shown to activate p70S6 in different cell types [Nishimura and Deuel, 1983;
Blenis et al., 1984; Trevillyan et al., 1984]. To investigate the effect of TPA on the p70S6
expression in the long-term culture of ARC, Western blot analysis of the extracts prepared
from cells cultured in the presence of 200 nM TPA for a week was performed using the anti-
p70S6 kinase antibody. The results of the Western blot analysis demonstrated that the expres-
sion of the kinase was up regulated in the cells, which where grown in the TPA containing
medium (Fig.33A lane b). If the p70S6 inhibitor rapamycin was added to the cultures together
with TPA, then the expression of the p70S6 kinase returned to the control levels (Fig.33A lane
c). A week treatment of the cardiomyocytes with 1 nM rapamycin alone resulted in the strong
decrease of the p70S6 expression (Fig.33A lane d).

A

97 kDa

66 kDa

a   b   c   d

45 kDa

31 kDa

B

97 kDa

66 kDa

a   b   c   d

45 kDa

31 kDa
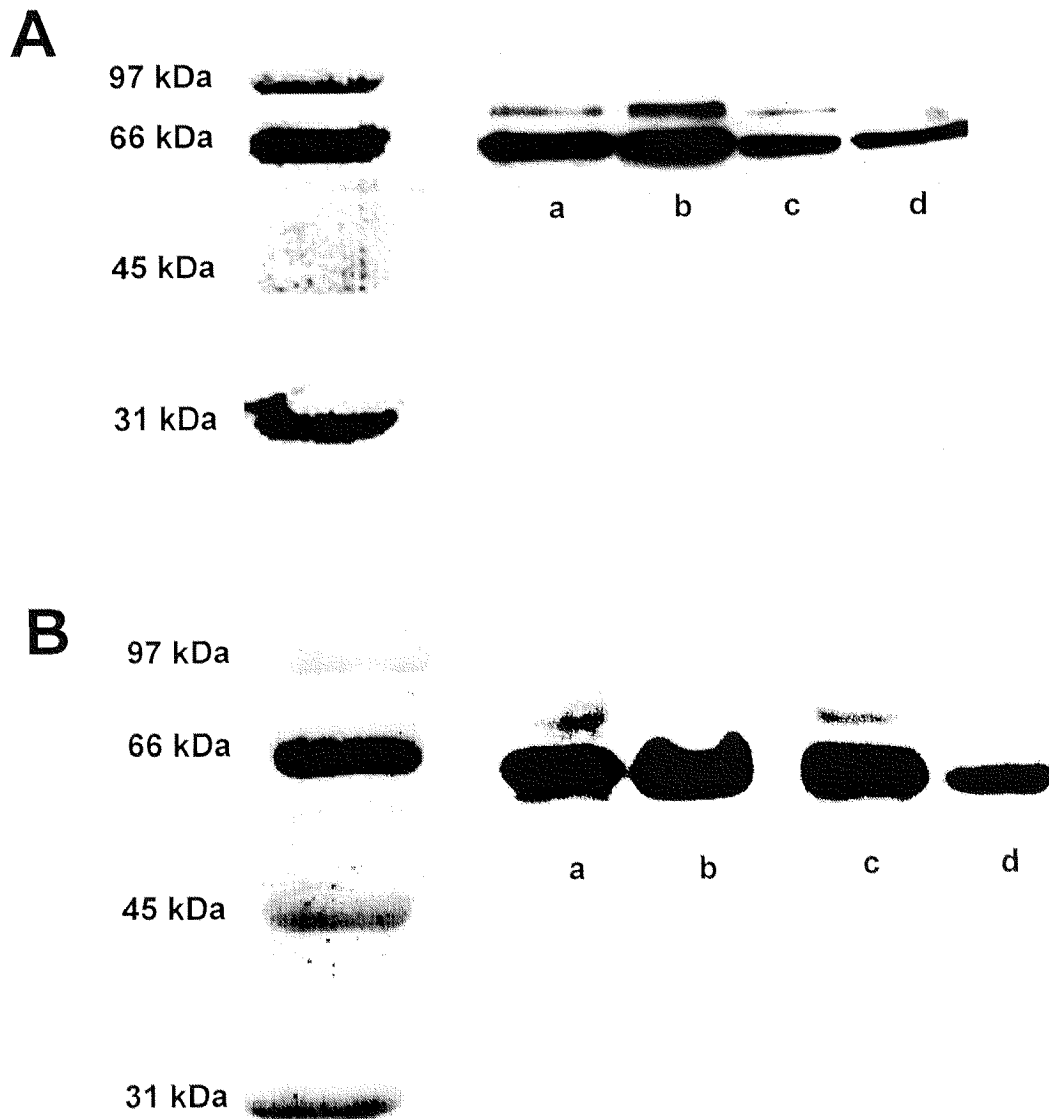
Fig.33 TPA Increases the p70S6 Expression in the Cultured Cardiomyocytes

A - The cell extracts of the 14 day untreated cardiomyocytes (a) and cardiomyocytes incubated with TPA (b), TPA and rapamycin (c), and rapamycin for a week were analysed by Western blotting with the anti-p70S6 antibody.

B- Western blot analysis of p70S6 in the cytosolic (a, c) and membrane (b, d) fractions of the cells treated with TPA (a and b) or TPA and rapamycin. (c and d)
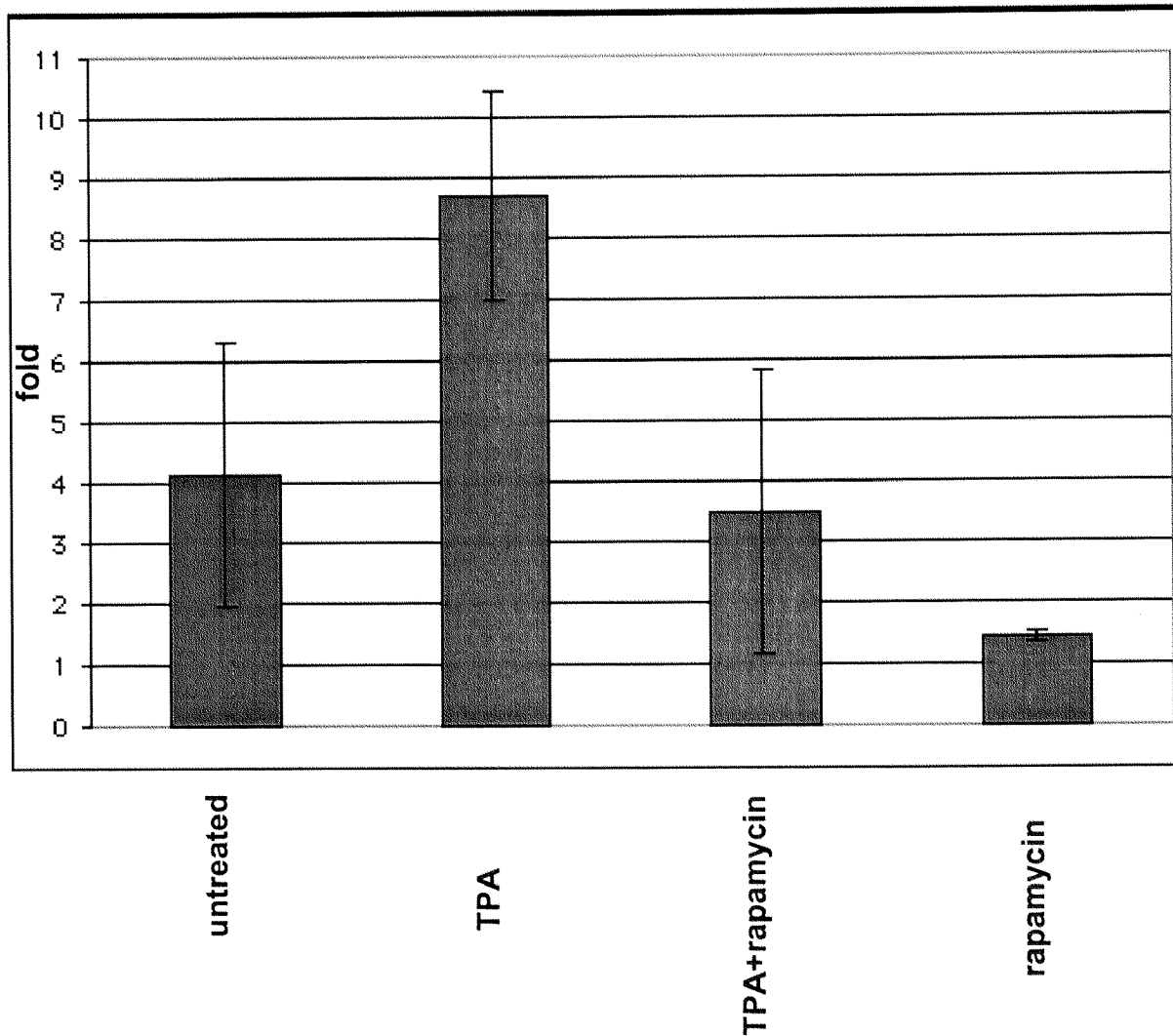
Fig.34 Effect of TPA on the p70S6 Kinase Activity in ARC

14 day cardiomyocytes were treated with 200 nM TPA, 200 nM TPA and 1 nM rapamycin, or 1 nM rapamycin for 7 days in culture. The activity of the p70S6 kinase immunoprecipitated from the cell extracts was assessed by S6 kinase assay. The control activity of the heat inactivated enzyme is designated as 1. The results shown are the mean± SD of four experiments, P<0.005.

Examination of the cytoplasmic and membrane fractions of the cardiomyocytes incubated with TPA or TPA and rapamyocin together demonstrated that TPA treatment significantly increased the amount of the membrane-associated p70S6 in the cells (Fig.33B lane b). Addition of rapamycin to the TPA treated cultures resulted in a specific down regulation of the membrane-anchored enzyme.

Measuring its ability to phosphorylate the S6 peptide in vitro assessed the p70S6 kinase activity. The p70S6 kinase was imunoprecipitated from the untreated, TPA-treated, TPA-and-rapamycin-treated and rapamycin-treated cultures and 1 µg of the protein from each sample was used for the S6 peptide assay (see Activation of p70S6 during the growth and re-differentiation of ARC in vitro). Data shown in Fig.34 demonstrate that the S6 peptide phosphorylation was significantly enhanced if the enzyme from the TPA-treated cells was used for the reaction. The statistical analysis showed that a week treatment of the cells with 200 nM TPA increased the enzyme activity by 2-fold in comparison to that in the cells cultured with no special treatments. The cardiomyocytes incubated with 200 nM TPA and 1 nM rapamycin together demonstrated the same level of the p70S6 kinase activity as that in the untreated cells. The p70S kinase activity in the cardiomyocytes incubated with 1 nM rapamycin was significantly lower than in the untreated cells. It did not differ much from a base line value measured with the heat-inactivated kinase.

2.2.4   Selective p70S6 Inhibitor Rapamycin Blocks the TPA-stimulated modification of Cx43 in the Cardiomyocytes

Starting at day 7, cardiomyocytes were treated either with 200 nM TPA, or with 200 nM TPA and 1 nM rapamycin, or solely with 1 nM rapamycin for one more week in vitro. The cells were fixed and immunolabelled with two different anti-Cx43 antibodies and Cy5-coupled phalloidin to check whether a selective p70S6 inhibitor rapamycin can affect the TPA-induced modification of the Cx43 molecule. As was described before, treatment of the cardiomyocytes with TPA resulted in the epitope masking and loss of the sensitivity of the monoclonal antibody raised against a synthetic peptide, which corresponds to the Cx43 C-terminal region between amino acid residues 252-271 and contains several phosphorylation sites. The other anti-Cx43 antibody used for the immunofluorescent analysis was polyclonal. It was produced against the Cx43 region between residues 314-322, which does not contain any phosphorylation sites, so that the antibody was able to recognise all three isoforms of the protein.

In the untreated cells, the signals from both Cx43 antibodies colocalised in the sites of the intercellular contacts (Fig.35A), whereas the signal from the polyclonal anti-Cx43 antibody only could be detected in the junctional membrane of the cells treated with TPA. The signal from the monoclonal anti-Cx43 antibody, which recognises solely the non-phosphorylated isoform of Cx43, was concentrated in the perinuclear region of the cardiomyocytes after the TPA treatment (Fig.35B). The distribution of both anti-Cx43 antibodies could be seen again in

the regions of cell-cell contacts between cardiomyocytes, if TPA and rapamycin were simultenously added to the cell culture medium (Fig.35C). Double immunostaining of the cardiomyocytes treated with rapamycin alone showed the patterns of the Cx43 distribution for both antibodies similar to those in the untreated ARC (Fig.35D).
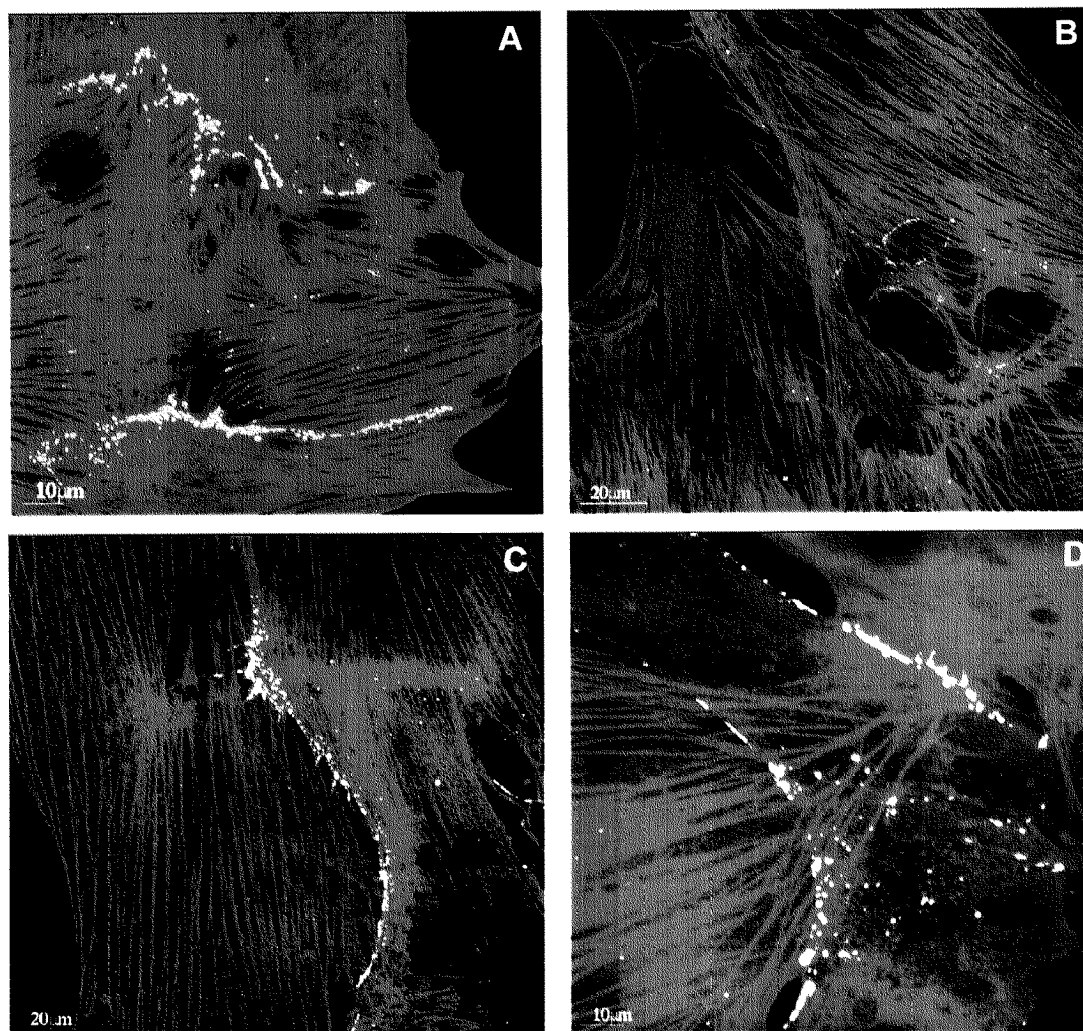
Fig.35 Rapamycin Prevents the TPA-induced Reduction of the Monoclonal Anti-Cx43 Antibody Staining in the Cell Contact Regions of Cultured Cardiomyocytes

14 day cultures of untreated cardiomyocytes (A) or the cells treated with TPA (B), TPA and rapamycin (C), and rapamycin (D) were indirectly immunolabelled with the monoclonal (FITC, green) and the polyclonal (Cy5, blue) anti-Cx43 antibodies. Actin cytoskeleton of the cells is visualised by rhodamin-conjugated phalloidin (red). White colour indicates the colocalisation of the signals from all three fluorescent probes; yellow - superimposition of the monoclonal anti-Cx43 antibody and actin stainings; violet - superimposition of the polyclonal anti-Cx43 antibody and actin stainings.

The non-phosphorylated isoform of Cx43 was concentrated in the perinuclear region of the TPA treated cardiomyocytes. The triple immunostaining of these cells with the monoclonal anti-Cx43 antibody, with an anti-ABL-70 antibody used as a marker for Golgi apparatus and Cy5-phalloidin demonstrated that the intracellular non-phosphorylated isoform of Cx43 accumulated in the medial Golgi cisternal membrane (Fig.36) under the experimental conditions.
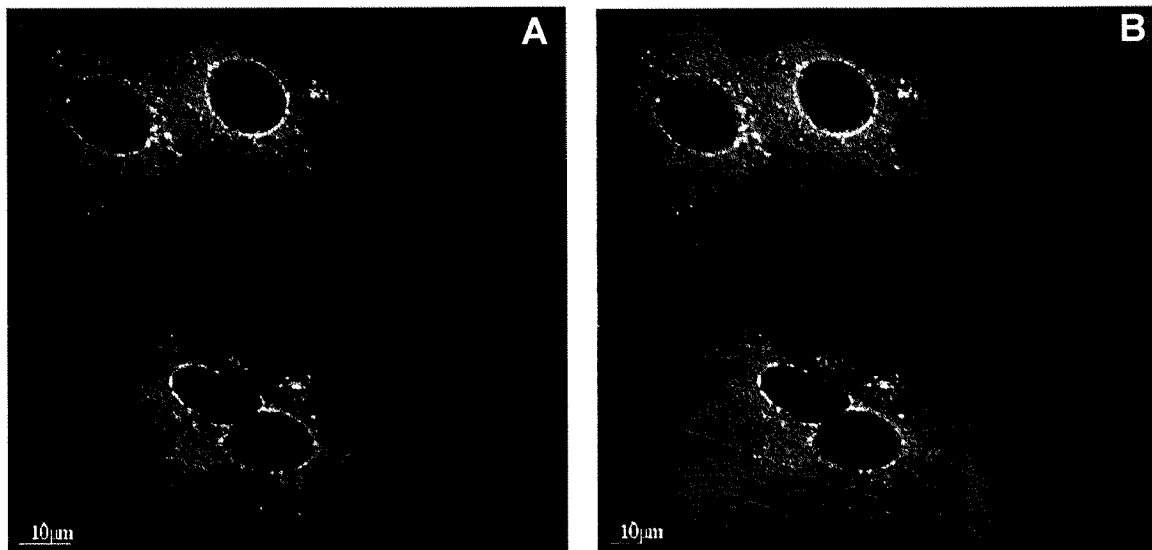
Fig.35 Cx43 Accumulates in the in Medial Golgi Cisternal Membrane in the TPA Treated Cells

Cardiomyocytes incubated in the presence of TPA for a week were fixed and subjected to the immunostaining with a mouse monoclonal anti-Cx43 antibody (FITC, green), a rat monoclonal anti-ABL-70 antibody (Tx Red, red) and Cy-5 labelled phalloidin. Images obtained with the confocal microscope were simultanously processed to monitor the colocalisation of the Cx43 antibody and the Golgi marker (A) and all three probes (B). A - the non-phosphorylated Cx43 and the medial Golgi cisternal membrane protein are shown in green and red respectively, yellow indicates the colocalisation of both signals in the perinuclear regions of the cells. B - overlay of the image shown in A with the total F-actin staining of the same cells.

To investigate the effect of TPA and rapamycin on the Cx43 expression and phosphorylation on the protein level, the lysates of the untreated cardiomyocytes and cardiomyocytes cultivated in the presence of TPA, TPA and rapamycin, and rapamycin alone were subjected to the immunoblot analysis using the polyclonal anti-Cx43 antibodies first. In the untreated

cells, the non-phosphorylated (NP) and two phosphorylated (P1 and P2) isoforms of Cx43 were detected (Fig.37A lane a). As it was shown before, the long-term exposure of cardiomyocytes to TPA resulted in the increase of total Cx43 protein in the cells (Fig.37A lane b). However, addition of rapamycin at the same time as TPA caused inhibition of the phosphorylation of Cx43 in the cardiomyocytes: both, Cx43P1 and Cx43P2 isoforms were absent (Fig.37A lane c). Rapamycin by itself induced a decrease in total Cx43 protein expression (Fig.37A lane d). However, the ratio between the phosphorylated isoforms and the non-phosphorylated one was not altered. After immunoblotting with the polyclonal anti-Cx43 antibody, the membranes were incubated in the stripping buffer (62.5 mM Tris, pH 6.7, 2% SDS, 100 mM β-mercaptoethanol) for 30 min at 50°C in order to dissociate the antibody-antigen complex and remove the antibody. After washing, the same blots were re-used for the Western blot analysis with the monoclonal anti-Cx43 antibody (Fig.37B). This antibody recognises only the non-phosphorylated isoform of Cx43, which has a higher electrophoretic mobility on the SDS-PAGE. The lysates of the cardiomyocytes treated with TPA (lane b) demonstrated an increase of Cx43-NP content in comparison to the untreated cultures (lane a). In addition to the 42-kDa non-phosphorylated isoform of Cx43, the antibody recognised a weak 43 kDa band, which was different from the phosphorylated isoforms detected with the poyclonal anti-Cx43 antibody in the lysates of the same cells. If ARC were incubated with TPA in the presence of rapamycin, the protein expression was found to return to the control level (lane c) and only the 42-kDa band was detected by Western blot. Rapamycin alone did not change the level of the protein expression in comparison to that in the control cultures (lane d).

In summary, the data described above demonstrate that a long-term treatment of cardiomyocytes with TPA results in a general increase in the Cx43 expression. They also imply that TPA induces the Cx43 phosphorylation in the C-terminal region between amino acid residues 252-271 of the protein, which can be abolished by the p70S6 inhibitor rapamycin. Moreover, the blockage of the TPA-stimulated Cx43 phosphorylation by rapamycin prevented the subsequent phosphorylation of the protein in the membrane.
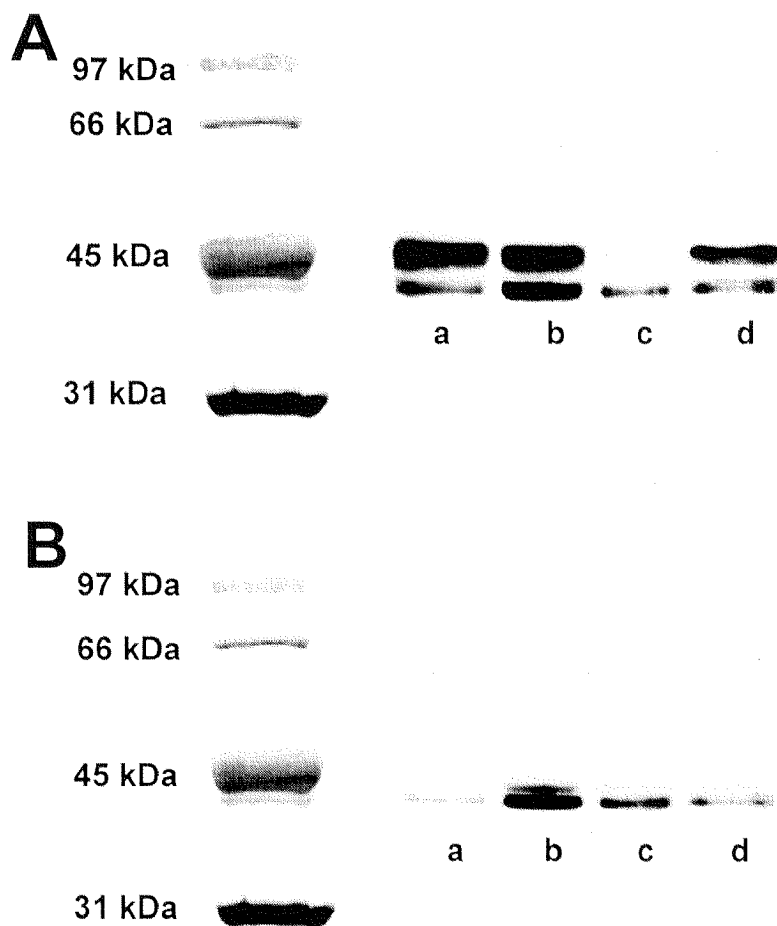
Fig.37 Effects of TPA and Rapamycin on the Cx43 Expression in the Cultured Cardiomyocytes

The cardiomyocyte extracts obtained from 14 day untreated cells (a), cells incubated with 200 nM TPA (b), 200 nM TPA and 1 nM rapamycin (c) and 1 nM rapamycin (d) for a week were analysed for Cx43 by immunoblotting with the monoclonal (A) and polyclonal (B) anti-Cx43 antibodies

2.2.5 The p70S6 Kinase and the TPA-induced Cx43 Phosphorylation

The inhibitory effect of rapamycin on the Cx43 phosphorylation raised the possibility that the C-terminal region of the connexin molecule between residues 252-271 may be a substrate for the p70S6 kinase. To check a possible intercellular colocalisation of Cx43 and p70S6, triple immunostaining of the cells was performed using the polyclonal anti-p70S6 antibody, the monoclonal anti-Cx43-NP antibody and Cy-5 phalloidin, which binds to filamentous actin. Immunocytochemical analysis revealed only the partial colocalisation of the p70S6 kinase with Cx43 in the regions of cell-cell contacts between untreated cells (Fig.38A). The treatment of the cells with TPA resulted in the accumulation of the non-phosphorylated Cx43 to the perinuclear region. The intensity of the p70S6 immunostaining in the membrane, within and around the cell nuclei increased in the same cultures. The distribution of Cx43-NP and p70S6 in the TPA treated cells demonstrates that both proteins colocalise in the perinuclear region (Fig.38B). If the cardiomyocytes were simultaneously exposed to TPA and rapamycin, the non-phosphorylated Cx43 was observed in the cell membrane again (Fig.25C). Association of p70S6 with the cell contact membrane was reduced. In cells treated with rapamycin, the pattern of the intracellular distribution of the non-phosphorylated Cx43 was the same as in the untreated cultures (Fig.38D). The intracellular level of p70S6 was lower than under control conditions. However, the membrane p70S6 colocalised with Cx43 in the contact regions between the cells. Hence, the immunocytochemical analysis showed that the p70S6 kinase and the non-phosphorylated isoform of Cx43 might have similar spatial distribution in the cells.

The amino acid sequence of rat Cx43 reveals that the region of the molecule between amino acid residues 252-271 contains two serines, which can be potential phosphorylation sites. The synthetic peptide corresponding to this region of the Cx43 molecule was used for the p70S6 kinase assay to test whether the kinase can phosphorylate it directly in vitro. The experimental samples contained the p70S6 kinase immunopurified from the cardiomyocyte cultures treated with TPA or TPA and rapamycin. The samples with addition of the denatured enzyme were used as controls. The results of the in vitro phosphorylation are presented in Fig.39. The incorporation of γP^{32}-ATP into the Cx43 peptide was increased 4-fold if the kinase from the TPA treated cells was used as the enzyme source for the reaction. Rapamycin inhibited the ability of the kinase to phosphorylate the Cx43 peptide. The activity of p70S6 in the cultures incubated with TPA and rapamycin together did not differ from controls. However, the enzyme was able to phosphorylate the S6 peptide in both cases as shown in Fig.34. Theses

data demonstrated that the synthetic peptide derived from the C-terminal region of Cx43 between residues 252-271 is a substrate for the TPA-activated p70S6 kinase in vitro.
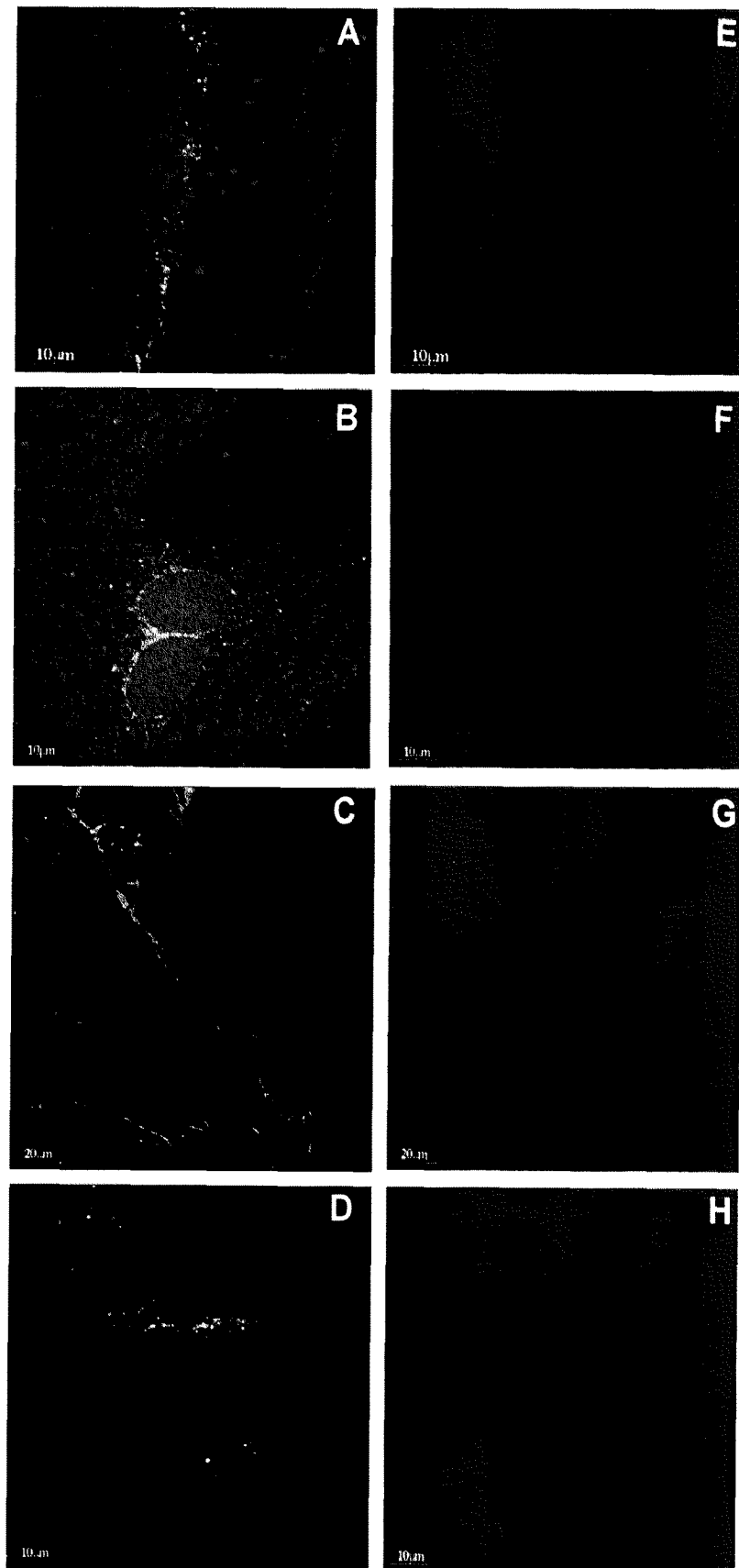
Fig.38 Effects of TPA and Rapamycin on the Subcellular Distribution of Cx43 and p70S6 in ARC

Cardiomyocytes cultured under standard conditions (A, E) or in the presence of TPA (B, F), TPA and rapamycin (C, G), and rapamycin (D, H) were imunostained for the non-phosphorylated isoform of Cx43, p70S6 (TxRed, red) and filamentous actin (Cy-5-phalloidin, blue). A, B, C, D - double immunostainig of the cells with the monoclonal anti-Cx43 antibody (FITC, green) and the polyclonal anti-p70S6 antibody (TxRed, red). E, F, G, H - F-actin staining of the cells (Cy-5-phalloidin, blue) shown in A, B, C and D respectively.

TPA   **TPA + rapamycin**
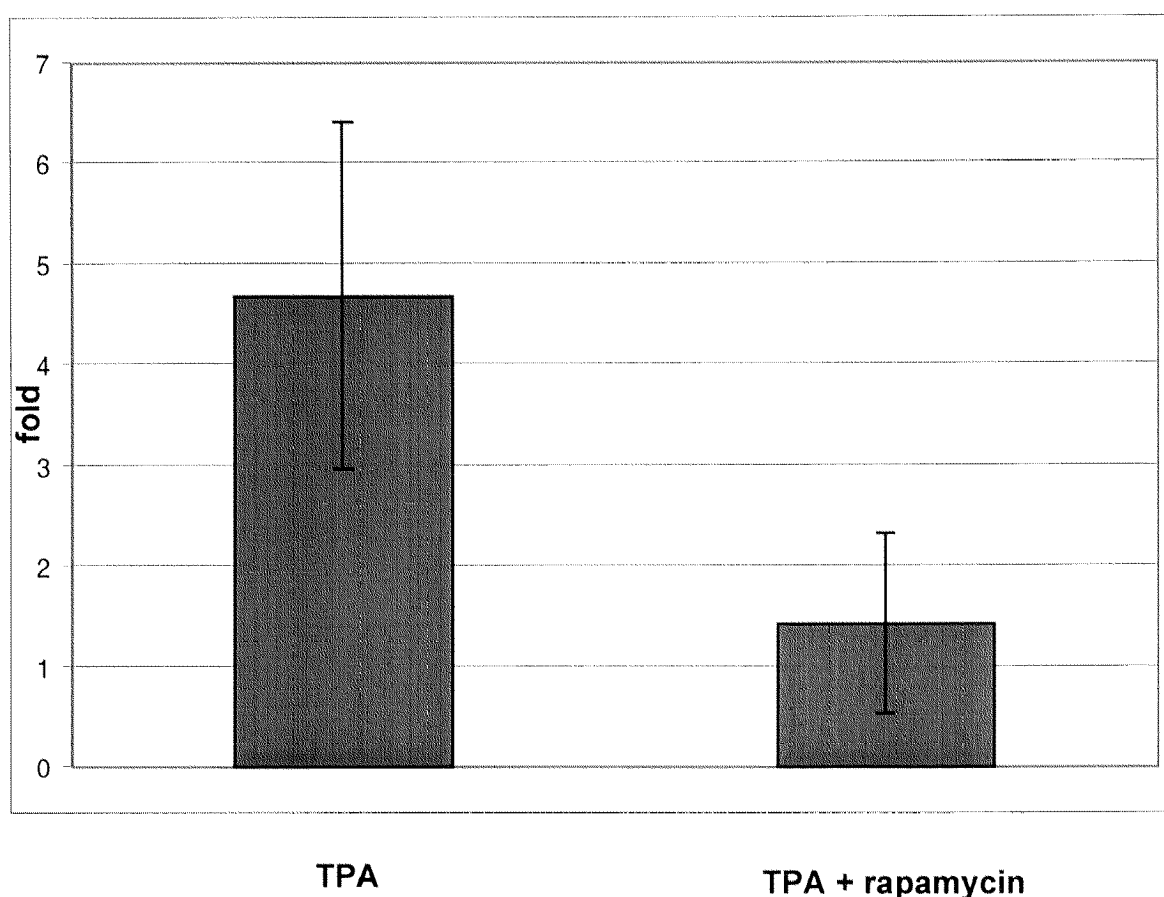
Fig.39 The p70S6 kinase is Able to Phosphorylate the Synthetic Cx43 Peptide In Vitro

The p70S6 kinase was immunoprecipitated from the cell extracts and incubated with the synthetic Cx43 peptide in the reaction buffer with γP^{32}-ATP. The aliquots of the supernatant were spotted onto P81 paper (Whatman), washed, dried and counted by the Cherenkov technique. The activity of the kinase, purified from the boiled lysates was designated as 1.0. The results shown represent the mean± SD of four experiments, $P < 0.005$.

Discussion

1. Expression of Connexins

1.1 Role of the Cx43 Phosphorylation during the Re-establishment of Intercellular Contacts between the Cardiomyocytes

Immunoblot and immunofluorescent analysis of freshly isolated and cultured cardiomyocytes using specific anti-connexin antibodies demonstrated that Cx40, Cx43 and Cx45 form gap junctions between cardiac cells in vivo and in vitro.

Cx43 is the major connexin expressed in the mammalian heart. It is a phosphoprotein and a target for protein kinases [Lau et. al., 1991]. The extent of the Cx43 phosphorylation and the presence of distinct phosphorylated forms are tissue specific and influenced by different signal transduction pathways [Kadle R. et.al., 1991]. In the present work, we detected three Cx43 isoforms: a non-phosphorylated form (NP) and two phosphorylated forms (P1 and P2). All three reside in the plasma membrane of freshly isolated cardiomyocytes. P1 and P2 disappeared when the adult cardiomyocytes in culture start to round up and spread out during the first few days in vitro. They reappeared parallel to the reformation of the intercalated disc-like structures between the cultured cells. The newly organised cell-to-cell contacts of re-differentiated adult cardiomyocytes contained all three types of specific intercellular junctions (desmosomes, adherens junction and gap junctions) and had re-established their link to myofibrillar structures via adhesion associated proteins [Hertig et al., 1996]. It has been shown before that the phosphorylation of gap junction proteins seems to depend on the presence of the intercellular adhesion molecules. For example, transfection of severely communication-deficient S180 cells with a cDNA encoding L-CAM corrected both the gap junction communication and the connexin 43 phosphorylation defects [Mege et. al., 1988]. Here it was demonstrated that the main connexin phosphorylation events in cultured cardiomyocytes take place during and after the assembly of gap junctions within the "mature", cytoskeleton associated regions of the cell-cell contacts. The intercellular adhesive complexes contain a number of proteins possessing a kinase activity. Recently it has been shown that the γ isoform of PKC is specifically associated with the junctional membrane of adult cardiomyocytes [Rouet-Benzineb et al.,

1996]. Conceivably, gap junction proteins may be a substrate for this or other adhesion associated kinases as well.

Cardiac connexins turn over very rapidly [Darrow et al., 1995]. The phosphorylation may serve to affect the degradation of connexins, thus contribute to the changes of their protein levels observed in the cultured cells. The degradation of proteins has been demonstrated to occur via either the lysosomal or proteosomal pathways. The lysosomal proteolysis is typical for the membrane and extracellular proteins, whereas cytosolic, nuclear and misfolded proteins transporting through endoplasmic reticulum and Golgi apparatus are mainly digested in proteosomes [Kopito, 1997]. Beardslee et al. [1998] has shown that perfusion of adult rat hearts with lysosomal inhibitors led to selective accumulation of phosphorylated isoforms of Cx43. This fact indicates that they reside in the plasma membrane of the cells. Treatment of the hearts with the proteasomal inhibitor caused an increase in the non-phosphorylated isoform and resulted in accumulation of Cx43 immunoreactivity at the cell surface. The last observation was inconsistent with the hypothesis that Cx43 phosphorylation is necessary for the hemi-channel formation and assembly in plasma membrane [Musil and Goodenough, 1991]. The results of the present study demonstrate that oligomeres formed by dephosphorylated Cx43 also reside in the cell membrane. Moreover, their number increases if the adherent junctions are artificially disrupted by Ca^{2+} depletion. The dephosphorylated Cx43 is able to stay in the non-junctional membrane of the former contact sites even when the other main protein of the cell adhesion complexes N-cadherin – gets internalised. Therefore, the Cx43 phosphorylation may be a consequence of the molecular clustering during the formation of adhesion complexes between the cells. This process has been shown to involve microfilaments in MHD-1 and RL C19 cells [Wang and Rose, 1995]. In general, connexin phosphorylation may be required to effectively increase the affinity of the lateral and/or homophilic interactions of connexons, which is important for the stabilisation of the cell-cell contacts when the re-differentiated cardiomyocytes regain their ability to contract in culture. In contrast, the non-phosphorylated Cx43 seems to form the hemichannels, which freely diffuse in the non-junctional membrane of the cells. It seems to be difficult to determine whether these non-junctional connexons are formed by not-yet-phosphorylated or already dephosphorylated Cx43. Therefore, the non-junctional connexons may represent a pool of either pre-existing hemichannels reserved for the subsequent quick delivery to the newly assembled site of the cell-to-cell contacts or the aggregates of misfolded proteins prepared for the degradation. However, it was found that the non-phosphorylated Cx43 recognised by the specific monoclonal antibody is still correctly targeted to the plasma membrane of single cardiomyocytes, which are not able to form cell-to-

cell contacts during their growth in culture. The existence of the non-junctional, plasma membrane Cx43 hemichannels has been demonstrated by Li et al. [1996]. These connexons could be induced to open upon reduction of extracellular calcium in LA35-NRK cells and in response to extracellular ATP in mouse macrophages expressing Cx43 [Steinberg et al., 1987]. The gating of the hemichannels has been found to be regulated by PKC and p60v-src tyrosine kinase in LA35-NRK cells. Therefore the Cx43 hemichannels observed in the non-junctional membrane of cultured cardiomyocytes should be closed under normal conditions, but could influence a conductive properties of the cell membrane in response to the specific stimuli.

Taken together these data demonstrate that the non-phosphorylated isoform of Cx43 forms connexons that are delivered to the cell surface. They are targeted to the cell-to-cell contacts as well as to the non-junctional area of plasma membrane and may represent two functionally different populations of hemichannels. One group of the connexin oligomeres is phosphorylated upon the insertion into the intercalated disk-like structures during the re-establishment of the intercellular communication between adult rat ventricular myocytes in vitro. The other group of connexons resides in the non-junctional cell membrane, stays unphosphorylated and shows no association with the cell adhesion structures.

1.2 Expression of Cx40 and Cx45 in Re-Differentiated Adult Ventricular Cardiomyocytes

The gap junction phosphoprotein Cx45 is expressed in ventricular cardiomyocytes. The gene transcription activity and the protein expression are high at the early stages of the heart development and cease with a progression to adulthood [Coppen et al., 1999]. Less than 10% of freshly isolated ventricular myocytes showed a positive signal after immunostaining with anti-Cx45 antibody. As for Cx43, the Cx45 expression was significantly down regulated in cardiomyocytes during the first two days after isolation, not allowing detection of the protein in cell pairs by the immunocytochemical technique. However, analysis of Cx45 in re-differentiated cardiomyocytes by a combination of the immunoblotting and immunostaining techniques showed a significant enhancement of the protein due to the increase of the cell population expressing this gap junction protein. Cx45 was present in the gap junctions of almost all cardiomyocytes after 2 weeks in vitro.

Expression of Cx40 has been detected in cardiomyocytes isolated from adult rat ventricles and cultured for longer periods. The antibody was able to recognise two bands with a molecular weight of 38 and 41 kDa, which corresponded to the non-phosphorylated and phosphorylated isoforms of Cx40. These results are consistent with the finding that Cx40 is present in phosphorylated and unphosphorylated forms in mouse heart during development [Delorme et. al., 1995]. The phosphorylation of Cx40 is strongly down regulated in rat ventricular cardiomyocytes during the transition from the neonatal to the adult stage, but the phosphorylation was found to be up regulated again in the re-differentiated heart muscle cells in culture.

Immunostaining of the cardiomyocytes showed the proper localisation of all three gap junction proteins in the regions of the cell-cell contacts. The co-localisation of Cx43 and Cx40 or Cx45 in the same gap junction documented in the present study raised the possibility of existence of heterotypic and/or heteromeric gap junction channel formation during the re-differentiation of ARC in vitro. The co-localisation of Cx40 and Cx45 could not been checked because of the polyclonal origin of the antibodies against the two connexins.

Presence of cardiac gap junction channels displaying asymmetric voltage dependence had been demonstrated between chicken embryonic cardiomyocytes (Chen and DeHaan, 1996). Since they express three different connexins, i.e. Cx42, Cx43 and Cx45, this has been attributed to heterotypic channels. The number of such channels has been shown to decrease with cardiac development and differentiation. Adult ventricular myocytes in long-term culture have been shown before to display adaptive changes in morphology and metabolism when a re-differentiated phenotype appear and re-expression of foetal genes could be observed [Eppenberger et al., 1994]. Therefore the Cx40 phosphorylation as well as the activation of the Cx45 expression in cultured adult ventricular cardiomyocytes may be the results of another switch to an early developmental program when the co-expression of cardiac connexins might be essential for the heart morphogenesis.

1.3 Regulation of Gap Junction Communication: an In Vitro Model of Myocardium Remodelling

The gap junction conductance is determined by the number of channels involved, the conductance of individual channels and their open-state probability. The number of gap junction channels between two cells seems to be depending on the size of the membrane contact area and the expression level of connexins. Cell isolation procedures disrupt intercellular contacts

in the cardiac tissue and produces single rod-shaped cardiomyocytes. The gap junctions show a dense organisation in the intercalated disc-like structures occupying its whole length after 2 days in culture (see Fig.22B and Fig.24B). Cultured cardiomyocytes establish in the first place new contacts by adherents junctions; their formation precedes the localisation of connexins to the contact membranes of the cells [Hertig et al., 1996]. However, it seems that the area of the gap junctional structure does not increase in parallel. The immunofluorescent labelling of connexins demonstrates a more dotted and disperse pattern of gap junctions in re-differentiated cardiomyocytes. Similar alterations in the organisation of gap junctions in vivo have been observed during the active phase of healing along the edges of infarction regions in dog hearts. Imunofluorescent studies have documented that viable myocytes lose the normal pattern of large gap junctions concentrated at the apical ends of myocytes and exhibit many small junctions which become uniformly distributed over the whole length of the cell contact [Peters et al., 1997]. In addition, the spatial remodelling of gap junctions in cultured adult car-diomyocytes represents the reverse process of the age-related changes in the distribution pat-terns of the intercellular junctions during postnatal development of human ventricular myocar-dium [Peters et al., 1994]. In the neonate, Cx43 gap junctions had a punctuate distribution over the entire surface of the ventricular myocytes. With advancing age, gap junctions become progressively confined to the transverse terminals of the cells. The fascia adherens junctions showed a similar progression. All these observations emphasise once more the importance of the in vitro studies of the adult cardiomyocyte re-differentiation.

The expression of Cx43 and Cx45, which form the low conductive gap junction channels is elevated as the process of the cardiomyocyte spreading and re-differentiation goes on. Therefore, the increase of the number of gap junction channels in the expanding area of cell-to-cell contacts is counterbalanced by a decrease of their single channel conductance. The dif-ferential expression of connexins forming the gap junction channels with specific transfer properties may help to maintain the quasi-constant level of the intercellular communication during the whole period of the cell development in vitro. Conceivably, the increase in cell vol-ume together with the nearly constant gj may lead to an acceleration of the electrical impulse in hypertrophic cardiac tissue, provided the excitatory inward currents remain constant.

2. Co-ordinated Regulation of the Cardiac Cell Growth and Cell-to-cell Communication.

2.1 TPA-Stimulated Increase of the Intercellular Communication between the Adult Rat Ventricular Cardiomyocytes *In Vitro*

Phorbol esters such as TPA, which are structural analogs of diacylglycerol are known to directly activate PKC in many cell types. In the heart, PKC has been implicated to be an intracellular mediator of some of the effects of α_1-adrenergic agonists, angiotensin, tumor promoters and growth factors. Irrespective of the mechanism of activation PKC has been shown to be involved in the hypertrophic response to α_1-adrenoreceptor stimulation in cardiomyocytes in vivo and in vitro [for a review see Schluetter and Piper, 1999]. Effects of TPA on cardiomyocytes have been investigated using different cell culture models, which were exposed to the drug for short and long periods. All experiments have demonstrated a critical role of TPA in various cellular processes in cardiomyocytes. Thus, Claycomb and Moses [1988] have shown that a long-term treatment of ventricular cardiomyocytes with TPA resulted in the alteration in the overall morphology of the cells. Terminally differentiated adult rat cardiac muscle cells lost their highly structured myofibrillar organisation: irregular Z-densities were often found in association with aggregation of thick and thin filaments. This has been shown earlier in vitro grown skeletal muscle cells by Doetschman and Eppenberger [1984]. In addition, TPA stimulated DNA synthesis and increases cellular RNA seemingly reverting ARC to a less-differentiated state when they were less structurally organised, but actively synthesised DNA. It is interesting that growth factors in the serum, which is normally added to the culture medium, had a similar effect on the reactivation of DNA synthesis in the adult cardiomyocytes [Claycomb and Brandshaw, 1983]. The other common response observed in TPA-treated cardiomyocytes was the accumulation of rough endoplasmic reticulum and free ribosomes. The presence of well-developed Golgi complexes was indicative of an increase in secretory activity. In neonatal cardiomyocytes, one of the consequences of PKC activation by TPA is the activation of transcription [Allo et al., 1991]. This may be at least partially mediated by the binding of the activator protein (AP-1) complex to a consensus sequence TRE (TPA responsive element) present in the promoter region of many genes [Deutsch, 1988].

Most of the cellular effects of TPA have been implicated in the regulation of the cardiomyocytes growth via PLCγ/PKC pathway. The role of TPA in the intercellular communication between cardiac muscle cells in culture has not been wel investigated yet. Only of Kwak [1995b], it has been shown that a short-term (10 min) exposure to 100 nM TPA increased macroscopic conductance, but decreased permeability and single channel gap junction conductance in the neonatal cardiomyocytes. The mechanisms of such an effect have not been revealed, but the result points to an opposite modulation of electrical and metabolic coupling of cardiac cells as evoked by TPA.

In the present study, it was demonstrated that a prolonged exposure of adult rat cardiomyocytes to 200 nM TPA increases metabolic coupling between the cells. It was shown by Western blot analysis that the Cx43 expression was elevated in the TPA treated cells, while the expression of Cx40 and N-cadherin were not altered. As it was mentioned before, TPA may facilitate the transcription of mRNA for different proteins. To examine whether TPA increased the transcription of the Cx43 gene, Northern blot analysis of the Cx43 mRNA isolated from control and induced cells was performed. This experiment did not reveal any difference in the level of the Cx43 mRNA in the cells grown with and without TPA. Therefore, the observed upregulation of Cx43 seems to be controlled at the level of protein translation, posttranslational modifications and targeting to plasma membrane.

Activation of PKC, PI3-kinase, and p70S6 kinase has been identified as key steps in stimulation of protein synthesis under α_1-adrenoreceptor stimulation [Simm et al., 1998]. Activated p70S6 phosphorylates the S6 protein of the 40-S subunits of the ribosomes and thus contributes to the increase of their translational activity. TPA and serum have been shown to activate p70S6 in several cell types [Nishimura and Deuel, 1983; Trevillyan et al., 1984; Blenis and Erikson, 1985]. Here it was demonstrated that both agonists are able to induce the p70S6 kinase activation in the cultured adult rat ventricular cardiomyocytes. The interesting fact was, that the effects of serum and TPA on p70S6 were cumulative. This allows to assume that growth factors and TPA contribute to the p70S6 activation via different signalling pathways, which lead to the initiation of growth in adult cardiomyocytes. Activation of cell growth may also result in the acceleration of the metabolic coupling between cardiomyocytes, which was observed in our cultures treated with TPA. Because Cx43 is a major connexin in the heart, its expression seems to be affected the most in the TPA-stimulated cells.

2.2 p70S6 Kinase and the Cx43 Phosphorylation

Besides the upregulation of total Cx43 protein in the adult cardiomyocytes, TPA induced loss of the monoclonal anti-Cx43 antibody binding capacity to the antigen detected by immunofluorescent analysis of the cells. Most probably, this was due to the modification of the native epitope in the Cx43 molecule. The antibody was raised against the synthetic peptide GPLSPSKDCGSPKYAYFNGC, which corresponds to the amino acid residues 252-271 of the C-terminal region of the rat Cx43 and contains two serine and two tyrosine residues. Cx43 is commonly phosphorylated; therefore, phosphorylation of Cx43 in the region between residues 252-271 of the C-terminus may be responsible for the epitope masking and the complete loss of antibody sensitivity to the antigen. A similar effect of TPA on the immunoreactivity of this antibody was observed in the neonatal cardiomyocytes treated with bFGF, where it was attributed to the phosphorylation of Cx43 in the C-terminal region of the molecule between residues 252-271 [Doble et al., 1996]. As already described before the p70S6 kinase is one of the enzymes, which has been shown to be activated by both, growth factors and TPA. Recent studies of de Groot et al. [1994] have demonstrated that in addition to the S6 protein of ribosomes p70S6 acts also on other targets in non-cardiac cells.

However, further experiments demonstrated that the signal from the monoclonal anti-Cx43 antibody, which recognises only the non-phosphorylated isoform of Cx43 on Western blot, was concentrated in the Golgi apparatus of the cardiomyocytes treated with TPA for a week. There was just no positive staining of the cell contacts. Similar pictures of the Cx43 accumulation in the Golgi were detected in the neonatal cardiomyocytes treated with monensin to inhibit the protein transport to plasma membrane [Puranam et al., 1993]. In this work it has also been demonstrated that Cx43 was initially phosphorylated to yield the intermediate Cx43 isoform immediately after synthesis or in the Golgi apparatus as well. The final Cx43 phosphorylation and conversion to the Cx43-P1 and Cx43-P2 has been predicted to occur at locations distal to the sites of monensin blockage in the Golgi. Therefore, it seems that Cx43 is phosphorylated at a specific site prior to phosphorylation at further sites in the cell membrane.

In the present work, Western blot analysis of Cx43 in the TPA treated cells was performed using the monoclonal anti-Cx43 antibody. In addition to the conventional 42-kDa band of the non-phosphorylated Cx43, the antibody recognised another band, which run at 43 kDa (Fig.37B lane b). This band was different from the highly phosphorylated isoforms of the protein detected with the polyclonal anti-Cx43 antibody. Therefore, TPA seemed to activate the

Cx43 expression and induced trapping of a significant amount of the partially phosphorylated protein in the trans-Golgi.

The p70S6 kinase assay performed with the synthetic Cx43 peptide, which corresponds to the amino acid residues 252-271 of the connexin C-terminus showed that the TPA-stimulated p70S6 kinase can phosphorylate the Cx43 peptide in vitro. The γP^{32}-ATP incorporation in the Cx43 peptide was smaller than in the S6 peptide determined under the same conditions. The lower radioactive signal detected from the Cx43 peptide could have several experimental reasons. Firstly, the filter-binding assay used in the experiments, needs the peptide to be positively charged to be able to bind to the negatively charged filter. The net positve charge of the Cx43 peptide was lower than that of the S6 peptide, so the amount of the Cx43 peptide absorbed by filters is expected to be less. Secondly, there are two serine residues, which are phosphorylated by p70S6 in the S6 peptide, but it could be possible that the kinase can phosphorylate only one of residue in the Cx43 peptide. Thirdly, equal amounts of the Cx43 peptide and S6 peptide were used for the reactions. However, the p70S6 kinase probably has different affinities and K_m's for each peptide. Taken together, these facts can explain the lower extend of the Cx43 peptide phosphorylation by p70S6 in vitro in comparison to the S6 peptide phosphorylation under the same conditions.

The selective p70S6 inhibitor rapamycin appeared to prevent the TPA induced activation of the Cx43 phosphorylation. After treatment of the cardiomyocytes with TPA and rapamycin, the non-phosphorylated isoform of Cx43 could be detected again in the regions of cell-to cell contacts by immunofluorescence. However, immunoblot analysis of the cell lysates with the polyclonal anti-Cx43 antibody demonstrated that the phosphorylation of the protein was dramatically inhibited: both phosphorylated isoforms of the protein were hardly detectable. The p70S6 kinase purified from these cells did not phosphorylate the Cx43 peptide. All these data point to the fact that the TPA-stimulated phosphorylation of the Cx43 molecule in the C-terminal cytoplasmic region between amino acid residues 252-271 may be mediated by p70S6. Moreover, this phosphorylation seems to be essential for further steps of the posttranslational modification of the protein in the membrane. It is interesting that the treatment of the cardiomyocytes with rapamycin alone, which inhibited the serum activated p70S6, did not affect the phosphorylation state of Cx43. It seems that TPA and serum activate the isoforms of the p70S6 kinase, which have different subcellular localisations. The active isoform of the p70S6 kinase was found to reside in the cytoplasm as well as in plasma membrane of cultured cells. TPA, which is soluble in the membrane, was shown to predominantly influence the membrane

associated p70S6, whereas the cytoplasmic pool of the kinase may be the target for growth factors. Subsequently, rapamycin preferentially downregulated the membrane-anchored p70S6 kinase, which is activated by TPA, and just slightly affected the cytoplasmic form of the enzyme. Therefore, the dramatic decrease in the Cx43 phosphorylation observed after the incubation of the cell with TPA and rapamycin could be explained by a loss of activity of the membrane-anchored p70S6 kinase.

In summary, long-term exposure of cardiomyocytes to TPA results in the activation of p70S6. Stimulation of the cytoplasmic pool of the kinase induces an increase in the Cx43 expression in the cells. The high level of the protein expression heightened its accumulation and processing in the Golgi apparatus. Activation of the membrane-associated p70S6 facilitates the incorporation of the increased amount of Cx43 into cell-to-cell contacts by phosphorylation of the specific cytoplasmic region of the protein. A co-ordinated increase in the Cx43 synthesis and phosphorylation stimulates the formation of new functional gap junctions and elevates the level of a metabolic co-operation between the cells. In that way the cardiac cell growth and cell-to-cell communication are coordinately regulated.

Open Questions and Outlooks

A long-term primary culture of adult cardiomyocytes represent a unique experimental system to study the mechanisms of heart tissue remodelling at the cellular level. Cardiomyocytes cultivated in serum-containing medium grow in size, establish new functional cell-to-cell contacts and form tissue-like sheets with no signs of cell migration or cell division. Eventually they restore spontaneous rhythmic activity.

The processes of cell growth and establishment of the intercellular communication are obviously mutually linked. However, details of the complex pathways mediating the transduction of growth signals and requiring multiple protein-protein interaction are only beginning to be uncovered. Participating in the activation of protein synthesis, the ribosomal S6 kinase probably plays a key role in the control of cell growth. Significant progress has been made during the last decade in the characterisation of the molecular mechanisms involved in the regulation of the enzyme activity, but the functional aspects of the kinase activation and its cellular distribution have not been properly investigated yet. The data obtained in the present study suggest that both inactive and active p70S6 isoforms have particular sites of location in cultured cardiomyocytes. The sensitivity of the enzyme isoforms to activators seems to depend on their subcellular localisation. Altered p70S6 localisation may also change accessibility of the kinase to protein substrates and thus affect its function. Indeed, it was found that a specific activation of the membrane-bound isoform of the p70S6 kinase by TPA facilitates the Cx43 phosphorylation in the sites of cell-to-cell contacts. Many questions remain to be answered. E.g. how does TPA trigger the activation or translocation of p70S6 into plasma membrane and where does the kinase encounter TPA? What is the role of the membrane lipids or lipid metabolites in the enzyme activation? What factors facilitate the kinase activity of the membrane form of p70S6 to interact with Cx43? Could the Cx43 phosphorylation induce the binding of other proteins to create clusters?

Similar to PKC isoenzymes and several other signalling proteins, isoform specificity of the p70S6 kinase may be mediated in part by association with special anchoring proteins. Therefore, it is interesting to pursue whether activation of p70S6 results in shuttling of the enzyme between different binding proteins and if so, what are the molecular mechanisms underlying these processes.

Organisation of proteins in a multiprotein complex might promote a cross talk between diverse signalling mechanisms. Intercalated disk-like structure established between ARC in

culture represent such association of specific proteins, which co-ordinate cellular functions like adhesion, intercellular communication and signal transduction, filtrating the input and output stimuli. Therefore, the potential therapeutic value of the selective regulators of these complexes is of great interest to both basic research and the pharmaceutical industry. Further characterisation of the intercalated disk structure at the molecular level should reveal new tiers for a potential cross talk between their structural and regulatory components. Various fluorescently tagged fusion proteins and peptides can directly be introduced into living cells to characterise the dynamic interactions and to determine the role of individual molecules in the cell function. Furthermore, these constructs can be used in high throughput assays to identify new drugs with selective inhibitor or activator activity.

References

Al A.F., Hatch D.S., Picot V., Crow D.S. (1991). Evidence that heart connexin 43 is a phosphoprotein. *J Mol.Cell. Cardiol..* **23**:659-663.

Allo S.N., MsDermott P.J., Carl L.L., Morga H.E. (1991). Phorbol ester stimulation of protein kinase C activity and ribosomal DAN transcription. *J.Biol.Chem.* **266**:22003-22009.

Aonuma S., Kohama Y, Akai K, Iwasaki S. (1980). Studies on heart. II. Further effects of bovine ventricle protein (BVP) and antiarrhythmic peptide (AAP) on myocardial cells in culture. *Chem.Pharm.Bull.* **28**:3340-3346.

Barr L., Dewey M.M., Berger W. (1965). Propagation of action potentials and the structure of the nexus in cardiac muscle. *J.Gen.Physiol.* **48**:797-823.

Barrio L.C., Handler A., Bennett M.V.L. (1993). Inside-outside and transjunctional voltage dependence of rat connexin 43 channels expressed in pairs of Xenopus oocytes. *Biophys.J.* **64**:A191.

Bastiaanse L.E.M., Jongsma H.J., van der Laarse A., Takens-Kwak B.R. (1993). Cardiac gap junctional conductance depends on the fluidity of membranous cholesterol-rich domains. *J.Membr.Biol.* **136**:135-145.

Bastide B., Neyses L., Ganten D., Paul M., Willecke K., Traub O. (1993). Gap junction protein connexin 40 is preferetially expressed in vascular endothelium and conductive bundles of rat myocardium and is increased under hypertensive conductions. *Circ.Res.* **73**:1138-1149.

Beardslee M.A, Laing J.G., Beyer E.C., Saffitz J.E. (1998). Rapid turnover of connexin 43 in the adult rat heart. *Circ.Res.* **83**:629-635.

Bevans C. G., Harris A. L. (1999a). Regulation of connexin channels by pH. Direct action of the protonated form of taurine and other aminosulfonates. *J Biol Chem..* **274**:3711-3719

Bevans C. G., Harris A. L. (1999b). Direct high affinity modulation of connexin channel activity by cyclic nucleotides. *J Biol Chem..* **274**:3720-3725.

Beyer E.C., Veenstra R.D., Kanter H.L., Saffitz J.E. (1995) in *Cardiac Electrophysiology. From Cell to Bedside.* (2nd edn) (Zipes D., Jalife J., eds), pp. 31-38, W.B. Saunders.

Blenis J., Erikson R.L. (1985). Regulation of a ribosomal protein S6 kinase activity by the Rous sarcoma virus transforming protein, serum, or phorbol ester. *Proc.Natl.Acad.Sci.USA.* **82**:7621-7625.

Boheler K.R., Chassagne C., Martin X., Wisnewsky C., Schwartz K. (1992). Cardiac expression of α-and β-myosin heavy chains and sarcomeric α-actinin are regulated through transcriptional mechanisms. *J.Biol.Chem.* **267**:979-985.

Brink P.R., Dewey M.M. 1980. Evidence for fixed charge in the nexus. Nature. 285:101-102.

Bukauskas F.F., Elfgang C., Willecke K., Weingart R. (1995). Biophysical properties of gap junction channels formed by mouse connexin 40 in induced pairs of transfected human HeLa cells. *Biophys.J.* **68**:2289-2298.

Bukauskas F. F., Peracchia C. (1997). Two distinct gating mechanisms in gap junction channels: CO_2-sensitive and voltage-sensitive. *Biophys J.* **72**: 2137-2142.

Burt J.M. (1987). Block of intercellular communication: interaction of intracellular H^+ amd Ca^{2+}. *Am.J.Physiol.* **253**:C607-C612.

Burt J.M., Spray D.C. (1988). Single-channel events and gating behavior of the cardiac gap junction channels. *Proc.Natl. Acad. Sci.USA..* **85**:3431-3434.

Burt J.M. and Spray D.C. (1988). Inotropic agents modulate gap junctional conductance between cardiac myocytes. *Am.J.Physiol.* **254**:H1206-1210.

Burt J.M., Spray D.C. (1989). Volatile anesthetic block intercellular communication between neonatal rat myocardiac cells. *Circ.Res.* **65**:829-837.

Burt J.M. (1989). Uncoupling of cardiac cells by doxyl stearic acids: specificity and mechanism of action. *Am.J.Physiol.* **256**:C913-924.

Calero G., Kanemitsu M., Taffet S.M., Lau A.F., Delmar M. (1998). A 17mer peptide interferes with acidification-induced uncoupling of Cx43. *Circ.Res.* **82**:929-935.

Camacho J.A., Peterson C.J., White G.J., Morgan H.E. (1990). Accelerated ribosome formation and growth in neonatal pig hearts. *Am.J.Physiol.* **258**:C86-C91

Campos-de-Carvalho A.C, Tamowitz H.B., Wittner M., et al. (1992). Gap junction distribution is altered between cardiac myocytes infected with *Trypanosoma cruzi.* *Circ.Res.* **70**:733-742.

Cascio M, Gogol E, Wallace BA (1990). The secondary structure of gap junctions. Influence of isolation methods and proteolysis.*J Biol Chem..* **265**:2358-64.

Caspar D.L.D., Goodenough D.A., Makowski L., Phillips W.C. (1977). Gap junction structures. I. correlated electron microscopy and X-ray diffraction. *J.Cell.Biol.* **74**:605-628.

Caulfield, J.B., and Wolkowica, P. (1988). Inducible collageneolytic activity in isolated perfused rat hearts. *Am.J.Pathol.* **131**: 199-205.

Chen. (1995). Identification of two regulatory elements within the promoter region of the mouse connexin 43 gene. *J.Biol.Chem.* **270**:3863-3868.

Chen Y.H., DeHaan R.L. (1996). Asymmetric voltage dependence of embryonic cardiac gap junction channels. *Am.J.Physiol.* **270**:C276-C285.

Chien K.R., Knowlton K.U., Zhu H., Chien S. (1991). Regulation of cardiac gene expression during myocardial growth and hypertrophy: molecular studies of an adaptive physiologic response. *FASEB J.* **5**:3037-3046.

Chilian W.M., Marcus M.L.(1987). Coronary vascular adaptations to myocardial hypertrophy. *Annu.Rev.Physiol.* **49**:477-487

Chou M.M. and Blenis J. (1995). The 70 kDa kinase: regulation of a kinase with multiple roles in mitogenic signalling. *Current Opinion in Cell Biology.* **7**:806-814.

Chung J., Kuo C.J., Crabtree G.R., Blenis J. (1992). Rapamycin-FKBP specifically blocks growth-dependent activation of and signalling by the 70 kDa S6 protein kinases. *Cell.* **358**:1227-1236.

Claycomb W.C., Palazzo M.C. (1980). Culture of the terminally differentiated adult cardiac muscle cells. A light and scanning electron microscopy study. *Dev.Biol.* **80**:466-482.

Claycomb W.C., Bradshaw H.D.Jr. (1983). Acquisition of multiple nuclei and the activity of DNA polymerase a and reinitiation of DNA replication in terminally differentiatedadult cardiac muscle cells in culture. *Dev.Biol.* **90**:331-337.

Claycomb W.C., Moses R. (1988). Growth factors and TPA stimulate DNA synthesis and alter the morphology of cultured terminally differentiated adult rat cardiac muscle cells. *Dev.Biol.* **127**:257-265.

Coppen S.R., Severs N.J., Gourdie R.G. (1999). Connexin 45 (alpha 6) expression delineates an extended conduction system in the embryonic and mature rodent heart. *Dev.Genet.* **24**:82-90.

Crow D.S., Beyer E.C., Paul D.L., Kobe S.S., Lau A.F. (1990). Phosphorylation of connexin 43 gap junction protein in infected and Rous sarcoma virus-transfored mammalian fibroblasts. *Mol.Cell.Biol.* **10**:1754-1763.

Dahl E., Winterhager E., Traub O., Willecke K. (1995). Expression of gap junction genes, connexin 40 and connexin 43, during fetal mouse development. *Anat.Embryol.* **191**:267-278.

Darrow B.J., Laing J.G., Lampe P.D., Saffitz J.E., Beyer E.C. (1995). Expression of multiple connexins in cultured neonatal ventricular myocytes. *Circ.Res.* **76**(3):381-387.

Davis L.M., M.E. Rodefeld, K.Green, E.C. Beyer, J.E.Saffitz. (1995). Gap junction protein phenotypes of the human heart and conduction system. *J Cardiovasc Electrophysiol.*. **6**:813-822

De Groot R.P., Ballou L.M., Sassone-Corsi P. (1994). Positive regulation of the cAMP-responsive activator CREM by the p70S6 kinase: an alternative route to the mitogen-induced gene expression. *Cell.* **79**:81-91.

Decker S. (1981). Phosphorylation of ribosomal protein S6 in avian sarcoma virus- transformed chicken embryo fibroblasts. *Proc.Natl.Acad.Sci. U.S.A.* **78**:4112-4115.

Dekker L.R., Fiolet J. W., VanBavel E., Coronel R., Opthof T., Spaan J. A., Janse, M.J. (1996). Intracellular Ca^{2+}, intercellular electrical coupling, and mechanical activity in ischemic rabbit papillary muscle. Effects of preconditioning and metabolic blockade *Circ.Res.***79**:237-246.

De la Bastie D., Levitsky D., Rappaport L., Mercardier J.-J., Marrote F., Wisnewsky C., Brovkovich V., Schwartz K., Lompre A.-M. (1990). Function of the sarcoplasmic reticulum and expression of its $Ca^{2(+)}$- ATPase gene in pressure overload-induced cardiac hypertrophy in the rat. *Circ.Res.* **66**:554-564.

De Leon J.R., Buttrick P.M., Fishman G.I. (1994). Functional analysis of the connexin 43 gene promoter in vivo and in vitro. *J.Mol.Cell Cardiol.* **26**:379-389.

Delorme B., Dahl E., Jarry-Guichard T., Marics I., Briand J.P., Willecke K., Gros D., Theveniau-Ruissy M. (1995). Developmental regulation of connexin 40 gene expression in mouse heart correlates with the differentiation of the conduction system. *Dev.Dyn.* **204**:358-371.

De Maziere A., Analbers L., Jongsma H.J., Gros D. (1993). Immunoelectron microscopic visualization of the gap junction protein connexin 40 in the mammalian heart. Eur.J.Morph.

De Mello W.C. (1976). Conductances, diffusion and streaming potentials in the rat proximal tubule. *J.Physiol.* **263**:171-197.

De Mello W.C. (1989). Effect of isoproterenol and 3-isobutyl-1-methylxanthine on junctional conductance in heart cell pairs. *Biochim.Biophys.Acta.* **101**:291-298.

De Mello W.C. (1994). Is an intracellular renin-angiotensin system involved in control of cell communication in heart? *J.Cardiovasc.Pharmacol.* **23**:640-646.

De Mello W.C. (1997). Influence of alpha-adrenergic-receptor activation on junctional conductance in heart cells: interaction with beta-adrenergic adrenergic agonists. *J.Cardiovasc.Pharmocol.* **29**:273-277.

Delorme B., Dahl E., Jarry-Guichard T., Marics I., Briand J.P., Willecke K., Gros D., Theveniau-Ruissy M. (1995). Developmental regulation of connexin 40 gene expression in mouse heart correlated with the differentiation of the conduction system. *Dev.Dyn.* **204**:358-371.

Delorme B., Dahl E., Jarry-Guichard T., Briand J.P., Willecke K., Gros D., Theveniau-Ruissy M. (1997). Expression pattern of connexin gene products at the early developmental stages of the mouse cardiovascular system. *Circ.Res.* **81**:423-437.

Deutsch P.J. (1988). Cyclic AMP and phorbol ester-stimulated transcription mediated by similar DNA elements that binds distinct proteins. *Proc.Natl. Acad.Sci.USA.* **85**:7922-7926.

Dhein S., Manicone N., Mueller A., Gerwin R., Ziskoven U., Irankhahi A., Minke C., Klaus W. (1994). A new synthetic antiarrythmic peptide reduces dispertion of epicardial activation recovery interval and diminishes alteration of epicardial activation patterns induced by regional ischaemia. A mapping study. *Naunyn-Schmiedeberg's Arch.Pharmacol.* **350**:174-184.

Dhein S., Poeppel P., Kruesemann K., Gottwald M. (1997). Changes in the intracellular distribution of connexin 43 after 24 hours of atrial fibrillation. Abstract in the Proceedings of International gap junction conference, Key Largo, USA.

Dhein S., (1998). Gap junction channels in the cardiovascular system: pharmacological and physiological modulation. *Trends Pharmacol Sci.* **6**:229-241.

Dillon M.S., Allessie M.A., Ursell P.C., Wit A.L. (1988). Influences of anisotropic tissue structure on reentrant circuits in the epicardial border zone of subacute canine infarcts. *Circ.Res.* **63**:182-206.

Doble B.W., Chen Y., Bose D.G., Litchfield D.W., Kardami E. (1996). Fibroblast growth factor-2 decreases metabolic coupling and stimulates phosphorylation as well as masking of connexin43 epitopes in cardiac myocytes. *Circ.Res.* **79**:647-658.

Doetschman C., Eppenberger H.M. (1984). Comparison of M-line and other myofibril components during reversible phorbol ester treatment. *Eur.J.Cell.Biol.* 33:265-274.

Dreifuss J.J., Girardier L., Forssmann W.B. (1966). Etude de la propagation de l'excitation dans le ventricule de rat au moyen de solutions hypertoniques. *Pfluegers Arch.* 232:13-33.

Dunnmon P.M. (1990). Phorbol esters induce immediate-early genes and activate cardiac gene transcription in neonatal rat myocardial cells. *J.Mol.Cell.Cardiol.* 22:901-910.

Ek J.F., Delmar M., Perzova R., Taffet S.M. (1994).Role of histidine 95 on pH gating of the cardiac gap junction protein connexin43. *Circ.Res.* 74:1058-1064.

Eppenberger M.E., Hauser I., Baechi T., Schaub M.C., Brunner U.T., Dechasne C.A., Eppenberger H.M. (1988). Immunocytochemical analysis of the regeneration of myofibrils in long-term cultures of adult cardiomyocytes of the rat. *Dev.Biol.* 130:1-15.

Eppenberger-Eberhardt M, Flamme I, Kurer V, Eppenberger H.M. (1990). Reexpression of alpha-smooth muscle actin isoform in cultured adult rat cardiomyocytes. *Dev Biol.* 139:269-278.

Eppenberger-Eberhardt M, Messerli M., Eppenberger H.M., Reinecke M. (1993). New occurence of atrial natriuretic factor and storage in secretorially active granules in adult rat ventricular cardiomyocytes in long-term culture. *J.Mol.Cell.Cardiol.* 25:753-757.

Eppenberger H.M., Hertig C., Eppenberegr-Eberhardt M. Adult rat cardiomyocytes in culture. (1994). A model system to study the plasticity of the differentiated cardiac phenotype at the molecular and cellular levels. *Trends Cardiovasc.Med.* 4:187-192

Ewart J.L., Cohen M.F., Meyer R.A., Huang G.Y., Wessels A., Gourdie R.G., Chin A.J., Park S.J., Lazatin B.O., Villabon S., Lo C.W. (1997). Heart and neural tube defects in transgenic mice overexpressing the Cx43 gap junction gene. *Development.* 124:1281-1292.

Falk M.M., Kumar N.M., Gilula N.B. (1995). In: *Intercellular communication through gap junctions. Progress in cell research* (**vol.4**). Kanno Y., Kataoka K., Shiba Y., Shibata Y., Shimazu T., eds. pp.319-322, Elsevier.

Ferrari S., Bannwarth W., Morley S.J., Totty N.F. Thomas G. (1992). Activation of p70s6k is associated with phosphorylation of four clustered sites displaying Ser/Thr-Pro motifs. *Proc.Natl.Acad.Sci. USA.* 89:7282-7286.

Francis D., Stergiopoulos K., Ek-Vitorin J. F., Cao F. L., Taffet S. M., Delmar M. (1999). Connexin diversity and gap junction regulation by pHi. *Dev.Gen.* 24:123-136.

Franco R. and Rosenfeld M.G. (1990). Hormonally inducible phosphorylation of a nuclear pool of ribosomal protein S6. *J.Biol.Chem.* **265**:4321-4325.

Fukiishi Y., Morris-Kay G.M. (1992). Migration of cranial neural crest cells to the pharyngeal and heart in rat embryos. *Cell Tissue Res.* **268**:1-8.

Fuller S.J., Gaitanaki C.J., Sugden P.H. (1990). Effects of catecholamines on protein synthesis in cardiac myocytes and perfused hearts isolated from adult rats. Stimulation of translation is mediated through the alpha 1-adrenoceptor. *Biochem.J.* **266**:727-736.

Gottwald E., Gottwald M., Dhein M. (1998). Enhanced dispertion of epicardial activation-recovery intervals at sites of histological inhomogeneity during regional cardiac ischemia and reperfusion. *Heart.* **79**:474-480.

Gourdie R.G., N.J. Severs, C.R. Green, S. Rothery, P. Germroth, R.P. Thompson. (1993). The spatial and relative abundance of gap-junctional connexin 40 and connexin 43 correlate to functional properties of components of the cardiac atrioventricular conduction system. J Cell *Science* . **105**: 985-991.

Gros D.B., Mosquard J.P., Challice C.E., Schrevel J. (1978). Formation and growth of gap junctions in mouse myocardium during ontogenesis. *J.Cell.Sci.* **30**:45-61.

Gros DB, Jongsma HJ. (1996). Connexins in mammalian heart function. *BioEssays..* **18**:719-730.

Grove J.R., Banerjee P., Balasubramanyam A., Coffer P.J., Price D.J., Avruch J., Woodgett J.R. (1991). Cloning and expression of two human p70S6 kinase polypeptides differing only at their amino termini. *Mol.Cell.Biol.* **11**:5541-5550.

Gupta I., Berthoud V.K., Atal V.M., Jarillo N., Beyer E.C. (1994). Bovine connexin 44, a lens gap junction protein: molecular cloning, immunologic characterization and functional expression. Invest. Ophtalmol. *Vis. Sci.* **35**:3747-3758.

Han J.-W., Pearson R.B., Dennis P.B., Thomas G. (1995). Rapamycin, wortmannin, and the methylxanthine SQ20006 inactivate p70^{s6k} by inducing dephosphorylation of the same subset of sites. *J.Biol.Chem.* **36**:21396-21403.

Henrich C.J., Simpson P.C. (1988). Differential acute and chronic response of protein kinase C in cultured neonatal rat heart myocytes to alpha 1-adrenergic and phorbol ester stimulation. *J.Mol.Cell.Cardiol.* **20**:1081-1085.

Hertig C.M., Butz S., Koch S., Eppenberger-Eberhardt M., Kemler R., H.M. Eppenberger. (1996). N-cadherin in adult rat cardiomyocytes in culture. II. Spatio-temporal appear-

ance of proteins involved in cell-cell contacts and communication. Formation of two distinct N-cadherin/catenin complexes. *J Cell Sci.* **109**:11-20.

Hertzberg E.L. (1997). Biochemistry of gap junctions: isoelectric focusing indicates that covalent modification(s) otheer than phosphorylation alteer connexin pIs. Abstract in the Proceedings of International gap junction conference, Key Largo, USA.

Homma N., Alvarado J.L., Coombs W., Stergiopoulos K., Taffet S.M., Lau A.F., Delmar M. (1998). A particle-receptor model for the insulin-induced closure of connexin 43 channels. *Circ.Res.* **83**:27-32.

Hoyt R.H., Cohen M.L., Saffitz J.E. (1989). Distribution and three-dimentional structure of intercellular junctions in canine myocardium. *Cir. Res.* **64**:563-574.

Huang G.Y., Thomas M., Michel P., Cooper E., Lo C.W. (1997). A role for CX43 gap junctions in the modulation of neural crest migration. *Mol.Biol.Cell.* **8**: 95a

Huang G.Y., Wessels A., Smith B.R., Linask K.K., Ewart J.L., Lo C.W. (1998). Alteration in connexin 43 gap junction gene dosage impairs conotrancul heart development. *Dev.Biol.* **198**:32-44.

Hunter T. (1995). When is a lipid kinase not a lipid kinase? When it is a protein kinase. *Cell.* **83**:1-4.

Izumo S., Lompre A.M., Matsuoka R., Koren G., Schwartz K., Nadal-Ginard B., Mahdavi V. (1987). Myosin heavy chain messenger RNA and protein isoform transitions during cardiac hypertrophy. Interaction between hemodynamic and thyroid hormone-induced signals. *J.Clin.Invest.* **79**:970-977.

Jacobson S.L. (1977). Culture of spontaneously contracting myocardil cells from adult rats. *Cell.Struct.Funct.* **2**:1-9.

Jefferies H.B.J., Fumagalli S., Dennis P.B., Reinhard C., Pearson R.B., Thomas G. (1997). Rapamycin supresses 5'TOP mRNA translation through inhibition of p70s6k. *EMBO J.* **16**:3693-3704.

Jeno P., Ballou L.M., Novak-Hofer I., Thomas G. (1988). Identification and characterization of a mitogen-activated S6 kinase. *Proc.Natl.Acad.Sci. U.S.A.* **85**:406.

Johnson M.F., Simon S.A., Ramon F. (1980). Interaction of anesthetics with electrical synapse. *Nature(Lond.).* **286**:498-500.

Johnson R.G., Meyer R.A., Lampe P.D. (1989). Gap junction formation: a "self-assembly" model involving membrane domains of lipid and proteins. In:*Cell interactions and gap junctions.* N. Sperelakis and W.Cole, editors. CRC Press, Boca Raton, FL. pp.159-179.

Joyner R.W., van Capelle F.J.L. (1986). Propagation through electrically coupled cells:how a small SA node drives a large atrium. *Biophys. J.* **50**:1157-1164.

Kadle R., Zhang J.T., B.J. Nickolson. (1991). Tissue specific distribution of differentially phosphorylated forms of Cx43. *Mol.Cell. Biol.* **11**:363-369.

Kanemitsu M.Y., Lau A.F. (1993). Epidermal growth factor stimulates the distruption of gap junctional communication and connexin 43 phosphorylation independent of 12-O-tetradecanoylphorbol, 13-acetate-sensitive protein kinase C: the possible involvement of mitogen-activated kinase. *Mol.Biol.Cell.* **4**:837-848.

Kanter H.L., Saffitz J.E., Beyer E.C. (1994). Molecular cloning of two human cardiac gap junction proteins, connexin 40 and connexin 45. *J.Mol.Cell.Cardiol.* **26**:861-868.

Kardami E., Liu L., Kishore S., Pasumarti B., Doble B.W., Cattini P.A. (1995). Regulation of basic fibroblast growth factor (bFGF) and FGF receptors in the heart. *Ann.NY Acad.Sci.* **752**:353-369.

Kirfhoff S.I., Nelles E., Hagendorf A., Krueger O., Traub O., Willecke K. (1998). Reduced cardiac conduction velocity and predisposition to arrhythmias in connexin40-deficient mice. *Curr.Biol.* **8**:299-302.

Koltin Y., Faucette L., Bergsma D.J., Levy M.A., Cafferkey R., Koser P.L., Johnson R.K. Livi G.P. (1991). Rapamycin sensitivity in Saccharomyces cerevisae is mediated by a peptidyl-prolyl cis-trans isomerase related to human FK506-binding protein. *Mol.Cell.Biol.* **11**:1718-1723.

Kopito R.R. (1997). ER quality control: the cytoplasmic connection. *Cell.* **88**:427-430.

Krutovskikh VA, Yamasaki H, Tsuda H, Asamoto M. (1998). Inhibition of intrinsic gap-junction intercellular communication and enhancement of tumorigenicity of the rat bladder carcinoma cell line BC31 by a dominant-negative connexin 43 mutant. *Mol Carcinog.* **23**(4):254-61

Kumar N.M. and Gilula N.B. (1996). The gap junction communication channel. *Cell.* **84**:381-388.

Kwak et al., (1995a). Differential regulation of distinct types of gap junction channels by similar phosphorylating conditions. *Mol.Biol.Cell.* **6**:1707-1719.

Kwak B.R. (1995b). TPA increases conductance, but decreases permeability in neonatal rat cardiomyocytes gap junction channels. *Exp.Cell.Res.* **220**:456-463.

Kwong K.F., Schuessler R.B., Green K.G., Laing J.G., Beyer E.C., Boineau J.P., Saffitz J.E. (1998). Differential expression of gap junction proteins in the canine sinus node. *Circ.Res.* **82**:604-612.

Laird D.W., Puranam K.L., Revel J.P. (1991). Turnover and phosphorylation dynamics of connexin 43 gap junction protein in cultured cardiac myocytes. *Biochem.J.* **273**:67-72.

Lal R. and Arnsdorf M.F. (1992). Voltage-dependent gating and single-channel conductance of adult mammalian atrial gap junctions. *Circ.Res.* **71**:737-743.

Lampe P.D., Kurata W.E., Warn-Cramer B.J., Lau A.F. (1998). Formation of a distinct connexin43 phosphoisoform in mitotic cells is dependent upon p34cdc2 kinase. *J. Cell. Sci.* **111**: 833-41.

Lane H.A., Fernandez A., Lamb N.J., Thomas G. (1993). p70^{s6k} function is essential for G1 progression. *Nature (Lond.)* . **363**:170-172.

Lau A.F., Kurata, W. E., Kanemitsu M. Y., Loo L. W., Warn-Cramer B. J., Eckhart W., Lampe P. D. (1996). Regulation of connexin43 function by activated tyrosine protein kinases. *J.Bioenerg. Biomembr.* **28**:359-368.

Li H., Liu T.-F., Lazrak A., Peracchia C., Goldberg G.S., Lampe P.D. (1996). Properties and regulation of gap junctional hemichannels in the plasma membranes of cultured cells. *J.Cell Biol.* **134**:1019-1030.

Lo C.W., Wessels A. (1998). Cx43 gap junctions in cardiac development. *Trend Cardio-vasc.Med.* **8**:264-269.

Luo H., Shan X., Wu J. (1996). Expression of human mitochondrial NADP-dependent isoci-trate dehydrgenase during lymphocyte activation. *J.Cell.Biochem..* **60**:495-507.

MacPhee D.J, Taylor C.V., Petrocelli T., Lye S.J. (1997). The relationship between Cx43 phosphorylation and trafficking during labour. Abstract in the Proceedings of International gap junction conference, Key Largo, USA.

Mazet F., Wittenberg B.A., Spray D.C. (1985). Fate of intercellular junctions in isolated adult rat cardiac cells. *Circ.Res.* **56**:195-204.

McNutt NS., Weinstein RS. (1970). The ultrastructure of the nexus. A correlated thin-section and freeze-cleave study. *Cell Biol* . **47**:666-88

McQuinn T. (1996). Molecular biological approaches to genetic cardiac diseases. *Prog.Pediat.Cardiol.* **6**:1-18.

Mege R.M., Matsuzaki F., Gallin W.J., Goldberg J.I., Cunningham B.A., Edelman G.M. (1988). Construction of epithelioid sheets by transfection of mouse sarcoma cells with cDNAs for chicken cell adhesion molecules. *Proc.Natl.Acad.Sci.* **85**:7274-72-78.

Meyuhas O., Avni D., Shama S. (1996). Translational control of ribosomal protein mRNA in eukaryotes. In Hershey J.W.B., Mathews M.B. and Sonenberg N. (eds.). *Translational Control.* Cold Spring Harbor Laboratory Press, Cold Spring Harbor, N.Y., pp363-388.

Ming X.-F., Burgering B.M.T., Wennstroem S., Claesson-Welsh L., Heldin C.H., Bos S., Kozma C., Thomas G. (1994). Activation of p70/p85S6 kinase by a pathway independent of p21ras. *Nature(Lond.)* **371**:426-429.

Moreno A.P., Eghbali B., Spray D.C. (1991). Connexin 32 gap junction channels in stably transfected cells: equilibrium and kinetic properties. *Biophys.J.* **60**:1267-1277.

Moreno A.P., Saez J.C., Fishman G.I., Spray D.C. (1994). Human connexin 43 gap junction channels. Regulation of unitary conductance by phosphorylation. *Circ.Res.* **74**:181-188.

Morgan H.E, Gordan E.E., Kira Y., Chua B.H.L., Russo L.A., Peterson L.J., McDermott P.J., Watson, P. A. (1987). Biochemical mechanisms of cardiac hypertrophy. *Annu.Rev.Physiol.* **49**:533-543.

Morgan H.E., Chua B.H.L., Russo L.A. In:Fozzard et al., (eds.). *The heart and cardiovascular system.* New York:Raven press. 1992. pp.1505-1524.

Morley G.E., Taffet S.M., Delmar M. (1996). Intramolecular interactions mediate pH regulation of connexin43 channels. *Biophys. J.* **70**:1294-1302.

Mueller A., Gottwald M., Tudyka T., Linke W., Klaus W., Dhein S. (1997a). Increase in gap junction conductance by an antiarrythmic peptide. *Eur.J.Pharmacol.* **327**:65-72.

Mueller A., Schaefer T., Linke W., Tudyke T., Gottwald M., Klaus W., Dhein S. (1997b). Action of the antiarrythmic peptide AAP10 on intercellular coupling. *Naunyn-Schmiedeberg's Arch.Pharmacol.* **356**:76-82.

Musil L.S., Cunningham B.A., Edelman G.M., Goodenough D.A. (1990). Differential phosphorylation of the gap junction protein connexin-43 in junctional communication-competent and –deficient cell lines. *J.Cell Biol.* **111**:2077-2088.

Musil L.S., Goodenough D.A. (1991). Biochemical analysis of connexin 43 intercellular transport, phosphorylation and assembly into gap junctional plaques. *J.Cell Biol.* **115**:1357-1374.

Musil L.S., Goodenough D.A. (1993). Multisubunit assembly of an integral plasma membrane channel protein, gap junction connexin 43, occurs after exit from the ER. *Cell.* **74**:1065-1077.

Nasmyth K. (1996). Retinoblastoma protein. Another role rolls in [news; comment]. *Nature.* **382**:28-29.

Nishimura J., Deuel T.F. (1983). Platelet-derived growth factor stimulates the phosphorylation of ribosomal protein S6. *FEBS Lett.* **156**:130-134.

Noma A., Tsuboi N. (1987). Dependence of junctional conductance on proton, calcium and magnesium ions in cardiac paired cells of guinea-pig. *J.Physiol.* **382**:193-211.

O'Brien J., Alubaidi M.R., Ripps H. (1996). Connexin 35: a gap-junctional protein expressed preferentially in the skate retina. *Mol.Biol.Cell.* **7**:233-243.

Ohayon, O., and Chadwick, R.S. (1990). Effects of collagen microstructure on the mechanics of the left ventricle. *Biophys.J.* **54**:1077-1088.

Oltra E., Werner R. (1997). Cloning of a potential regulatory protein involved in connexin 43 gene expression. Abstract in the Proceedings of International gap junction conference, Key Largo, USA.

Osawa H., Sutherland C., Robey R.B., Printz R.L., Granner D.K. (1996). Analysis of the signalling pathway involved in the regulation of hexokinase II gene transcription by insulin. *J.Biol.Chem.* **271**:16690-16694.

Ou, C. W., Orsino A.Lye S. J. (1997). Expression of connexin-43 and connexin-26 in the rat myometrium during pregnancy and labor is differentially regulated by mechanical and hormonal signals. *Endocrinology.* **138**:5398-5407.

Padua R.R., Fandrich R.R., Kardami E. (1993). Increased basic fibroblast growth factor accumulation and distinct patterns of localisation in isoproterenol-induced cardiomyocyte injury. *Growth Factors.* **8**:291-306.

Paul D.L. (1986). Molecular cloning of cDNA for rat liver gap junction protein. *J. Cell.Biol.* **110**:123-134.

Pearson R.B., Dennis P.B., Han J.W., Williamson N.A.,, Kozma S.C., Wettenhall R.E.H., Thomas G. (1995). The principal target of rapamycin-induced p70^{s6k} inactivation is a novel phosphorylation site within a concerved hydrophobic domain. *EMBO J.* **21**:5279-5287.

Pelech S.L., Olwin B.B., Krebs E.G. (1986). Fibroblast growth factor treatment of Swiss 3T3 cells activates a subunit S6 kinase that phosphorylates a synthetic peptide substrate. *Proc.Nat.Acad.Sci.USA.* **83**:5968-5972.

Perkins G, Goodenough D, Sosinsky G. (1997). Three-dimensional structure of the gap junction connexon. *Biophys J.* **72**:533-44

Peters N.S., Severs N.J., Rothery S.M., Lincoln C., Yacoub M.H., Green C.R. (1994). Spatiotemporal relation between gap junctions and fascia adherens junctions during postnatal development of human ventricular myocardium. *Circulation.* **90**:713-725.

Peters N.S. (1996). New insights into myocardial arrhythmogenesis:distribution of gap junctional couplinb in normal, ischaemic and hypertrophied human hearts. *Clin.Sci.* **90**:447-452.

Peters N.S., Coromilas J., Severs N.J., Wit A.L. (1997). Disturbed connexon 43 gap junction distribution correlates with the location of reentrant circuits in the epicardial border zone of healing canine infarcts that cause ventricular tachycardia. *Circulation.* **95**:988-996.

Price D.J., Grove J.R., Calvo V., Avruch J., Bierer B.E. (1992). Rapamycin-induced inhibition of the 70-kilodalton S6 protein kinase. *Science.* **257**:973-977.

Proud C.G. (1996). p70 kinase: an enigma with variations. Trends Biochem Sci. 21:181-185.

Pullen N. and Thomas G. (1997). The modular phosphorylation and activation of $p70^{s6k}$. *FEBS Letters.* **410**:78-82.

Puranam K.L., Laird D.W., Revel J.P. (1993).Trapping an intermediate form of connexin 43 in the Goldgi. *Exp. Cell Res.* **206**:85-92.

Rakusan K. In:Zak R.(ed.). *Growth of the heart in health and disease.* New York:Raven Press.1984. pp.131-164.

Reinhard C., Fernandez A., Lamb N.J.C., Thomas G. (1994). Nuclear localisation of p85s6k: functional requirement for entry into S phase. *EMBO J.* **13**:1557-1565.

Reaume A.G., de Sousa P.A., Kulkarni S., Langille B.L., Zhu D., Davies T.C., Juneja S.C., Kidder G.M.., Rossant J. (1995). Cardiac malformation in neonatal mice lacking Cx43. *Science.* **267**:1831-1834.

Revel J.P., Karnovsky M.J. (1967). Hexagonal array of subunits in intercellular junctions of the mouse heart and liver. *J.Cell.Biol.* **33**:C7-C10.

Rook M.B., Jongsma H.J., van Ginneken A.C.G. (1988). Properties of single gap junction channels between isolated neonatal rat heart cells. *Am.J.Physiol.* **255**: H770-H782.

Rouet-Benzineb P., Mohammadi K., Perennec J., Poyard M., El Houda Bouanani N., Croza-
tier B. (1996). Protein kinase isoform expression in normal and failing rabbit hearts.
Circ.Res. **79**:153-161.

Ruedisueli A., Weingart R. (1989). Electrical properties of gap junction channels in guinea-
pig ventricular cell pairs revealed by exposure to heptanol. *Pfluegers Arch.* **415**:12-21.

Rush P.S., Ek-Vitorin J.F., Delmar M., Lau A.F., Taffet S.M. (1997). In vitro phosphorylation
of Cx43 cytoplasmic tail is enhanced at lower pH. Abstract in the Proceedings of Inter-
national gap junction conference, Key Largo, USA.

Sadoshima J. and Izumo S. (1995). Rapamycin selectively inhibits angiotensin II-introduced
increase in protein synthesis in cardiac myocytes in vitro. Potential role of 70-kDa S6
kinase in angiotensin II-induce cardiac hypertrophy. *Circ.Res.* **77**:1040-1052.

Saffitz J.E., Kanter H.L., Green K.G., Tolley T.K., Beyer E.C. (1994). Tissue-specific deter-
minants of anisotropic conduction velocity in canine atrial and ventricular myocardium.
Circ.Res. **74**:1065-1070.

Saez J.C., Nairn A.C., Czernik A.J., Fishman G.I., Spray D.C., Hertzberg E.L. (1997). Phos-
phorylation of connexin 43 and the regulation of neonatal rat cardiac myocyte gap junc-
tions. *J.Mol.Cardiol.* **29**:2131-2145.

Schluetter K.-D., Piper H.M. (1999). Regulation of growth in the adult cardiomyocytes.
FASEB J. **13**: S17-S22.

Schwarzmann G., Wiegandt H., Rose B., Zimmermann A., Ben-Haim D., Loewenstein W.R.
(1981). Diameter of the cell-to-cell junctional membrane channels as probed with neu-
tral molecules. *Science (Wash.DC)*. **213**:551-553.

Seul K.-H., Tadros P.N., Beyer E.C. (1997). Mouse connexin40: gene structure and promoter
analysis. *Genomics.* **46**:120-126.

Severs N.J., Shovel K.S., Slade A.M., Powell T., Twist V.W., Green C.R. (1989). Fate of gap
junctions in isolated adult mammalian cardiomyocytes. *Cir.Res.* **65**:22-42.

Severs N.J., Slade A.M., Powell T., Twist V.W., Green C.R. (1990). Integrity of the dissoci-
ated adult cardiac myocyte: gap junction tearing and the mechanism of plasma mem-
brane resealing. *J.Muscle Res. and Cell Motility.* **11**:154-166.

Siehl D., Chau B.H.L., Lautensack-Belser N., Morgan H.E. (1985). Faster protein and ribo-
some synthesis in thyroxine-induced hypertrophy of rat heart Am.J.Physiol. 248:C309-
C319.

Simm A., Nestler M., Hoppe V. (1997). PDGF-AA, a potent mitogen for cardiac fibroblasts from adult rats. *J.Mol.Cell.Cardiol.* **29**:357-368.

Simon A.M, Goodenough DA, Paul DL.. (1998). Mice lacking connexin40 have cardiac conduction abnormalities characteristic of atriventricular block and bundle branch block. *Curr.Biol.* **8**:295-298.

Simm A., Schlueter K.-D., Diez C., Piper H.M., Hoppe J. (1998). Activation of p70S6k by b-adrenoreceptor agonists on adult cardiomyocytes. *J.Mol.Cell.Cardiol.* **30**:2059-2067

Sjoestrand F.S., Andersson-Cedergren E., Dewey M.M. (1958). The ultrastructure of the intercalated disc of frog, mouse and guinea pig cardiac muscle. *J. Ultrasruct.Res.* **1**:271-287.

Soehl G., Degen J., Teubner B., Willecke K. (1998). The murine gap junction gene connexin 36 is highly expressed in mouse retina and regulated during brain development. *FEBS Lett.* **428**:27-31.

Sporn M.B., Roberts A.B., Lalage M., Wakefield M., DeCrombrugghe B. (1987). Some recent advances in the chemistry and biology of transforming growth factor-beta. *J.Cell.Biol.* **105**:1039-1045.

Spray D.C., Harris L.A., Bennett M.V.L. (1981). Equilibrium properties of a voltage-dependent junctional conductance. *J.Gen.Physiol.* **77**:77-93.

Spray D.C., Burt J.M. (1990). Structure-activity relations of the cardiac gap junction channels. *Am.J.Physiology.* **258**:C195-C205.

Steere R.L., and Sommer J.R. (1972). Stereo ultrastructure of nexus faces exposed by freeze-fracturing. *J.Microsc.(Paris).* **15**:205-218.

Steinberg T.H., Newman A.S., Swanson J.A., Silverstein S.C. (1987). ATP^{4-} permeabilises the plasma membrane of mouse macrophages to fluorescent dyes. *J.Biochem.* **262**:8884-8888.

Stergiopoulos K., Alvarado J.L., Mastroianni M., Ek-vitorin J.F., Taffet S.M., Delmar M. (1999). Hetero-domain interactions as a mechanism for the regulation of connexin channels. *Circ.Res.* **84**:1144-1155.

Sugiura H., Toyama J., Tsuboi N., Kamiya K., Kodama I. (1990). ATP directly affects junctional conductance between paired ventricular myocytes isolated from guinea pig heart. *Circ.Res.* **66**:1095-1102.

Swenson K.I., Piwnica Worms H., McNamee H., Paul D.L. (1990). Tyrosine phosphorylation of the gap junction protein connexin 43 is required for the pp60v-src-induced inhibition of communication. *Cell.Regul* .**1**:989-1002.

Takano H., Komuro I., Zou Y., Kudoh S., Yamazaki T., Yazaki Y. (1996). Activation of p70S6 protein kinase is necessary for angiotensin II-induced hypertrophy in neonatal rat cardiac myocytes. *FEBS Lett.* **379**:255-259.

Takens-Kwak B.R., Jongsma H.J. (1992). Cardiac gap junctions: three distinct single channel conductances and their modulation by phosphorylating treatments. *Pfluegers.Arch.* **422**:198-200.

Thomas S. A., Schuessler R. B., Berul C. I., Beardslee M. A., Beyer E. C., Mendelsohn M. E., Saffitz, J. E. (1998). Disparate effects of deficient expression of connexin43 on atrial and ventricular conduction: evidence for chamber-specific molecular determinants of conduction. *Circulation.* **97**:686-691.

Trevillyan J.M., Kulkarni R.K, Byus C.V. (1984). Tumor-promoting phorbol esters stimulate the phosphorylation of ribosomal protein S6 in quiescent Reuber H35 hepatoma cells. *J.Biol.Chem.* **259**:897-902.

Tibbits T.T., Caspar D.L.D., Philips W.C., Goodenough D.A. (1990). Diffraction diagnosis of protein folding in gap junction connexons. *Biophys.J.* **57**:1025-103

Tokola H. (1994). Basal and acidic fibroblast growth factor-induced atrial natriuretic peptide gene expression and secretion is inhibited by staurosporine. *Eur.J.Pharm.* **267**:195-206.

Trevillyan J.M., Kulkarni R.K, Byus C.V. (1984). Tumor-promoting phorbol esters stimulate the phosphorylation of ribosomal protein S6 in quiescent Reuber H35 hepatoma cells. *J.Biol.Chem.* **259**:897-902.

Unger V.M., Kumar N.M., Gilula N.B., Yeager M. (1997). Projection structure of a gap junction membrane channel at 7A resolution. *Nature Struct.Biol.* **4**:39-43

Unger VM, Kumar NM, Gilula NB, Yeager M. (1999) Three-dimensional structure of a recombinant gap junction membrane channel. *Science.* **283**:1176-80.

Unwin P.N.T., Zampighi G. (1980). Structure of the junction between communicating cells. *Nature.* **283**:545-549.

Unwin P.N.T. (1987). Gap junction structure and the control of cell-to-cell communication. In: *Junctional complexes of epithelial cells.* New York: Wiley, 1987, p.78-91. (Ciba Foundation Symp. 125).

Valiunas V., Bukauskas F., Weingart R. (1997). Conductance and selective permeability of connexin 43 gap junction channels examined in neonatal rat heart cells. *Circ.Res.* **80**:708-719.

Van Kempen M.J., te Velde I., Wessels A., Oosthoek P.W., Gros D., Jongsma H.J., Moorman A.F., Lamers W.H. (1995). Differential connexin distribution accomodates cardiac function in different species. *Microsc.Res.Tech.* **31**:420-436.

Van Rijen H., van Kempen M. J., Analbers L. J., Rook M. B., van Ginneken A. C., Gros D., Jongsma H. J. (1997). Gap junctions in human umbilical cord endothelial cells contain multiple connexins. *Am. J. Physiol.* **272**: C117-30.

Vaughan-Jones R.D., Lederer W.J., Eisner D.A. (1983). Ca^{2+} ions can affect intracellular pH in mammalian cardiac muscle. *Nature (Lond.)* . **301**:522-524.

Veenstra R.D., Wang H.Z., Westphale E.M., Beyer E.C. (1992). Multiple connexins confer distinct regulatory and conductance properties of gap junctions in developing heart *Circ.Res.* **71**:1277-1283.

Veenstra R.D., Wang H.Z., Beblo D.A., Chilton M.G., Harris A.L., Beyer E.C., Brink P.R. (1995). Selectivity of connexin-specific gap junctions does not correlate with channel conductance. *Circ.Res.* **77**:1156-1165.

Verheulr S., van Kempen M.J.A., te Welscher P.H.J.A., Kwak B., Jongsma H.J. (1997). Characterization of gap junction channels in adult rabbit atrial and ventricular myocardium. *Circ.Res.* **80**:673-681.

Verrecchia F., Herve J.C. (1997). Reversible inhibition of gap junctional communication elicited by several classes of lipophilic compounds in cultured rat cardiomyocytes. *Can.J.Cardiol.* **13**:1093-1100.

Viragh S., Challice C.E. (1980). The development of the conduction system in the mouse embryo heart, III: the development of sinus muscle and sinoatrial node. *Dev.Biol.* **80**:28-45.

Wang H.-Z., Li J., Lemanski L.F., Veenstra R.D. (1992). Gating of mammalian cardiac gap junction channels by transjunctional voltage. *Biophys.J.* **63**:139-151.

Wang Y., Rose B. (1995). Clustering of Cx43 cell-to-cell channels into gap junction plaques: regulation by cAMP and microfilaments. *J.Cell.Sci.* **108**:3501-3508.

Warn-Cramer B.J., Lampe P.D., Kurata W.E., Kanemitsu M.Y., Loo L.W., Eckhart W., Lau A.F. (1996). Characterisation of the mitogen-activated protein kinase phosphorylation sites on the connexin-43 gap junction protein. *J.Biol.Chem.* **271**:3779-3786.

Warner A., Clemens D.K., Parkikh S., Evans W.H., DeHaan R.L. (1995). Specific motifs in the external loops of connexin proteins can determine gap junction formation between chick heart myocytes. *J. Physiol.* **288.** 721-728.

Weber, K.T., Pick, R.,Jalil, J.E., Janicki, J.S., and Carroll, E.P.(1989). Patterns of myocardial fibrosis. *J.Mol.Cell.Cardiol.* **21**(suppl.5):121-131.

Weihe, E., and Kalmbach, P. (1978). Ultrastructure of capillaries in the conduction system of the heart in various mammals. *Cell Tissue Res.* **192**: 77-87.

Weng Q.-P., Andrabi K., Kozlowski M.T., Grove J.R., Avruch J. (1995). Multiple independent inputs are required for activation of the p70 S6 kinase. *Mol.Cell.Biol.* **15**:2333-2340.

White R.L., Doeller V.K., Verselis V.K., Wittenber B.A. (1990). Gap junctional conductance between pairs of ventricular myocytes is modulated synergistically by H^+ and Ca^{2+}. *J.Gen.Physiol.* **95**:1061-1075.

Widers R., Jongsma H.J. (1992). Limitation of the dual voltage clamp method in assaying conductance and kinetics of gap junction channels. *Biophys.J.* **63**:942-953.

Willecke K., Buchmann A., Butzler C., Gabriel H-D., Hagendorf A., Jung D., Kirchhoff S., Kruger O., Nelles E., Schwarz M., Temme A., Traub O., Winterhager E. Biological functions of gap junctions revealed by targeted inactivation of mouse Cx32, -26 and –40 genes. In:Werner E. ed. *Gap junctions.* Amsterdam. Netherlands: IOS Press; 1998:304-308.

Woodcock-Mitchell J., Mitchell J.J., Low R.B., Kieny M., Sengel P., Rubbia L., Skalli O., Jackson B., Gabbiani G. (1989). Alpha-smooth muscle actin is transiently expressed in embryonic rat cardiac and skeletal muscles. *Differentiation* . **39**:161-166.

Wu J., McHowat J., Saffitz J.E., Yamada K.A., Corr P.B. (1993). Inhibition of gap junctional conductance by long-chain acylcarnitines and their preferential accumulation in junctional sarcolemma during hypoxia *Circ.Res.* **72**:879-889.

Yeager M., Gilula N.B. (1992). Membrane topology and quaternary structure of cardiac gap junction ion channels. *J.Mol.Biol.* **223**:929-948.

Zahringer J. and Klaubert A. (1982). The effect of triiodothyronine on the cardiac mRNA. *J.Mol.Cell.Cardiol.* **14**:559-571.

Zak R. (1973). Cell proliferation during cardiac growth. *Am.J. Cardiol.***31**:211-219

Seite Leer /
Blank leaf

TITANIUM DIOXIDE CERAMICS CONTROL

THE DIFFERENTIATED PHENOTYPE

OF CARDIAC MUSCLE CELLS IN CULTURE

Summary

A new approach, the cultivation of heart muscle cells on biocompatible scaffolds made from titanium dioxide ceramics was worked out to provide a mechanism for in vitro engineering of viable heart tissue. Terminally differentiated ventricular myocytes isolated from hearts of adult rats were kept in primary culture for long periods of time and used as an experimental model. The microenvironmental properties of titania ceramics helped to maintain the tissue-like structural organisation of the cardiac cells in vitro. Coating of the cell substrata with fine-grained titania ceramics imitating cell surface topography favoured the formation of focal adhesion complexes in the ventral plasma membrane of cardiomyocytes. It also promoted the cellular expression of vinculin, a protein that connects the ECM integrin receptors to the network of cytoplasmic filaments, which define cell shape. This topographical reinforcement of cell-material interactions led to the stabilisation of the molecular linkage between the extracellular contacts and the intracellular cytoskeleton and thus assisted the preservation and maintenance of the heart muscle cell differentiated phenotype in long-term primary culture. The results of this work demonstrate a promising pathway for the regulation of cellular organisation in vitro by local geometric control.

Zusammenfassung

Eine neue Methode wurde ausgearbeitet, welche die in vitro Konstruktion von lebensfähigem Herzgewebe zu ermöglich soll. Das Ziel war die Kultivierung von Herzmuskelzellen auf biokompatiblen Gerüststrukturen aus Titaniumdioxid-Keramik. Terminal differenzierte ventrikuläre Myozyten, die von Herzen adulter Ratten isoliert worden waren, wurden über längere Zeitperioden in Primärkulturen gehalten und als experimentelles Modell verwendet. Die Eigenschaften der Mikroumgebung von Titaniumkeramik halfen mit, die gewebeähnliche Organisation der Herzzellen in vitro zu erhalten. Das Bedecken der Zellsubstrate mit feinkernigen Titaniumkeramiken, welche die Topographie der Zelloberfläche imitieren, begünstigte die Bildung von konzentrierten Adhäsionskomplexen in der ventralen Plasmamembran von Kardiomyozyten. Ebenso wurde die zelluläre Expression von Vinculin gefördert, einem Protein, das u.a. die ECM Integrin-Rezeptoren mit dem Netzwerk der zytoplasmatischen Filamente verbindet, welche die Form der Zelle bestimmen. Diese topographische Verstärkung der Interaktionen von Zellen und Substrat führte zu einer Stabilisierung der Molekularen Bindung zwischen den extrazellulären Kontakten und dem intrazellulären Zytoskelett. Sie unterstützte so die Aufrechterhaltung des differenzierten Phenotyps der Herzmuskellzellen in langfristigen Primärkulturen. Die Resultate dieser Arbeit zeigen einen vielversprechenden Weg, wie die Zellorganisation in vitro durch lokale geometrische Kontrolle reguliert werden kann.

Introduction

1. Long-term Primary Culture of Adult Cardiomyocytes

Adult rat ventricular cardiomyocytes (ARCs) represent a cell culture model biomedical research on heart tissue [Jacobson and Piper, 1986]. They are frequently used to study cell-substrate and cell-cell interactions as well as signalling pathways under defined condition [Stemmer et al., 1992]. The advantage of such primary cell cultures is that the cells are fully differentiated and retain many characteristics of adult cardiomyocytes of intact heart, but lack interstitial tissue and other cell types which can complicate measurements in whole organs or animal models. The isolation procedure yields single rod shaped ventricular myocytes from adult heart tissue. During the first two days in culture in the presence of serum these cells attach to the bottom of a gelatine coated plastic dish and undergo a process of spreading and re-differentiation in which their morphology and myofibrillar apparatus are remodelled [Eppenberger et al., 1988]. Cardiomyocytes grow in size, establish new cell-cell contacts and restore rhythmic contraction without movement or cell division. The sequence of phenotypic changes is accompanied by the re-expression of a number of mRNA, e.g. for the precursor of atrial natriuretic peptide (ANF), as well as of isoforms of contractile proteins more typical for neonatal or fetal cardiomyocytes [Claycomb, 1988; Eppenberger- Eberhardt et al., 1990]. These processes are similar to the adaptive enlargement of myocytes during cardiac hypertrophy that may occur as a result of heart dysfunction [Eppenberger- Eberhardt et al., 1993].

To a certain extent the removal of ARC from the neurohumoral milieu and the absence of mechanical load in vitro may induce these developmental alterations. A number of investigations have been performed to design experimental conditions that favour the maintenance of the adult cardiac myocyte phenotype in long-term primary culture. Higher plating densities [Horakova and Mapplebeck, 1989] and defined media enriched with specific factors [Nag and Cheng, 1981] as well as the use of the suspension culture method [Qi et al., 1996] or serum-free culture technique [Ellingsen et al., 1993] help to preserve the elongated rod-shaped phenotype similar in morphology to the freshly isolated adult myocytes for up to 1 week in vitro, although cell atrophy and detachment inevitably occur over time.

2. Titanium Dioxide Ceramics as a Substrate for Cell Culture

The high biocompatibility of titanium has been demonstrated [Zarb and Branemark, 1985]. The positive influence is due to its passive layer on the surface, consisting of titania [Kasemo et al., 1988]. Titania shows a low solubility in water and exhibits a highly hydrophilic surface [Fartash et al., 1995]. It has already been shown that titania ceramics used as cell-culture substrate, have favourably influenced the maintenance of the original cardiomyocyte morphology in long-term culture [Polonchuk et al., 1997]. The substrates used in the above mentioned paper had a rough topography due to the granular material structure and due to its porosity [Eckert et al., 1997]. Therefore it was highly motivatius to investigate the role of the topography in the cellular response to titania ceramic scaffolds.

3. Focal Adhesion Complexes

3.1 Molecular Structure of Cell-extracellular Matrix Contacts

In cultured cells, cell-substrate contacts known as focal contacts (FC) play a central role in the maintenance of a reciprocal flow of signalling information between cells and the surrounding microenvironment. These submembrane junction complexes form three-dimensional networks of interacting proteins that link the integrin-type adhesion receptors to the cytoskeleton. FC are readily seen as vinculin-containing tear-shaped plaques at the ends of actin filaments [Koch-Schneidermann et al., 1994]. Their formation is associated with the process of cell spreading. Vinculin anchors myofibrils and stress fiber-like structures of cultured cariomyocytes to sarcolemma (see Fig.1). The protein is found only in adhesion complexes that are in direct contact with the extracellular matrix [Goncharova et al., 1992]. The focal contacts are likely to be dynamic and heterogeneous in molecular composition. Integrins, protein kinases and phosphatases, diverse signalling and docking molecules colocalise with vinculin in the adhesion plaque [for a review see Yamada and Geiger, 1997] (Fig.1). Therefore the regulation of the assembly and reassembly of these multi-protein complexes by changing substrate adhesivity provides the molecular mechanism for modulation of cell shape in culture. In

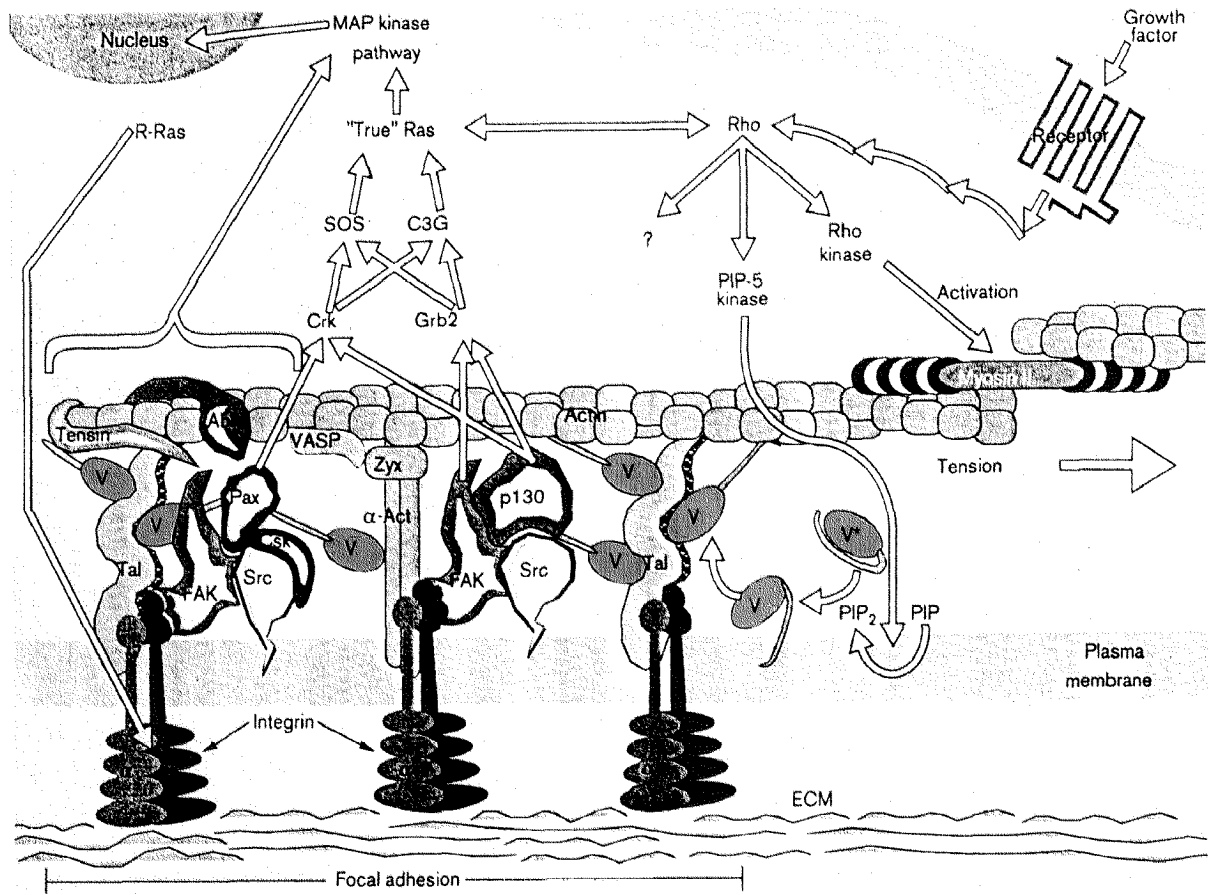addition, cell shape per se may cause cells to switch between different genetic programs [Chen et al., 1997].

Fig.1   Molecular Interactions in Cell Adhesion Complexes

(from Ben-Ze'ev A. (1997). "Cytoskeletal and adhesion proteins as tumor supressors". *Current Opinion in Cell Biology*. 9:99-108)

Actin filaments are linked to the ECM via αβ integrins and by the plaque proteins talin (Tal) and α-actinin (α-Act). Vinculin (V, pink) has actin-, tali- and α-actinin-binding sites and can stabilise the link between thses structural components, but can also fold into a conformation (V*) with masked binding sites. Membrane phospholipid phosphatidylinositol 4,5-biphosphate (PIP$_2$) can interact with a number of actin-binding proteins to promote actin polymerisation, and can stimulate the transition of vinculin from nonactive conformation (V*) to one capable of talin- and actin binding (V). Protein tyrosine kinases FAK, Src, Csk and Abl are also localise at focal adhesions. Paxillin (Pax), tensin, and p130cas (p130) are substrates for tyrosine phosphorylation. Other components of focal adhesion include an α-actinin-binding protein zyxin (Zyx) that can bind to vasodilator-stimulated phosphoprotein (VASP) which can, in turn, bind to actin filaments.

3.2 Use of Ventral Membrane Preparations to Study the Focal Adhesion Assembly in Cultured Cardiomyocytes

The formation of adhesion complexes is physically controlled when a cell attaches to an ECM substrate. In cultured cardiomyocytes, the ventral membrane was suggested to be involved in the formation of so-called submembraneous assembly sites (SAPs), which are thought to function as the nucleation sites for myofibril formation [Lu et al., 1992]. Visualisation of the cell-matrix adhesions formed in culture can be performed using the lysis-squirting technique. The procedure introduced by Mazia et al. [1974] has been successfully applied for the preparation of ventral membranes of several cell types [Clarke et al., 1975; Nermut, 1982; Cattelino et al., 1995]. The cells are first lysed in hypotonic buffer and then squirted with a stream of buffer from a syringe. It is obvious that structures, which withstand such a treatment, adhere firmly to the substratum and that structural elements found in the ventral membrane are specifically associated with it. Here for the first time an ultrastructural analysis of the protoplasmic surface of the plasma membrane of ventricular myocytes adherend to the substrate in culture has been made. It is thought to be a useful tool to characterise the three-dimensional structure of the cell-material interface.

Objective of the Study

Establishment of the appropriate differentiated phenotype in vivo and in cell culture depends on the co-ordinated interactions between cell adhesion molecules and the local environment. Cell attachment and spreading on the substrate induce myofibril organisation in cultured myocytes. These processes depend on the nature of the surface coating [Hilenski et al., 1989]. Therefore an alternative approach to influence the growth of cardiac cells in vitro may be the cultivation of the cells on biocompatible scaffolds that can determine the morphology of the developing culture.

In the present work the effect of surface topography on the cell phenotype in vitro was investigated. For this purpose, substrates with different topographies were coated with titania ceramics using the sol-gel technique [Elbel et al., 1998a]. By this procedure chemically uniform coatings were produced on different substrates. These coatings mask not only the difference in chemical composition of the substrates, but also impose an additional topography in the nanometer range [Elbel et al., 1998b]. This kind of topography is similar to that of the cell plasma membrane and may control the patterns of cell attachment, thus affecting local cell-material interactions at the molecular level. Hence, it was set out to determine whether the organisation of the focal adhesion complexes of cardiomyocytes grown on titania ceramics can be controlled solely by patterning the substrate.

The maintenance of morphological characteristics of cardiomyocytes grown on scaffolds coated with sol-gel derived titania was one parameter used to estimate the success of this cell culture method. After plating, primary adherence and phenotypic changes of cardiac cells grown on biocompatible scaffolds were investigated using scanning electron microscopy (SEM). Immunostaining and confocal microscopy (CLSM) were applied to characterise the heart cell structure. Focal adhesion sites were visualised in the cardiomyocyte ventral plasma membranes by SEM. Immunoblotting and immunofluorescence labelling of vinculin, a focal contact protein, were used to perform a quantitative and qualitative analysis of the focal contact assembly.

Materials and Methods

1. Preparation of Cell-Culture Scaffolds

Scaffolds with different surface roughness were prepared from commercially available glass cover slips (R_a= 0.075 +/- 0.041 um), commercially available alumina substrates (R_a=0.33625 um +/- 0.0092), (CeramTech, Germany) and titania ceramic discs (R_a= 0.97 +/- 0.256 um) [Blum et al., 1996]. These substrates were coated with a sol-gel derived titania layer. The titania sol was prepared by hydrolysing titaniumisopropoxide (Fluka, Switzerland) in isopropanol (Fluka, Switzerland) in a mixture of H_2O (dest.) and 65% HNO_3 (Fluka, Switzerland). The molar ratio was chosen as H_2O / Ti^{4+} = 200; H+ / Ti^{4+} = 0.2. To adjust viscosity and to prevent the coatings from cracking during heat treatment, hydroxyethylcellulose (HEC, Fluka, Switzerland) was added to the sol as a binder. Dip coating was performed by immersing the substrates into the sol and retracting them at a rate of 0.5-mm s-1. After 12 h drying in ambient atmosphere the coatings were sintered at 500° C for 1 h. The scaffolds were cleaned with ethanol and placed in 24-well culture dishes.

AFM surface characterisation of the substrates and the granular structure of the sol-gel-derived coatings was performed by a Nanoscope IIIa microscope (Digital Instruments). AFM investigations were performed by using tapping-mode" in air.

2. Cell Culture

Adult rat ventricular myocytes were isolated and cultured from adult female Sprague-Dawley rats as previously described [Eppenberger-Eberhardt et al., 1990]. Rats were anesthesised with Nembuthal, hearts were excised and then perfused retrogradely through the ascending aorta (Langendorff preparation) with a Ca^{2+}-free Joklik solution (Cell Culture Technologies, Switzerland) followed by the same buffer containing collagenase. After 30 min of perfusion, the atria and great vessels were removed, and the remaining ventricular tissue was minced, dissociated in the collagenase solution, filtered, and washed once with Joklik containing 0,5 mM Ca^{2+} for obtaining Ca^{2+} tolerance. The final pellet was resuspended in the standard cell culture medium M-199 supplemented with 2,5% horse serum, creatine, and penicillin/streptomycin, plated in 24-well cell culture dish (Nunc, Denmark) containing cell carriers and placed at 37°C, 5% CO_2, 95% humidity. Fibroblast growth was suppressed by addition of

cytosine arabinoside (10 μM) throughout the whole period of the heart cell cultivation. Medium change was done after 2 and 7 days.

3. MTT Cytocompatibility Assay

Cell survival was assessed by the MTT assay, which measures intracellular dehydrogenase activity [Mosmann, 1983]. At intervals, MTT stock solution (5 mg/ml) was added to each well of the 24-well culture plate being assayed to equal one tenth the medium volume and incubated 1,5h at 37°C. Absorbance of converted dye was measured at a wavelength of 580 nm after ethanol elution.

4. Scanning Electron Microscopy

After 9 days in culture, cells were fixed in 3% glutaraldehyde in PBS, dehydrated in a graded alcohol series, critically point dried with CO_2 and examined with a SEM (Hitachi S-2500C).

5. Ventral Membrane Preparation

The lysis squirting technique [Nermut, 1982] was used to expose ventral membranes of cardiomyocytes for microscopic observation. Cells were washed with ice-cold PBS and incubated for 2 min on ice in PIPES buffer (20m PIPES, 100mM KCl, 5mM $MgCl_2$, 3 mM EGTA, pH6). After washing with 20% hypotonic PIPES buffer they were squirted over by using a jet of the ice-cold buffer, immediately fixed with 3% glutaraldehyde and processed for SEM observations or immunofluorescence analysis.

6. Immunostaining

Ventricular cardiomyocytes were fixed according to conventional protocols [Asai, 1993] in 3% PFA (15 min at RT) and then permeabilised in 0,2% Triton X-100 (10 min at RT). Ventral membranes of the cells were prepared as described above, fixed with 3% glutaraldehyde and directly used for the immunolabelling reaction. The cells and ventral membrane samples were incubated with primary antibodies (overnight at +4°C), washed with PBS and

exposed to secondary antibodies for 1h at room temperature in the dark. The preparations were rinsed in PBS and mounted in galat-glycerol mounting medium.

The monoclonal antibodies against myomesin prepared in our laboratory have been characterised before [Grove et al., 1984]. The filamentous actin specific reagent phalloidin-RITC, which recognises all isoforms of actin, was purchased from Sigma. Immunolabelling of vinculin was performed with monoclonal anti-vinculin antibodies from Genex (Finland). The secondary antibodies, FITC-coupled goat anti-mouse IgG, were obtained from Cappell Research Reagents (USA).

7. Confocal Microscopy and Image Processing

A laser-scanning confocal microscope equipped with an argon/krypton mixed gas laser (Leica TCS NT), fitted onto a microscope (Leica DMIRB-E, FL APO objective lens 63, N.A. 1.4), was used to obtain optical sections of the cells from the top of the cells to the substratum level. Image processing was done on a Silicon Graphics Workstation using Imaris Image Analysis (Bitplane AG, Switzerland) [Messerli et al., 1993].

8. Protein Analysis and Western blot

Cells were rinsed with PBS and collected with sample buffer (62.5 mM TRIS , pH6.8, 2% SDS, 10 mM EDTA , 5% glycerol and 1mM PMSF). The lysates were boiled for 5 min and then centrifuged at 13000 g for another 5 min at $+4°C$. Supernatants were saved and mixed with Laemli electrophoresis buffer prior to electrophoresis. 2 µg of total protein were loaded on and resolved by an 8% SDS-polyacrylamide gel. Proteins were electrically transferred to nitrocellulose membranes using semi-dry blotting, stained with Ponceau red, and after block-ing with a milk blocker, finally incubated with primary antibodies. The monoclonal antibodies raised against human vinculin, but cross reacting with rat tissue were obtained from Genex (Finland). Secondary goat anti-mouse antibodies coupled to peroxidase (Pierce,USA) were detected with Super Signal Reagent (Pierce, USA).

9. Protein Assay

Protein content was estimated using the Lowry method [Lowry, 1951].

Results

1. General Morphology and Structure of Adult Rat Ventricular Myocytes *In Vitro*

1.1 SEM Observations

Enzymatic digestion of heart tissue yields individual myocytes. Fig.2A shows an adult rat ventricular cardiomyocyte right after isolation when it still mainains the cylindrical shape typical for muscle cells in the heart. The rod-like shape of the differentiated heart muscle cells is supported by the scaffold of the intracellular cytoskeleton linked to the attachment complexes in plasmalemma over the entire surface of the myocyte. Anchor fibers tug in plasmalemma to form a series of folds and thus give cardiac myocytes a scalloped surface. The periodic rib-like pattern of cardiac sarcolemma is termed costomeric. The regularly distributed grooves indicate the sites of extracellular contacts

Cardiomyocytes cultured in the presence of serum attach in their rod-shaped state to the bottom of gelatine coated cell culture dishes. After a few days they start to round up and to spread out. During the first week ARCs grow in size and undergo a sequence of phenotypic changes to form a tissue-like sheet of polygonal re-differentiated cells exhibiting spontaneous contractions in culture (Fig.3A).

1.2 The Structure of the Cardiomyocyte Contractile Apparatus

A cardiac muscle cell contains myofibrils, and their fundamental repeating unit is the sarcomere. The sarcomere consists of two interdigitating filament systems – thick myosin-containing filaments and thin actin-containing filaments – which slide past one another and generate the isometric muscle force. We used the combination of fluorescent labelling, confocal microscopy and 3-D image processing to visualise the native assembly of myofibrils in the heart muscle cells and the changes of their organisation in cultured ARCs.
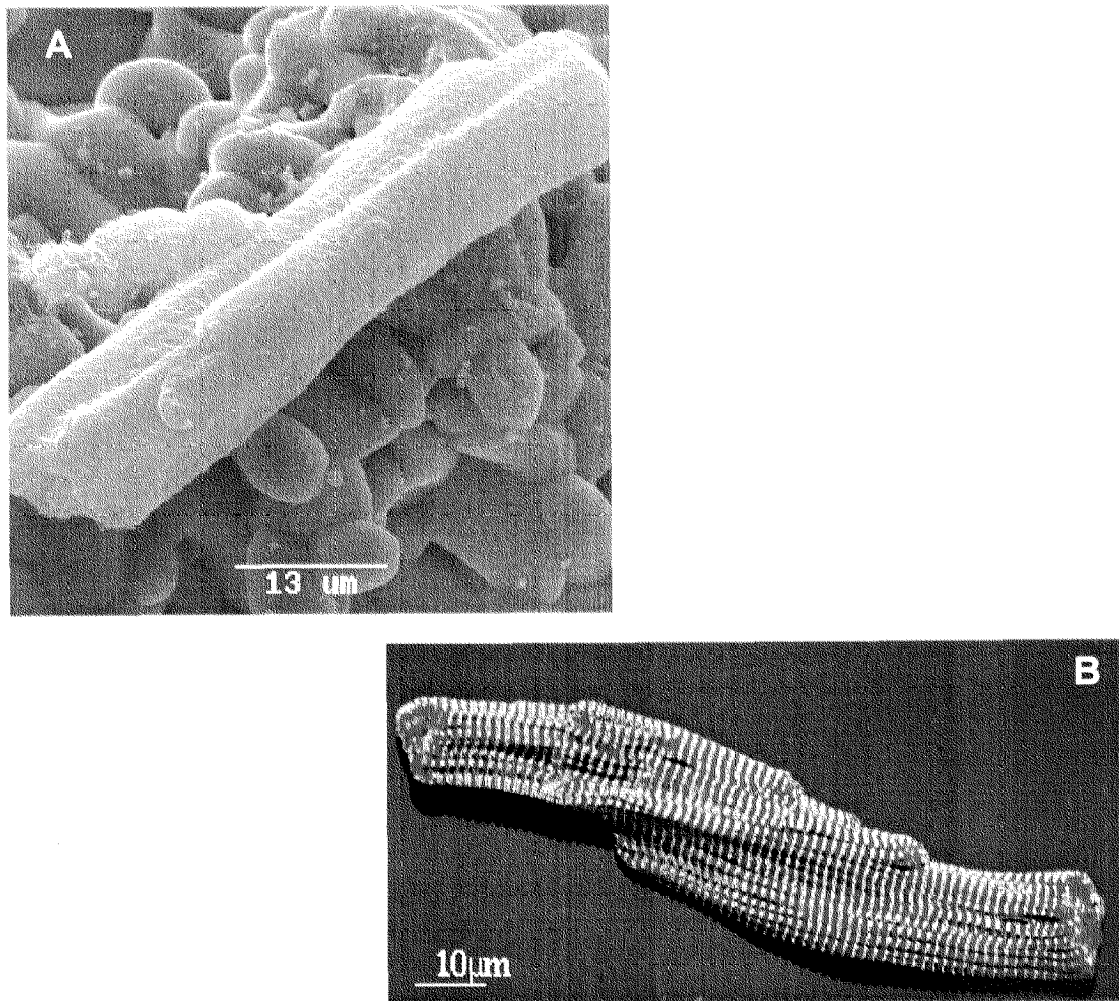
Fig.2   Freshly Isolated Adult Rat Ventricular Myocytes

A- SEM micrograph

B - 3-D reconstruction of confocal images. The cell was immunolabelled with anti-bodies against the myofibrillar protein myosin (green) and with rodamin-coupled phalloidin (red) which binds to the filamentous actin; yellow: superimposition of green and red.

Fig.2B demonstrates a 3-D image of a newly isolated ARC. The cell was stained with rhodamine isothiocyonate (RITC)-conjugated phalloidin that binds to the actin filaments (shown in red). In parallel, it was indirectly immunolabelled with antibodies against myo-mesin, the myosin filament assiociated protein, detected with fluorescein isothiocyonate (FITC)-conjugated secondary antibodies (depicted in green). The spatial distribution of fluo-rescently labelled proteins in cardiac cells was analysed by CLSM. 16 optical sections were

taken through an ARC from the bottom to the top, followed by a digital reconstruction to create a stereoscopic image of the cardiomyocyte myofibrillar structure.

The myofibrils from freshly isolated cells showed a regular organisation of both filament systems. Actin and myomesin were alternately arranged in sarcomeres of the intact myofibrils spread through the cell. After more than a week of hypertrophic growth in vitro, cardiomyocytes increased their size and altered the organisation of the contractile apparatus. During the process of spreading in culture, the cells developed a non-sarcomeric actin cytoskeleton termed stress fiber-like structures without clear sarcomeres as visualised by rhodamin-phalloidin (Fig.3B). They were located in the peripheral region of the cells. Assembled myofibrils with a cross-striated sarcomeric structure were detected by the myomesin staining. They concentrated in the perinuclear region. Therefore the functional myofibrils coexist with a nonsarcomeric cytoskeleton in adult rat ventricular myocytes in long-term primary culture.
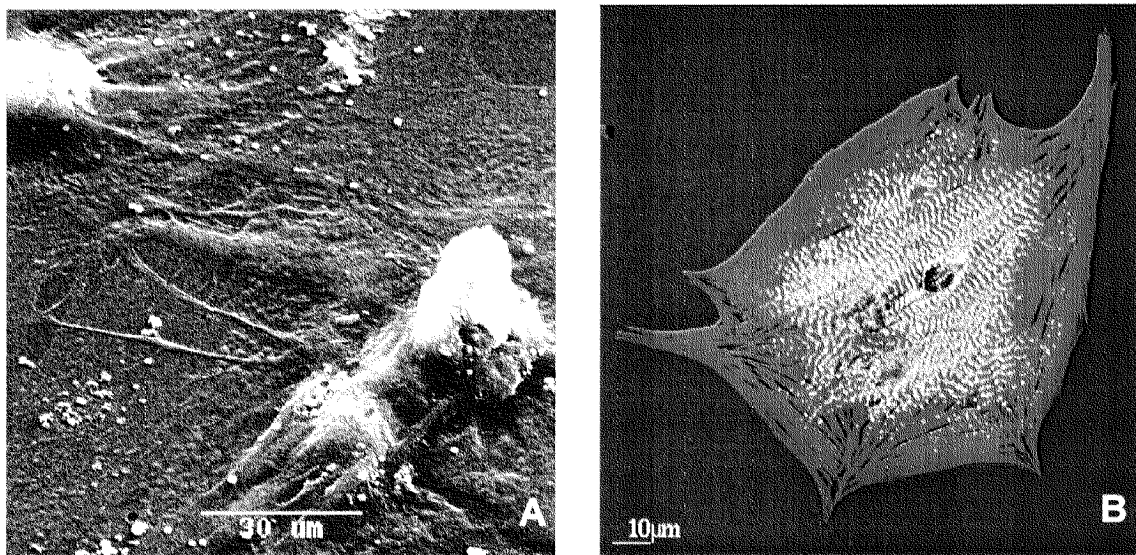
Fig.3   Adult Rat Ventricular Myocytes in Long-Term Primary Culture

Cells cultured for 9 days in a gelatine coated plastic cell culture dish.

A - SEM image

B - the 3D visualisation of the cell obtained by image processing of the CSLM data shows the distribution of myomesin (green) and F-actin (red); yellow: a superimposition of both colours.

2. Influence of the Sol-Gel Derived Titania Coating on the Cardiomyocyte Remodelling

Titania ceramic coatings were applied on the surfaces of glass, alumina ceramics and titania ceramics to create a range of samples with a gradual increase of roughness. To give an optical impression of the surface roughness of the different substrates, AFM surface plots with a total scan size of 50 µm in x- and y-direction and 10 µm in z- direction are presented in Fig.4A-C. To calculate the R_a-values, scan areas of 2500 µm^2 were examined. The values of surface roughness obtained for the sol-gel coated glass, alumina and titanium dioxide substrates were $R_a = 6$ nm, $R_a = 350$ nm and $R_a = 813$ nm respectively.

Scaffolds were seeded with freshly isolated cardiomyocytes and cells were cultured under standard conditions. Every three days viability of cardiomyocytes grown on different scaffolds was assayed by the MTT test, which measures activity of various intracellular dehydrogenases. Viable cells cleave the tetrazolium ring into a visible dark blue formazan reaction product, whereas dead cells remain uncolored. Cytocompatibility studies demonstrated no toxic effect of the materials on the cells. The initial viability of cardiomyocytes was ~ 90% from that of control cells plated into gelatine coated wells. The survival of the cells did not change significantly during the whole period of cell cultivation on any type of scaffold (Fig.5).

After 9 days, the structure of heart cells on different substrata was analysed using the immunolabelling technique and confocal microscopy. ARC were double immunostained with monoclonal antibodies against myomesin associated with myosin filaments and with phalloidin, which binds to filamentous actin. The 3-D computer reconstruction of the multichannel images showed the absence of the cardiomyocyte spreading and their myofibrillar apparatus remodelling on all substrata. The patterns of sarcomeric organisation of myomesin and actin were the same as those in freshly isolated cells (Fig.4 D-F). Hence, the structural components of the cardiac myofibrils did not undergo significant rearrangements during cell cultivation for longer periods of time.
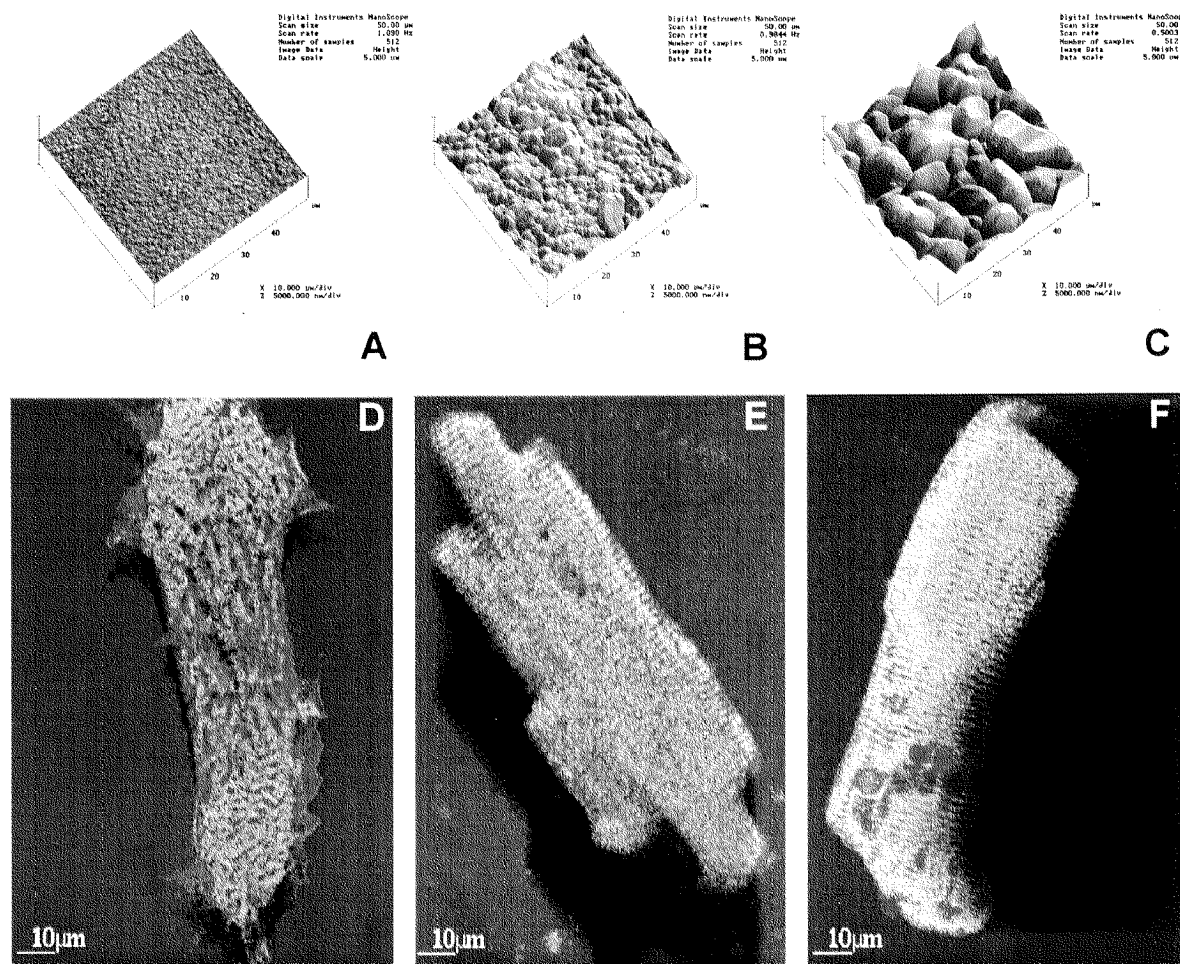
Fig.4 Growth of the Heart Cells on the Substrates Coated with the Sol-Gel Derived Titania Film

A - AFM-surface plot of the sol-gel coated glass, heat treated at 500°C; x- and y-direction 50 μm/div; z-direction 5 μm/div; surface roughness R_a = 6 nm. B - AFM-surface plot of the sol-gel coated alumina, heat treated at 500 °C; x- and y-direction 50 μm/div; z-direction 5 μm/div; surface roughness R_a = 350 nm. C - AFM-surface plot of the sol-gel coated titania, heat treated at 500 °C. x- and y-direction 50 μm/div; z-direction 5 μm/div. Surface roughness R_a = 813 nm.

The bottom part of the figure represents the volume visualisation of the confocal images of cells grown for 9 days on the sol-gel coated glass (D), alumina (E) and titanium dioxide ceramic (F) samples. The sarcomeric organisation of myomesin (M-line) and F-actin are shown in green and red respectively; yellow indicates a superimposition of both signals. A, B, C - SEM images of the cell carrier surfaces.
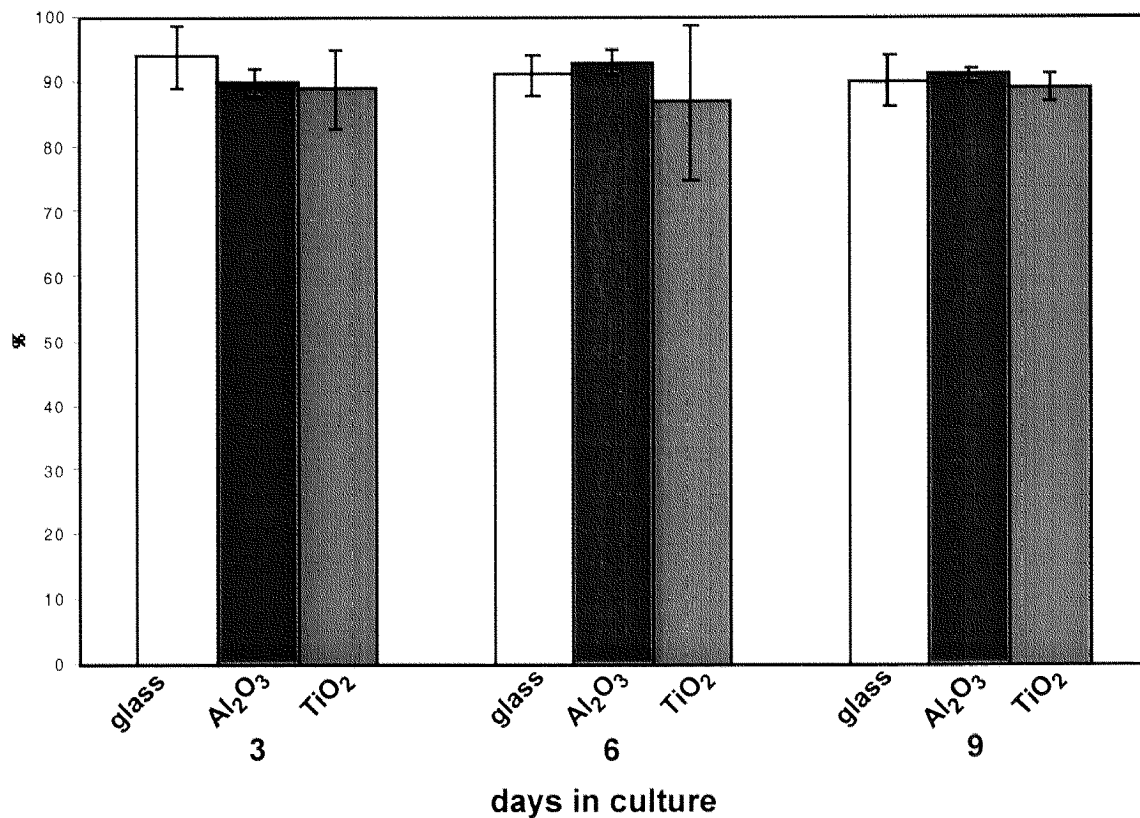
Fig.5 Survival of Adult Rat Ventricular Cardiomyocytes on Biocompatible Scaffolds

The cells were cultivated on glass, alumina and titania ceramics scaffolds coated with the sol-gel derived titania film. Cells were cultured in the 24-well cell culture plates. Cardiomyocytes grown in gelatine coated wells were used as positive controls. The results are given as percentages of control. Data are presented as means ± SD of four experiments.

3. Formation of Focal Adhesions on the Scaffolds with the Titania Surface Coating

The topographical structure in the nanometre range of fine-grained titania derived films physically mimic the surface of cardiac sarcolemma and may simulate the natural microenvironment of the heart cells in culture.

3.1   Ultrastructural Study of the Cell-Substratum Adhesion in Cardiac Cells

Among several detergent-free methods for breaking cells open we found the lysis-squirting technique most suitable for characterising the structure of the cardiomyocyte plasma membrane protoplasmic face. The squirting was always carried out with a syringe from a distance of 10 mm. The procedure yielded sheets of substrate adherent plasma membranes (Fig.6A-B). The membrane-associated cytoskeleton was visualised using SEM. Microscopic observations revealed structural features of the cytoplasmic surface of cardiac sarcolemma similar to those described in other cell types: a continuous web of microfilaments interacting with the globular complexes of transmembrane proteins [Bray et al., 1986]. Ventral membrane preparations of cardiomyocytes cultured on the coated titania ceramic samples (Fig.6C) exposed the macromolecular scaffold of the contact membrane with a well-developed network of focal adhesion points. At the same time, ventral membranes of the heart cells on the uncoated titania ceramics did not show such a high degree of a structural organisation (Fig.6D). Their cytoplasmic surface was smoother and the closely accumulated clusters of focal contacts were less abundant.

3.2   Characterisation of Vinculin Localisation in Isolated Ventral Membranes by Immunofluorescence Microscopy

Isolated ventral membranes of the cells grown on both coated and uncoated titania ceramics were labelled for adhesion complexes using an anti-vinculin antibody. We correlated the immunolabelling with the morphological studies using SEM. Fig.7 shows single optical sections of the ventral membrane adherent to the titania surface. These preparations were usually positive for vinculin indicating that the light squirting did not remove most of the membrane-associated components. A dot-like pattern of adhesion complexes was observed. Vinculin containing focal contacts were abundant and evenly distributed in the ventral membranes of cardiomyocytes cultured on the sol-gel derived titania surfaces (Fig.7A). In cardiomyocytes cultured on the uncoated substrates the degree of vinculin immunolabelling was considerably lower and was localised at the periphery of the adherent membrane fragments. The labelling is very weak in the central part of the contact membranes (Fig.7B).
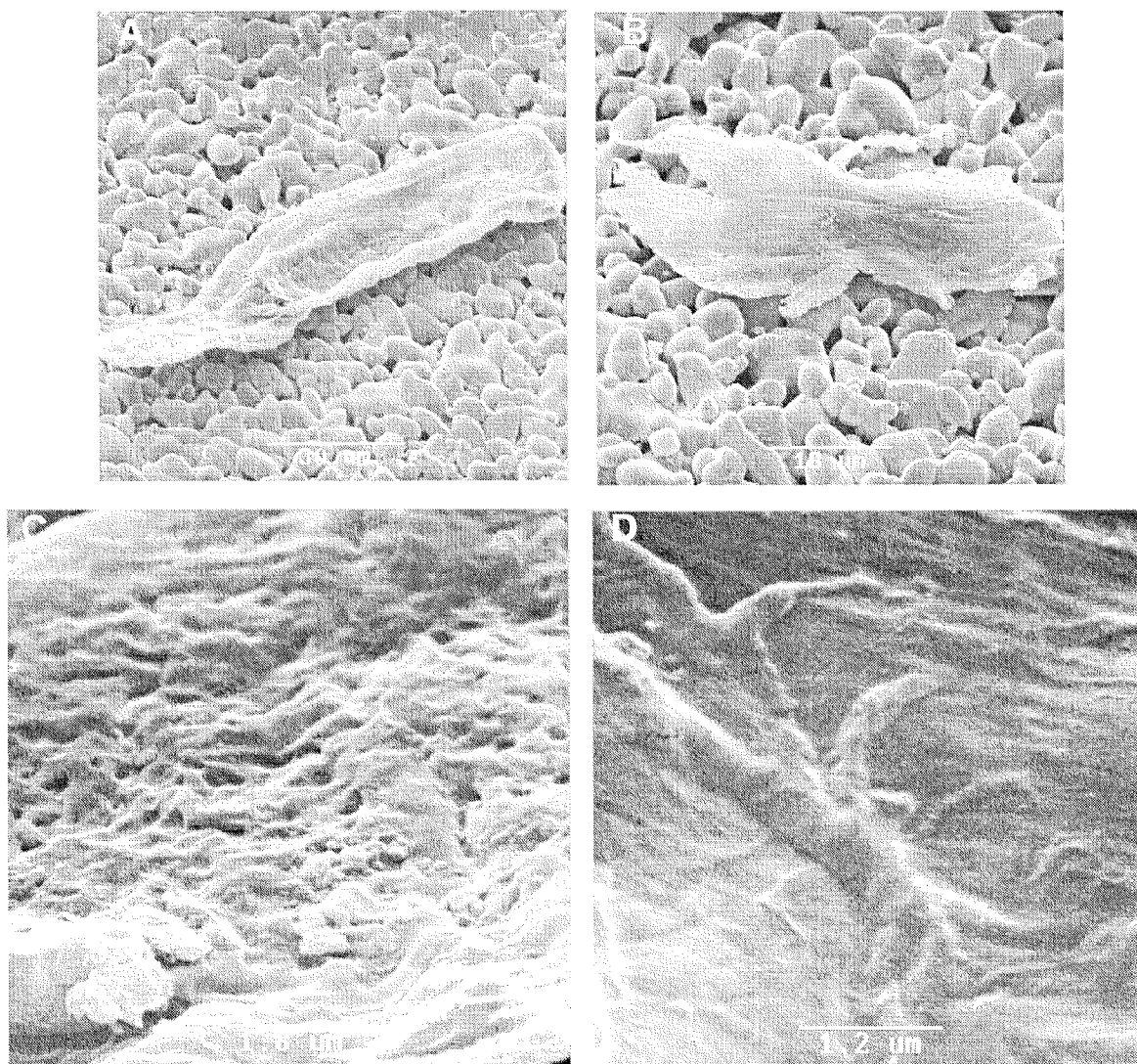
Fig.6 Structure of the Cardiomyocyte Ventral Membrane

Scanning electron micrographs of the ventral membrane preparations of the cells cultured for 9 days on the ceramic samples with (A, C) and without (B, D) sol-gel derived titania coatings. A and B - general view of the preparations at low magnification.

3.3 Biochemical Analysis of Vinculin Expression in the Cells

Cardiomyocytes, which have firmly attached to the carriers, were lysed with buffer containing detergents and protease inhibitors. Solubilised cellular proteins were then separated according to their molecular weight in a polyacrilamide gel, electrically transferred to a nitrocellulose membrane and incubated with anti-vinculin antibodies. After the detection proce-

dure, the antibody bound specifically to a protein with a molecular weight of 117 kDa on the blot, which corresponds to vinculin. Equal amounts of total cellular proteins from different samples were used for the immunoblotting experiments. Therefore the level of the specific protein expressed in the cells under different experimental conditions could be compared. Western blot analysis of vinculin demonstrated an elevation in protein expression in the cardiac cells attached to the fine-grained surface of the sol-gel derived titania coatings as compared to the cardiomyocytes grown on uncoated titania (Fig.8).
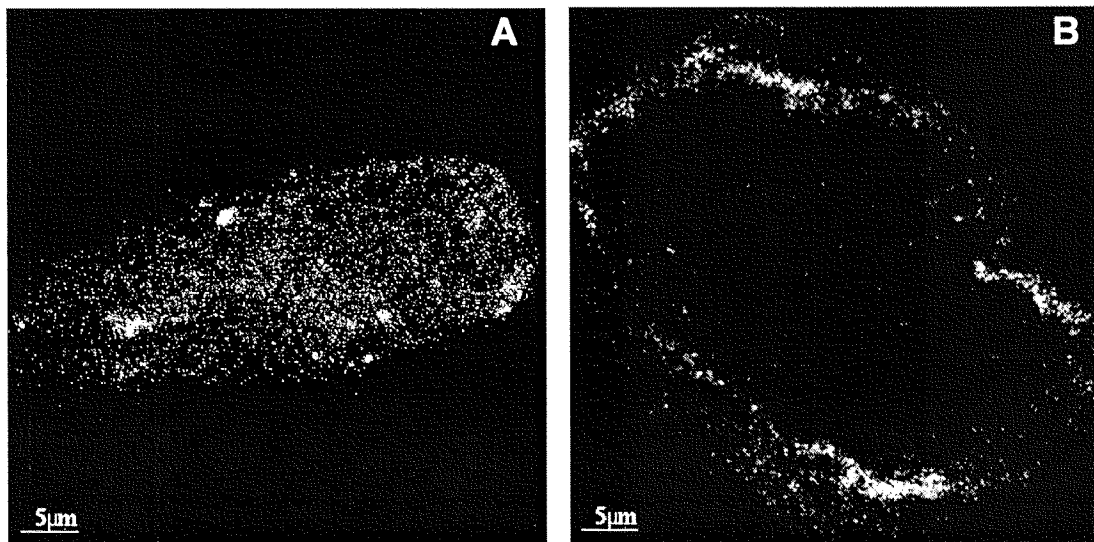

Fig.7   The focal Contact Organisation in ARC

Ventral plasma membranes of cardiomyocytes cultured for 9 days on the sol-gel coated (A) and uncoated (B) titania ceramics were immunolabelled against vinculin. Images represent the projections of all optical sections taken through the whole preparation onto a plane, which is parallel to the image layers. Vinculin staining shows the distribution of cell adhesion complexes.
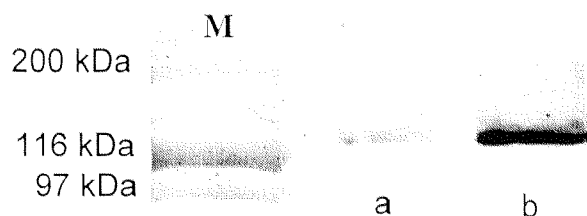

Fig.8   Western Blot Analysis of Vinculin Expression

ARCs were cultured for 9 day on the uncoated (lane a) and sol-gel coated (lane b) titania ceramics.

Discussion

The results of our previous work showed that heart muscle cells maintain the in vivo-like phenotype if cultured on porous titanium dioxide ceramics [Polonchuk et al., 1997]. The question, which occurs, is whether the positive influence on cell growth is induced by the chemical properties of the material or by the surface topography.

Development of sol-gel derived titania coatings [Elbel et al., 1998c] allowed the production of surfaces bearing the same chemical qualities, but exhibiting distinct topographical characteristics. Scaffolds with an increasing degree of surface roughness were coated with a sol-gel derived titania film to create a chemically identical substratum. These cell carriers were used to elucidate whether and how cardiac cells react to the topographical phenomena. This approach helped to distinguish between the effects of substrate chemistry and topography on the cells.

Adult rat cardiomyocytes preserved the regular sarcomeric organisation of myofibrils on all types of scaffolds coated with sol-gel derived titania. The cardiomyocyte did not react on the topographical changes in the micron diapason if the scaffolds have the same surface profiles in the nanometre range. Hence, the cytoskeletal organisation of the cells was mainly guided by the nanometre structure of the superficies.

A closer look at the surfaces coated with sol-gel derived titania showed that the coating consists of small granules of 20-50 nm diameter. The surface structure formed by these granules resembles the organisation of the plasma membrane in differentiated cardiomyocytes. Structuring the scaffold surface by means of such a coating may directly facilitate the short-distance interactions of the cell adhesion receptors with the extracellular material and thus regulate cell development in vitro.

Cells stabilise their shape using both internal structures and external adhesions. Formation of focal adhesion contacts in culture determines the cell response to changes in the local environment. The focal adhesion complexes (FAC) represent a point of convergence for transduction of three main types of extracellular signals: ECM, soluble factors and mechanical forces. Integrin, a membrane component of the attachment complex, forms the principal receptor for extracellular matrix proteins on the outer portion of the plasma membrane. Factors acting through integrins on individual cytoskeletal links produce biochemical signals that are sufficient to modify cell organisation and function [Howe et al., 1998]. The FAC also contains several actin-associated proteins. They mechanically connect the cytoplasmic portion of integrins

to the internal actin cytoskeleton. Among them, vinculin seems to play a central role in trans-membrane coupling. It is required for integrin association with components of the actin cytoskeleton and for localisation to focal adhesions [Ezzel et al., 1997]. Modulation of vinculin levels by overexpression or suppression by antisense cDNA transfection demonstrated dramatic effects on cell spreading, anchorage-dependent growth and tumorigenicity [Rodriguez Fernandez et al., 1992; Rodriguez Fernandez et al., 1993]. Vinculin has actin, talin and α-actinin-binding sites. It can stabilise the link between these structural components within single adhesion points as well as facilitate the assembly many of FACs [Gilmore, 1996].

In cardiomyocytes, the cytoskeleton-matrix link strengthens during differentiation thereby compensating for the increased mechanical load in the developing heart. Reinforcement is controlled via alternative splicing of the b1 integrin [Belkin et al., 1997]. A new b1D isoform of the protein demonstrates the increased affinity for both the extracellular matrix ligand and the adhesion complex proteins. It completely displaces b1A integrin in the adult heart muscle cells. This leads to the increased stability of focal adhesion because of enhancement of the actin-membrane attachment. Stabilisation of the specific cytoskeleton-membrane link can also preserve the organisation of myofibrils and can therefore be involved in the establishment of the differentiated phenotype of cardiac cells. To check whether the formation and maintenance of adhesion complexes can be topographically controlled in cultured adult cardiomyocytes we analysed the structure of ventral membranes in the cells attached to titania ceramics with and without the sol-gel derived titania surface coating.

The experimental results clearly demonstrate that the increase of the scaffold surface roughness in the nanometer range by means of the sol-gel derived titania coating promotes the assembly and the even distribution of focal contacts in the plasma membrane. Immunochemical analysis showed that vinculin assembles with the adhesion complexes formed by ARC on the sol-gel derived titania coated ceramics over the entire cell-substrate contact area. The cells also express a significantly higher amount of vinculin under these conditions as compared to the cardiomyocytes cultivated on uncoated ceramics.

The lower degrees of vinculin staining and of protein expression do not necessarily indicate the absence of the proper cell-substrate contacts in the cells cultured on uncoated ceramics. It has been shown that malignant cells lacking vinculin can still form focal contacts [Volberg et al., 1995] using other molecular mechanisms for their organisation.

However, vinculin most probably assists in cross-linking the adhesion complexes and in maintaining their integrity within the plasma membrane of the cells cultured on coated ceram-

ics. The fine-grained surface structure of a sol-gel titania derived coating may topographically create and determine the distribution of sites for cell-material interactions and focal contact formation. As adhesion proceeds, vinculin targeted to the cell membrane folds into a conformation with unmasked binding sites for talin and actin [Johnson et al., 1995], thereby helping to assemble adhesion complexes and anchorage myofibrils into cardiac sarcolemma and define cell shape. The surface topography of the sol-gel derived titania coating mimics the cell surface and promotes the expression of the protein involved in the cell-material interaction and its recruitment to the sites of ECM binding. In that way the linkage between the cytoskeleton and cell-ECM adhesions via vinculin is strenthened and might therefore stabilise the cellular extensions, permitting the cell to exert forces against the substrate and to adopt a distinctive morphology.

Conclusion and Outlooks

The present work demonstrate that adult rat ventricular cardiomyocytes cultured on titanium dioxide ceramics survive in a differentiated state for long periods of time in vitro. Structural patterning of the cell carrier surface at the nanometre scale promotes formation of focal adhesion complexes. The subsequent reinforcement of the cytoskeleton-membrane link might lead to the stabilisation of cell shape and in that way contribute to the preservation of tissue-like cell morphology in culture.

This observation suggests that cellular organisation is being achieved by local geometric control. Such a result demonstrates an appreciable way towards engineering the rebuilding of heart tissue. In the future, it will be interesting to pursue whether and how the fabrication of the topography influences the chemical properties of the scaffolds used for the cell cultivation and production of devices for tissue repair.

References

Adams J.C., Watt E.M. (1993). Regulation of development and differentiation by extracellular matrix. *Development.* **117**:1183-1198.

Antibodies in Cell Biology. Asai D.J. (Ed); *Method in Cell Biology* v 37, London, Academic Press Ltd, 1993.

Belkin A.M., Retta S.F., Pletjushkina O.Y. et al. (1997). Muscle b1D integrin reinforced the cytoskeleton matrix link: modulation of integrin adhesive function by alternative splicing. *J. Cell.Biol.* **139**:1538-1595.

Blum J., Eckert K.-L., Schroeder A., Petitmermet M., Ha S.-W., Wintermantel E., (1996). In vitro testing of porous titanium dioxide ceramics. *The Proceedings of the 9th Int. Symposium on Ceramics in Medicine.*

Bray D., Jeath J., Moss D. (1986). The membrane associated "cortex" of animal cells: its structure and mechanical properties. *J Cell Sci.* **4**:71-88

Cattelino A, Longhi R., de Curtis I. (1995). Differential distribution of two cytoplasmic variants of the alpha6 beta1 integrin laminin receptors in the ventral plasma membrane of embryonic fibroblast. *J Cell Sci.* **108**:3067-3078

Chen Ch.S., M. Mrksich, Sui Huang, G.M. Whitesides, D.E. Ingber. (1997). Geometric control of cell life and death. *Science.* **276**:1425-1428.

Clarke M, G.Schatten, D.Mazia, J.A.Spudich. (1975). Visualization of actin fibers associated with the cell membrane in amoebae of Dictyostelium discoideum. *Proc.Natl.Acad.Sci.USA.* **72**:1758-1769.

Claycomb W.C. (1988). Atrial natriuretic factor mRNA is developmentally regulated in heart ventricles and actively expressed in cultured ventricular cardiac muscle cells of rat and human. *Biochem. J.* **255**:617-620.

Curtis A., Wilkinson Ch. (1997). Topographical control of cells. *Biomaterials.* **18**:1573-1583.

Eckert K.-L., Ha S.-W., Ritter S., Wintermantel E. (1997). Precipitation of calcium phosphate on titania ceramics. *The Proceedings of the 10th International Symposion on Ceramics in Medicine.* p.3 -6.

Elbel, J., Polonchuk, L. O., Eckert, K.-L., Eppenberger, H., Wintermantel, E., (1998a). Sol-gel derived titania coatings for cell-culture substrates. *The Proceedings of the 11th International Symposion on Ceramics in Medicine.* p. 305 - 308.

Elbel, J., Polonchuk, L., Eckert, K.-L., Eppenberger, H., Wintermantel, E., (1998b). Surface Characteristics of sol-gel derived titania coatings for cardiomyocyte cell culturing, IEKC 6 "Advanced Ceramics and Composites", Stuttgart, Germany; in press.

Elbel, J., Polonchuk, L., Eckert, K.-L., Eppenberger, H., Wintermantel, E., (1998c). Sol-gel derived titania coatings for cardiomyocyte cell-culture scaffolds. *The Proceedings of the 2nd International Conference on Biomaterials Biosurf II.* B20

Ellingsen O., Davidoff A.J., Prasad S.K. et al. (1993). Adult rat ventricular myocytes cultured in defined medium: phenotype and electromechanical function. *Am.J.Physiol.* **265**:H747-H754.12.

Eppenberger M.E., Hauser I., Baeci T., Schaub M.C., Brunner U.T., Dechesne C.A., Eppenberger H.M. (1988). Immunohistochemical analysis of the regeneration of myofibrils in long-term culture of adult cardiomyocytes of the rat. *Dev. Biol.***130**:1-15.

Eppenberger-Eberhardt M., Flamme I., Kurer V., Eppenberger H.M. (1990). Reexpression of alfa-smooth muscle actin isoform in cultured adult rat cardiomyocytes. *Dev. Biol.* **139**:269-278.

Eppenberger-Eberhardt M., Messerli M., Eppenberger H.M., Reinecke M. (1993). New occurence of atrial natriuretic factor and storage in secretorially active granules in adult ventricular cardiomyocytes in long-term culture. *J. Mol. Cell. Cardiol.* **25**:753-757.

Ezzel R.M., Goldmann W.H., Wang N., Parasharama N., Ingber D.E. (1997). Vinculin promotes cell spreading by mechanically coupling integrins to the cytoskeleton. *Exp.Cell.Res.* **231**:14-26

Fartash, B., Liao, H., Li, J., Fouda, N., Hermansson, L., (1995). Long-term evaluation titania-based ceramics compared with commercially pure titanium in vivo. *Journal of Materials Science: Materials in Medicine.* **6**:451-454.

Gilmore A.P., Burridge K. (1996). Regulation of vinculin binding to talin and actin by phosphatidyl-inositol-4-5-biphosphate. *Nature.* **381**:531-535.

Goncharova E.J., Kam Z.M., Geiger B. (1992). The involvement of adherens junction components in myofibrillogenesis in cultured cardiac myocytes. *Development.* **114**:173-183.

Grove B.K., Kurer V., Lehner C., Doetschman T.C., Perriard J.C., Eppenberger H.M. (1984). Monoclonal antibodies detect new 185000 dalton muscle M-line protein. *J.Cell Biol.* **98**:518-524.

Hilenski L.L., Terracio L., Sawyer R., Borg T. (1989). Effects of extracellular matrix on cytoskeletal and myofibrillar organisation in vitro. *Scanning Microsc.* **3**: 535-548.

Horakova M., Mapplebeck C. (1989). Electrical contractile and ultrastructural properties of adult rat and guinea pig ventricular myocytes in long-term primary cultures. *Can. J. Physiol. Pharmacol.* **164**:113-131.

Howe A., Aplin A.E., Alahan S.K., Juliano R.L. (1998). Integrin signalling and cell growth control. *Curr.Op.Cell.Biol.* **10**:220-231.

Jacobson S.L., Piper H.M. (1986). Cell culture of adult cardiomyocytes as models of the myocardium. *J. Mol. Cell. Cardiol.* **18**: 661-667.

Johnson R.P., Cralg S.W. (1995). F-actin binding sites masked by the intramolecular association of vinculin head and tail domain. *Nature.* **373**:261-264.

Kasemo, B. Lausmaa, J., (1988). Biomaterial and Implant Surfaces: A Surface Science Approach. *The Int. Journ. of Oral and Maxillofacial Implants.* **3**: 247 - 259.

Koch-Schneidermann S., P.Gehr, B.Rutishauser, H.M.Eppenberger. (1994). Attachment of adult rat cardiomyocytes (ARC) on laminin and two laminin fragments. *J.Struc.Biol.* **113**:107-116.

Lowry O.H., Rosebrough N.J., Farr A.L., Randall R.J. (1951). Protein measurement with the folin phenol reagent. *J. Biol.Chem.* **193**:265-275.

Lu M.H., Dilulo C., Schultheiss T., Holtzer S., Murray J.M., Choi J., Fishman D.A., Holtzer H. (1992). The vinculin/sarcomeric-alpha-actinin/alpha-actin nexus in cultured cardiac myocytes. *J.Cell.Biol.* **117**:1007-1022.

Mazia D., Sale W.S., Schatten G. (1974). Polylysine as an adhesive for electron microscopy. *J.Cell.Biol.* **63**:212a.

Mosmann T. (1983) Rapid colorimetric assay for cellular growth and survival: applcation to proliferation and cytotoxicity assays. *J.Immuno.Methods.* **65**:55-63.

Nag A.C., Cheng M. (1981). Adult mammalian cardiac muscle cells in culture. *Tissue Cell.* **13**:515-523.

Nermut M.V. Advanced method in electron microscopy of viruses. In: *New developments in practical virology.* C.Howard (ed.); New York, Alan Lis., 1982a:1-58.

Nermut M.V. (1982b). The "cell monolayer technique" in membrane research. Eur. J.Cell Biol., 28: 160-172.

Polonchuk, L.O., Blum, J., Eckert K.-L., Wintermantel, E., Eppenberger H.M. (1997). Establishment of cardiac tissue-like culture using biocompatible scaffolds. *The Proceedings of the Society for Biomaterials 23rd Annual Meeting.* p.248

Qi He, Cahil C.J., Spiro M.J. (1996). Supension culture of differentiated rat heart myocytes on non-adhesive surfaces. *J.Mol.Cell.Cardiol.* **28**:1177-1186.

Rodriguez Fernandez J., Geiger B., Salomon D., Ben-Ze'ev A. (1992). Overexpression of vinculin supresses cell motility in Balb/C 3T3 cells. *Cell Motil Cytoskeleton.* **22**:127-134.

Rodriguez Fernandez J., Geiger B., Salomon D., Ben-Ze'ev A. (1993). Suppression of vinculin expressionby antisense transfection confers changes in cell morphology, motility and anchorage-dependent growth of 3T3 cells. *J. Cell.Biol.* **122**:1285-1294.

StemmerP., Wisler P.L., Watanabe A.M. Isolated myocytes in experimental cardiology. New York: Raven Press Ltd, 1992:387-400.

Volberg T., Geiger B., Kam Z. et al. (1995). Focal adhesion formation by F9 embryonal carcinoma cells after vinculin gene disruption. *J.Cell.Sci.* **108**:2253-2260.

Yamada K.M., Geiger B. (1997). Molecular interactions in cell adhesion complexes. *Curr.Opin.Cell.Biol.* **9**:76-85.

Zarb G.A., P.-I. Branemark, Tissue Integrated Protheses: Osteointegration in Clinical Practice, Quintessence, Chicago, 1985.

Acknowledgements

Time I spent in Switzerland doing my PhD at the ETH-Zurich became a very interesting and important period in my life.

I would like to thank Prof.Dr. Hans M. Eppenberger for giving me the opportunity to work in his group, for his trust and continuous support.

I also would like to express my gratitude to Dr.Monika Eppenberger for sharing her experience in the exciting world of the cardiac cell culture.

I am very thankful to Prof.Dr. Robert Weingart and Dr.Virgis Valiunas from the Physiological Institute of Bern University for a very interesting collaboration we had.

My specials thank goes to the colleagues from the Chair of Biocompatible Materials Science and Engineering ETH-Zurich - Jorg Elbel, Dr.Ludwig Eckert, Dr. Janaki Blum and Prof.Dr. Erich Wintermantel.

I am very grateful to my Diploma supervisor and friend Dr. Antonina Dunina-Barkovskaya for introducing me into the gap junction field and community, for her constant interest and encouragement.

I would like to thank Prof. Jean Claude Perriard for stimulating critical discussions at early Friday morning seminars.

I was very glad to work with all former and present fellows of Prof. Eppenberger's and Prof. Perriard's groups, whose professional help and advice as well as friendship I appreciate very much: Irina Agarkova, Dr. Sigrid Aigner, Daniel Auerbach, Daniel Daetwyler, Dr. Elisabeth Ehler, Julia Feucht, Pierre Giro, Dr. Beatrice Harder, Martin Hefti, Verena Kurer, Martin Leu, Dr. Mohamed Nemir, Dr. Josef Magyar, Evelyne Perriard, Reto Pusterla, Christian Zuppinger.

I enjoyed my time in the Institute for Cell Biology very much and I would like to thank all members and the staff.

I would like to thank a lot all my friends around the world for keeping in touch and cheering me up, for their love and care.

Finally I would like to say that all I have achieved in my life would not be possible without a very strong love and support my dear mother gave to me.

Abstracts and publications

Publications:

Polonchuk L.O. (1996). Single gap junctiion conductance in HeLa cells transfected with Cx32. *Futura* 1: 74-76.

Polonchuk L.O., Frolov V.A., Yuskovich, A.K., Dunina-Barkovskaja, A.Ja. (1997). The effect of arachidonic acid on junctional conductance in isolated murine hepatocytes. *Membr Cell Biol.* 11(2): 225-242.

Polonchuk L.O., Valiunas V., Haefliger J.-A., Weingart R., Eppenberger H.M. Expression and regulation of connexins in cultured ventricular myocytes isolated from adult rat hearts. *Circulation Research*, submitted.

Polonchuk L.O., Elbel J., K.-L. Eckert Blum, J., Wintermantel E., Eppenberger H.M. titanium dioxide ceramic control the differentiated phenotype of adult rat ventricular myocytes in vitro. *Biomaterials*, submitted

Polonchuk L.O., Eppenberger H.M. Re-establishment of cell-cell contacts and the Cx43 phosphorylation during the growth of adult rat ventricular myocytes in long-term culture: involvement of p70S6 kinase; in preparation

Abstracts/Posters

1996:

Cardiovascular biology and clinical implications 3rd Meeting; Interlaken,Switzerland.

Zuppinger Ch., Polonchuk L.O., Eppenberger-Eberhardt M., Schaub M.C., Eppenberger H.M. Cell-cell contacts and cell communication in the redifferentiation process of adult rat cardiomyocytes in long-term and coculture.

1997:

2nd International workshop on cardiac cells in culture: Molecular mechanisms of hypertrophy; Monte Verita, Ascona, Switzerland.

29 Annual Meeting of Swiss Society for Cell and Molecular Biology; Geneva, Switzerland.

Polonchuk L.O. and H.M. Eppenberger. TPA increases the intercellular communication between adult rat cardiomyocytes in culture.

Cardiovascular biology and clinical implications 4th Meeting; Interlaken, Switzerland.

Valiunas V., **Polonchuk L.O.**, Eppenberger H.M, Weingart R. Redifferentiated rat ventricular myocytes: Localization and electrical properties of gap junction channels.

1998:

2nd Symposium of Biological Department ETH-Zurich; Davos, Switzerland.

Polonchuk L.O., Elbel J., Wintermantel E, Eppenberger H.M. Growth of cultured adult rat cardiomyocytes on biocompatible scaffolds: topographical control of cells.

11th International Meeting on Bioceramics; New York, USA.

Elbel J., **Polonchuk L.O.**, Eckert K.-L., Eppenberger H.M., Wintermantel E. Sol-gel derived titania coatings for cell-culture substrates.

1999:

6th Meeting of European Ceramic Society; Brighton, UK.

Elbel J., **Polonchuk L.O.**, Eckert K.-L., Eppenberger H.M., Wintermantel E. Microstructural characterization of sol-gel derived titania coatings for cardiomyocyte cell culturing.

16th European Society for Animal Cell Technology Meeting; Lugano, Switzerland.

Polonchuk L.O., Elbel J., .Eckert K.-L., Blum J., Wintermantel E., Eppenberger H.M. titanium dioxide ceramics control the differetiated phenotype of cardiac muscle cells in culture.

1999 International Gap Junction Conference; Gwatt, Switzerland.

Polonchuk L.O., Eppenberger H.M. gap junction in the long-term culture of adult rat ventricular cardiomyocytes.

Presentations

1997:

Society for Biomaterials 23rd Annual Meeting; New Orleans, LA U.S.A.

Polonchuk L.O., Blum J., Eckert K.-L., Wintermantel E., Eppenberger H.M. Establishment of cardiac tissue-like culture using biocompatible scaffolds.

1999:

Scanning Microscopy International – Cells and materials meeting. Bone & Soft Tissue Biomaterial Interactions, Davos, Switzerland.

Francz G., Hauert R., **Polonchuk L.O.**, Eppenberger H.M., Schroeder A., Riner M., Mayer J., Wintermantel E. XPS analysis of coatings and materials for biomediacal applications.

Acknowledgments:

Eppenberger H.M., Zuppinger Ch. (1999). In vitro reestablishment of cell-cell contacts in adult rat cardiomyocytes. Functional role of transmembrane components in the formation of new intercalated disk-like cell contacts. *The FASEB Journal.* **13**:S83-S89.

CURRICULUM VITAE

Lioudmila Olegovna Polontchouk

Personal

Date of Birth: November 11, 1971

Place of Birth: Moscow, Russia

Citizenship: Russia

Languages: Russian, English, German

Education

1979-1982: Primary School, Moscow Russia

1982-1987: Secondary School, Moscow, Russia

1987-1989: Biological Gymnasium Moscow State University, Moscow, Russia

1990-1995: M.Sc. Biophysics Curriculum, Biological Department of Moscow State University named after M.V.Lomonosov, Moscow, Russia.

Supervisor: Dr.A.J.Dunina-Barkovskaja

1995-1999: Graduate Studies at the Institute for Cell Biology, ETH-Zurich, Switzerland

Mentor: Professor Dr. H.M.Eppenberger